UNIVERSITY OF CALIFORNIA, SAN DIEGO

Exit of the intracellular pathogen *Nematocida parisii* from host *Caenorhabditis elegans* intestinal cells

A dissertation submitted in partial satisfaction of the requirements for the degree

Doctor of Philosophy

in

Biology

by

Suzannah Clark Szumowski

Committee in charge:

Professor Emily Troemel, Chair
Professor Andrew Chisholm
Professor Malene Hansen
Professor Amy Kiger
Professor Victor Nizet
Professor Peter Novick

2015

The Dissertation of Suzannah Clark Szumowski is approved, and it is acceptable in quality and form for publication on microfilm and electronically:

Chair

University of California, San Diego

2015

Table of Contents

List of Figures

List of Tables

Preface

In this thesis I have included two chapters of background material. These introductory chapters were prepared for publication as a review article (Chapter 1) and a commentary article (Chapter 2). Chapter 1 focuses on how hosts respond to microsporidia infection. Chapter 2 is an overview of strategies used by different intracellular pathogens, including microsporidia, to exit from their host cells. This chapter introduces features of microsporidia exit that are covered more extensively in Chapter 3. Chapters 3-5 are publications that examine different stages in the exit process of the microsporidia *Nematocida parisii* from *Caenorhabditis elegans* host intestinal cells. Chapter 3 was published in the journal PLoS Pathogens and investigates the early phases of microsporidia exit from host intestinal cells in which *N. parisii* restructures the host cytoskeleton prior to spore formation. Chapters 4 and 5 focus on the later stages of microsporidia exit. The intracellular trafficking and exocytic fusion of exiting spores is the topic of Chapter 4, which was published in PNAS and highlights the importance of host RAB-11. Chapter 5 describes host factors needed for regulating ACT-5 localization to exocytosing spores and is presented in the format initially submitted to Cellular Microbiology. The contribution of these works to the field of microsporidian biology is highlighted in the Chapter 6, as are suggestions for future lines of inquiry relating to these studies. The Appendix is a compilation of unpublished work, including an imaging mass spectrometry project; information on live imaging techniques; and figures prepared for a manuscript currently in preparation about spore-filled vesicles that appear very late in the *N. parisii* infection cycle.

Acknowledgements

I have been blessed with an incredibly encouraging network of family and friends, whose unconditional love and support has been instrumental in my growth as both a scientist and a person. Thank you to: Emily, Steve, and Mark Szumowski; Allison Kretchman; Dave and Janice Szumowski; Grace King, Joost Hol and Annie Virnig; Chris Koehler and Jenn Tsau; Tiffany Dunbar, Katie Estes, Malina Bakowski, Kirthi Reddy, and Sarah Boyer. I am also grateful for the support of all the members of the Troemel Lab over the years; the UCSD Biological Sciences Program, including Gabriele Wienhausen, Cathy Pugh, and Jackie Vignes; the 2009 incoming graduate student cohort; and the many friends I've made in San Diego. Lastly, I would like to thank my advisor Emily Troemel for her mentorship and support throughout my tenure in her lab.

Chapter 1, in full, is currently being prepared for submission for publication of the material. The dissertation author was the primary investigator and author of this material.

Chapter 2, in full, is reprinted from Worm, 1, Szumowski, S.; Estes, K.; Troemel, E., Preparing a discreet escape: Microsporidia reorganize host cytoskeleton prior to non-lytic exit from *C. elegans* intestinal cells, 207-211, (2012), with permission from Landes Bioscience. The dissertation author was the primary investigator and author of this material.

Chapter 3, in full, is reprinted from PLoS Pathogens, 7, Estes, K.; Szumowski, S.; Troemel, E., Non-lytic, actin-based exit of intracellular parasites from *C. elegans* intestinal cells, e1002227, (2011), with permission from PLoS. The dissertation author

was the second author of this paper. Author contributions to manuscript are as follows: Estes, K.: Figure 1, Figure 2, Figure 3, Figure 4, Figure 5, Figure 6A, 6B, 6C, Figure 8, all Supplemental Figures; Szumowski, S.: Figure 7, all experiments requested for peer review; Troemel, E.: Figure 6D.

Chapter 4, in full, is reprinted from Proceedings of the National Academy of Sciences, 111, Szumowski, S.; Botts, M.; Popovich, J.; Smelkinson, M.; Troemel, E., RAB-11 directs polarized exocytosis of the intracellular pathogen *N. parisii* for fecal-oral transmission from *C. elegans*, 8215-20, (2014), with permission from Proceedings of the National Academy of Sciences. The dissertation author was the primary investigator and author of this material. Author contributions to manuscript are as follows: Szumowski, S.: Figure 1, Figure 2, Figure 3A, 3B, 3D, 3E, Figure 4, Figure 5, all Supplemental Figures, all experiments requested for peer review; Botts, M.: Figure 3C; Popovich, J.:, Figure 5A, Figure S6D; Smelkinson, M.: Figure S2D.

Chapter 5, in full, is currently being prepared for re-submission and publication, Szumowski, S.; Estes, K.; Popovich, J.; Botts, M.; Sek, G.; Troemel, E., Small GTPases promote actin coat formation on pathogens exocytosing from *C. elegans* intestinal cells. The dissertation author was the primary investigator and author of this material. Author contributions to manuscript are as follows: Szumowski, S.: Figure 2, Figure 3, Figure 4, Figure 5A, 5C, 5D, Figure 6, Figure S1A, Figure S1C, Figure S2; Estes, K.: Figure 1, Figure S1B; Popovich, J.: Figure 3A; Botts, M.: Figure 5B; Sek, G.: Figure 3A.

Vita

2015 Ph.D., Biology, University of California San Diego

2009 B.A., Biology, Macalester College

Publications

Szumowski, S., Estes, K., Popovich, J., Botts, M., Sek, G., Troemel, E. Small GTPases promote actin coat formation on pathogens exocytosing from *C. elegans* intestinal cells. 2015; Cellular Microbiology *In review*

Szumowski, S., Botts, M., Popovich, J., Smelkinson, M., Troemel, E. The small GTPase RAB-11 directs polarized exocytosis of the intracellular pathogen *N. parisii* for fecal-oral transmission from *C. elegans*. Proceedings of the National Academy of Sciences. 2014; 111: 8215-20.

Szumowski, S., Estes, K., Troemel, E. Preparing a discreet escape: Microsporidia reorganize host cytoskeleton prior to non-lytic exit from *C. elegans* intestinal cells. Worm. 2012; 1: 207-11.

Szumowski, S., Boyer, S. Hornbach, D., Hove, M. Genetic diversity of two common freshwater mussel species, *Lampsilis cardium* and *Quadrula pustulosa* (Bivalvia: Unionidae), in a large federally protected waterway (St. Croix River, Minnesota/Wisconsin, U.S.A.). American Malacological Bulletin. 2012; 30: 59-72.

Estes, K., **Szumowski, S.**, Troemel, E. Non-lytic, actin-based exit of intracellular parasites from *C. elegans* intestinal cells. 2011; 7: e1002227

Honors, Fellowships, Awards

2013 Best Graduate Student Talk, UCSD Biology Divisional Retreat
2011 NSF Graduate Research Fellowship 2012-2015
2010 NIH Genetics & Genomics Training Grant Fellowship 2010-2012
2009 Graduate *magna cum laude*, Macalester College

ABSTRACT OF THE DISSERTATION

Exit of the intracellular pathogen *Nematocida parisii* from host *Caenorhabditis elegans* intestinal cells

by

Suzannah Clark Szumowski

Doctor of Philosophy in Biology

University of California, San Diego, 2015

Professor Emily Troemel, Chair

A crucial stage in the transmission of diseases that are caused by intracellular pathogens is the exit of these pathogens from their replicative host cell niche. Leaving the host cell allows the pathogen to disseminate to new cells or organisms not yet compromised by infection. Microsporidia are a poorly understood group of

intracellular pathogens that must carry out a host cell exit process. A species of microsporidia called *Nematocida parisii* is a naturally occurring intracellular pathogen of the laboratory model organism *Caenorhabditis elegans*. Using this host-pathogen pair, we have discovered many interesting details of a carefully orchestrated microsporidian host cell exit strategy. *N. parisii* forms spores that exit by exocytosis from the apical side of *C. elegans* intestinal cells. Even prior to spore formation, a dramatic restructuring of the host cytoskeleton occurs, including ectopic localization of actin filaments and gaps in the intermediate-filament dense terminal web structure. Through a genetic screen we found that intracellular membrane-bound spores co-opt the host endocytic recycling system and become coated in *C. elegans* RAB-11 protein. RAB-11 is necessary for spores to fuse with the host apical membrane and thus for exocytosis of spores into the intestinal tract of the host animal. In addition to RAB-11 and other key members of the endocytic recycling system, an isoform of host actin called ACT-5 is strongly required for spore exit. We believe that ACT-5 plays several roles in spore exit, including forming a distinctive coat on spores fused with the apical membrane. Together these findings comprise the bulk of what is known about microsporidia exit from any host cell and illustrate the complexity and intimacy of interactions between intracellular pathogens and their hosts.

1 Introduction: Host response to microsporidia infection

Microsporidia comprise a phylum of fungal-related, obligate intracellular parasites. This phylum contains species that parasitize almost all types of animals, including humans, fish, bees, and other insects. Over 1400 species of microsporidia have been described thus far and new species are being discovered each year (Andreadis et al., 2013; Morsy et al., 2013; Sapir et al., 2014). Some species of microsporidia have a very narrow host range, while others have a relatively broad host range, including vertebrates and invertebrates. Transmissible microsporidia spores are often described as ubiquitous and have been detected in diverse environments ranging from deep sea vents (Sapir et al., 2014) to intercontinental dust (Favet et al., 2013). Microsporidia spores invade hosts with a polar tube to inject themselves directly into the host cell, where they undergo their entire replicative life cycle, and then ultimately differentiate back into spores to return to the environment. These microbes are widespread, but poorly understood, despite their importance to human health and agriculture.

The medical relevance of microsporidia was appreciated when they were found to be responsible for lethal diarrhea in AIDS patients, and death in transplant and immunocompromised patients. Microsporidia can infect any organ system, but predominantly infect the intestine in humans. There is a lack of drugs that are both safe and effective for treating microsporidiosis. For example, fumagillin is one of the few compounds that are effective in killing some species of microsporidia but unfortunately it is toxic to humans (Desoubeaux et al., 2013). Some groups report that the prevalence of microsporidia infections in humans increasing, with many individuals carrying latent and asymptomatic infections (Kotkova et al., 2013; Sak et al., 2011a; Sak et al., 2011b). For further details on the clinical relevance of

microsporidia, we refer readers to a recent review of this topic (Ashfaq and White, 2013).

Microsporidia also affect agriculturally relevant animals, predominantly through infections of fish and insects. Microsporidia have been responsible for the collapse of fisheries, and they have also been implicated in honey bee colony collapse disorder, a disease that is decimating the honey bees that pollinate many essential crops. Recently, progress has been made in developing vaccines and cell lines for study of fish infections by microsporidia (Harkness et al., 2013; Kumar et al., 2014; Mc et al., 2014; Saleh et al., 2014a; Saleh et al., 2014b). Due to space limitations, we direct the reader to existing reviews of microsporidia infections and treatments in fish (Sanders et al., 2012; Stentiford et al., 2013), and in honey bees (van den Heever et al., 2014).

Here we focus primarily on progress made in the basic research of microsporidia-host interactions. We review findings from genomic, transcriptional, cell biological, immunological, and behavioral studies published in the last two years that provide new insight into how hosts respond to these ubiquitous intracellular pathogens.

1.1 Analysis of microsporidian genomes and host-interacting proteins

There has been a rapid increase in the number of microsporidian genome sequences available, which has helped address questions of phylogeny, evolution and pathogenesis of the microsporidia. Microsporidia were originally classified as protists, but are now generally accepted to be a sister taxa to the fungi based on phylogenomic analysis (Capella-Gutierrez et al., 2012; Cuomo et al., 2012). Because of the challenges in manipulating microsporidia in the lab, it has been difficult to use

this newly acquired microsporidian genome information to perform functional analysis. However, new findings have emerged that are providing insight into the microsporidian obligate intracellular lifestyle. A particular focus has been on the proteins secreted by microsporidia into the host cell, since these factors likely hold the key to microsporidia survival within the host cell. Importantly, two recent reports have experimentally verified secretion of some of these proteins from pathogen cells. The first example relates to the finding that many microsporidia genomes encode a secretion signal sequence on the enzyme hexokinase, which catalyzes the first step in glycolysis and the pentose phosphate pathway (Cuomo et al., 2012). This secretion sequence was shown to be functional in a heterologous yeast expression system, where it could direct traffic through the yeast secretory system, supporting a model where microsporidia hexokinase could be directed into the host cell and perhaps promote anabolic metabolism *in vivo* (Cuomo et al., 2012). Hexokinase secretion was recently verified experimentally using antibodies directed against hexokinase of *Antonospora locustae*, a species of microsporidia that infects locusts (Senderskiy et al., 2014). Interestingly, hexokinase localized to the nucleus in these studies, suggesting that it could alter host gene expression. This study also provided experimental confirmation for other pathogen proteins previously predicted to be secreted into host cells. A second set of microsporidia proteins that recently were experimentally verified as secreted came from genomic and proteomic analysis of *Spraguea lophii*, which infects *Lophius* monkfish (Campbell et al., 2013). The authors identified proteins released into the extracellular media from spores that were germinated *in vitro*, and found several microsporidia-specific proteins, as well as RICIN-B lectin-like proteins. The RICIN-B lectin-like proteins are also encoded in the

genomes of other microsporidian species, and could possibly interact with carbohydrates found on host proteins. It will be exciting to functionally connect some of these secreted proteins with phenotypes long known to be caused by microsporidia infection, such as the dramatic 'xenoma' growths induced by many microsporidia infections in fish (Lom and Dykova, 2005). The past few years have seen many newly published microsporidia genomes, and these are covered in a recent review to which we direct readers for more information relating to progress in deciphering microsporidian biology using genomics (Corradi and Selman, 2013).

Using this newly acquired genome information, several studies have focused on proteins that are unique to microsporidia, to learn more about the biology that characterizes these parasites and how they interact with their hosts. In particular, microsporidia-specific proteins such as spore wall proteins and polar tube proteins have received attention (Chen et al., 2013; Dang et al., 2013; Meng et al., 2014; Wang et al., 2014; Yang et al., 2014; Zhu et al., 2013). Some of these studies suggest a role for these unique proteins in promoting host cell entry. For example, it is thought that spore wall proteins may aid in adherence of spores to the host cell and thereby contribute to spore infectivity. The Zhang group recently reported that blocking either spore wall protein 16 (SWP16) or spore wall protein SWP11 using *in vitro* antibody treatments caused a 20% decrease in the adherence of *Nosema bombycis* spores to host cells in each case (Wang et al., 2014; Yang et al., 2014). Further studies of proteins unique to microsporidia may provide insight into what underlies the unique properties of these parasites.

1.2 Host transcriptional response to microsporidia infection

Despite microsporidia being ubiquitous and significant parasites, very little was known about how host animals alter their gene expression in response to infection until just recently. This gap in our understanding has now been filled through analysis of the microsporidia-induced host response for several species, including insect hosts that have been studied for decades, as well as the nematode *C. elegans*, which has only recently been studied as a host for microsporidia infection. See Table 1 for a summary of pathways subjected to transcriptional regulation upon microsporidia infection in the host species that are discussed below.

Table 1-1. Differentially regulated host pathways upon microsporidia infection.

Differentially regulated host pathways	Host/microsporidia		
	C. elegans *N. parisii*	*B. mori* *N. bombycis*	*A. mellifera* *N. ceranae*
Autophagy		✔	
Ubiquitin proteasome	✔	✔	✔
Melanization		✔	✔
Innate Immunity- Toll		✔	
Innate Immunity- IMD			
Innate Immunity- JAK/STAT		✔	
C type lectins	✔	✔	
Antimicrobial peptides		✔	
Metabolism	✔	✔	✔
References	Bakowski *et al.*, 2014	Ma *et al.*, 2013 Yue *et al.*, 2015	Aufauvre *et al.*, 2014 Vidau *et al.,* 2014

One of the first animals described as a host for microsporidia was the silkworm *Bombyx mori*, which can be infected by the microsporidia *Nosema bombycis*. Indeed, Louis Pasteur was one of the first scientists to describe microsporidia infection in silkworm, which causes a disease called pébrine. This disease is characterized by small larval size, delayed development, molting problems, and ‘prickly ash spots’. To understand more about the silkworm response to microsporidia

infection, the Zhou group recently conducted two studies using different techniques to assess changes in host transcription. One study used a genome-wide (23K) microarray chip for *B. mori* and examined host transcriptional response to *N. bombycis* at 2, 4, 6, and 8 days post infection (Ma et al., 2013). Then more recently, they extended these transcriptional studies by examining additional early timepoints with a more modern Digital Gene Expression (DGE) analysis method (Yue et al., 2015). In both studies, the authors highlight the differential expression of many genes active in the synthesis and metabolism of a key regulator of silkworm development, juvenile hormone. These changes in gene expression are likely responsible for increases in juvenile hormone during infection (Ma et al., 2013), which in turn is likely responsible for the small body size and delayed development that are symptoms of silkworm pébrine disease (Ma et al., 2013; Yue et al., 2015). Interestingly, juvenile hormone also accumulates upon infection in *Nosema ceranae*-infected honey bees. However, as opposed to causing stunted growth, in honey bees extra juvenile hormone may cause precocious foraging behaviors that are associated with microsporidia infection (Goblirsch et al., 2013), although the cause of precocious foraging is still disputed (McDonnell et al., 2013). The link between juvenile hormone regulation and symptoms of pébrine in silkworms is intriguing as a possible connection between changes in host gene expression and complex symptoms of disease. Additionally, the microarray study compared *N. bombycis*-induced transcriptional changes to changes resulting from infection by 4 non-microsporidian pathogens and found that 34/70 differentially regulated *B. mori* immune genes were uniquely regulated during infection by *N. bombycis*. Genes in the Toll and JAK/STAT pathways were found to be upregulated in expression, as well as several classes of

anti-microbial peptides (Ma et al., 2013). These findings were largely confirmed in the study using DGE (Yue et al., 2015).

In addition to the innate immune signaling pathways described above, many insects also use a melanization pathway to defend against microbes. The microarray study found genes of the serine protease cascade of the melanization pathway to be down-regulated upon infection with microsporidia. The authors postulate that secretion of serpins by the pathogen could be responsible for this down-regulation of host defense, and go on to show that hemolymph from *N. bombycis*-infected silkworms has slower rates of *in vitro* melanization than does uninfected silkworm hemolymph (Ma et al., 2013). Interestingly, the serine protease cascade was also found to be downregulated in an RNA-seq study of *Nosema ceranae*-infected honey bees (Aufauvre et al., 2014). The DGE study of silkworms on the other hand found that lysozyme and lectins, key players in the melanization defense pathway were upregulated upon silkworm infection with *N. bombycis* (Yue et al., 2015). However, lysozyme was downregulated in the honey bee system (Aufauvre et al., 2014). Taken together, these findings suggest that the melanization pathway may be a battleground for the ongoing arms race between host and pathogen, with each seeking to alter this important defense pathway to its own advantage.

A recently developed model host for studying microsporidia infection is the nematode *C. elegans*, which provides a tractable host with many genetic and molecular tools available for study. *Nematocida parisii* is a microsporidian species shown to naturally infect the intestines of *C. elegans* nematodes from around the world (Felix and Barkoulas, 2012; Troemel et al., 2008). The transcriptional response of *C. elegans* to *N. parisii* microsporidia infection was measured using RNA-seq at 5

timepoints during infection and compared to transcriptional responses to other pathogens of *C. elegans*. Genes upregulated by *N. parisii* infection were largely distinct from those upregulated by infection with the extracellular pathogens *Pseudomonas aeruginosa* or *Staphylococcus aureus*, although there was extensive overlap in the set of genes downregulated by these distinct infections (Bakowski et al., 2014). This finding is similar to the results of the *B. mori* microarray study described above, which found a high proportion of microsporidia-specific changes in gene induction compared to infection with other pathogens (Ma et al., 2013). Interestingly, there was a striking similarity in the *C. elegans* host genes upregulated during *N. parisii* infection as compared to genes upregulated by viral infection, indicating a common host response to these very distinct intracellular pathogens. Many of the commonly upregulated genes contain F-box, FTH, and MATH domains that are associated with ubiquitin-mediated degradation (Bakowski et al., 2014). The authors provide several additional lines of evidence to show that ubiquitin-mediated pathways are involved in the host response to microsporidia infection. In particular, they show that two downstream outputs of ubiquitin, the proteasome and autophagy, provide defense against infection. RNAi knock-down of proteasome subunits, as well as autophagy factors LGG-1 (Atg8/LC3 homolog) or ATG-18 led to increased pathogen load. Furthermore, they showed that ubiquitin as well as autophagy markers are targeted to parasite cells, and that the parasite may suppress that targeting (Bakowski et al., 2014). Interestingly, in the silkworm model of microsporidia infection, DGE analysis of differentially expressed genes found that autophagy genes were regulated during infection by *N. bombycis*, particularly early in infection (6 hpi) (Yue et al., 2015). Although autophagy genes were not induced by *N. parisii* infection, they

did appear to play an important role in defense (Bakowski et al., 2014). Thus, autophagy and other ubiquitin-mediated processes may be a common host response to intracellular infection by microsporidia.

A growing theme in host defense in *C. elegans*, as well as in other hosts, is that immune defense genes are induced when core host processes commonly targeted by pathogens are perturbed (Cohen and Troemel, 2014). In keeping with this theme, *C. elegans* appears to induce intracellular defense genes in response to perturbation of proteasome function. In particular, E3 ubiquitin ligase components, which are induced by RNAi knock-down of proteasome subunits, as well as by pharmacological inhibitors of the proteasome, are also induced by microsporidia or viral infections (Bakowski et al., 2014). Thus, microsporidia infection may be detected through the increased demand placed on the proteasome, although there are likely to be other cues as well. A recent study using a proteomics technique also supports the hypothesis that microsporidia counteracts host degradation pathways (Vidau et al., 2014). Proteomic analysis of infected and uninfected honey bee midguts identified 14 differentially expressed proteins, one of which was a proteasome subunit that was about half as abundant upon *Nosema ceranae* infection. Perhaps challenging the host proteasome is a common mechanism of pathogenesis employed by different species of microsporidia.

1.3 Microsporidia use host intracellular trafficking pathways for exit and remodel host cytoskeleton

A critical stage in the life cycle of any intracellular pathogen is to exit from the host cell and be transmitted to a new host, which requires the pathogen to navigate and interact with host pathways. Very little was known about microsporidia exit from

host cells until recently. Previous analysis of microsporidia life cycles had assumed that microsporidia lyse host cells in order to exit. Indeed, several other intracellular pathogens such as *Chlamydia* have been shown to use such a strategy (Friedrich et al., 2012). However, recent discoveries in *C. elegans* have found microsporidia can use a very well-orchestrated, multi-step exit strategy that does not lyse cells, but rather enables the host to live for a surprising length of time during prolific pathogen production, although microsporidia infection does eventually kill this host (Estes et al., 2011; Troemel et al., 2008).

Earlier work in the *C. elegans* host system showed that host animals were alive while contagious, indicating that the *C. elegans*-infecting species of microsporidia, *Nematocida parisii* is able to exit from host intestinal cells and be excreted from the animal without causing death (Troemel et al., 2008). Additional studies of this host cell exit process indicated it to be non-lytic, because intestinal cells continued to exclude a small dye that enters perforated cells, even at timepoints when animals were actively excreting *N. parisii* spores (Estes et al., 2011). More recently, it was shown by electron microscopy that intracellular spores are contained in a separate membrane compartment that can fuse with the host plasma membrane (Szumowski et al., 2014). Importantly, *N. parisii* spores exit exclusively from the apical side of polarized intestinal cells, which allows them access to the lumen of the intestinal tract and therefore a route to excretion (Estes et al., 2011). The recycling endosome regulator RAB-11 was identified by an RNAi screen to be instrumental in orchestrating the fusion of microsporidia-containing compartments with the host apical membrane. RNAi against RAB-11 decreased spore exit and reduced the transmission of infection from infected animals to their neighbors (Szumowski et al.,

2014). The authors propose that the action of this polarized smGTPase, RAB-11, may be responsible for the apical-only direction of parasite exit, an example of elegant repurposing of host trafficking machinery in response to infection.

Another interesting finding from studies of microsporidia in the *C. elegans* model system, is the degree to which the host cytoskeletal system is remodeled during infection. It was first noted that exit of *N. parisii* from host cells requires an intestinal-specific isoform of *C. elegans* actin, ACT-5. This protein is also mislocalized early during infection (Estes et al., 2011). Interestingly, differential levels of host actin upon infection were identified in a proteomic study of the mosquito, *Aedes aegypti*, when it was co-infected with two species of microsporidia (Duncan et al., 2012). Although there are many possible roles actin could play during intracellular infection by parasites, perhaps use of actin during host cell exit is a common strategy employed by many different species of microsporidia. This finding also suggests that researchers should be cautious about using actin gene levels to normalize expression in transcriptional studies, since actin genes may not be have consistent levels of expression during infection (Duncan et al., 2012).

1.4 Natural variation in host resistance and clearance of microsporidia

One recent study of microsporidia infection demonstrates how genetic variation in host responses to parasitic infections can affect host fitness across generations. In a study of the resistance of different strains of the roundworm *C. elegans* to its naturally occurring microsporidian parasite, *N. parisii*, the authors found that a strain of *C. elegans* from Hawaii had about 30-fold increased resistance to infection compared to the laboratory strain from England, as assessed by pathogen load. Furthermore, Hawaiian worms had more progeny than British worms after

infection, indicating that the increased resistance could lead to a selective advantage. The enhanced resistance and fecundity of this strain when challenged with *N. parisii* appears to be due to the surprising ability of this strain to clear intracellular infection, but only during early larval stages of development (Balla, 2015). Clearance of *N. parisii* from the intestinal epithelial cells of *C. elegans* in vivo is a striking finding, given that *C. elegans* does not have known professional immune cells. It would be interesting to analyze the mechanism of clearance in other hosts, to determine whether this epithelial clearance can also be used in hosts that have a professional immune system.

1.5 Changes in host behavior resulting from microsporidia infection

In addition to modulating host activities on a cellular level, microsporidia such as the honey bee-infecting species, *Nosema ceranae*, can also alter host behavior (Botias et al., 2013; Cepero et al., 2014; Natsopoulou et al., 2015; Naug and Gibbs, 2009). European honey bee populations have been decimated recently due to a phenomenon called 'colony collapse disorder' that may be at least partially due to infection by *Nosema ceranae.* A recent report suggests that "homing success", a measure of the bees' ability to return to the hive after kidnapping and being released from a far-away location, was significantly reduced in *N. ceranae*-infected bees compared to control animals (Wolf et al., 2014). This difference was largely due to decreased flight times and increased rest intervals of infected bees, rather than differences in navigation or other flight characteristics. The authors note that although this inability to return home can reduce colony size, it also can mitigate spread of infection throughout the colony, highlighting the complexity of factors at play in host response to microsporidia infections.

In another fascinating example of the complex behavioral changes that can occur upon microsporidia infection, Shi et al present data for a mechanism by which microsporidia infection can prevent locust swarming (Shi et al., 2014). In their paper, the authors propose that the locust-infecting microsporidia, *Antonospora* (*Nosema) locustae*, acidifies the hindgut of the host locust during infection, which reduces growth of a particular commensal bacterial species that is responsible for producing pheromones that promote swarming behavior. Volatiles from the feces of infected locusts were less attractive to healthy locusts than volatiles from the feces of uninfected animals. In addition to reducing the onset of aggregating behaviors, RNAseq data shows that microsporidia infection suppresses synthesis of dopamine, a neurotransmitter that helps maintain swarming (Shi et al., 2014). This study again illustrates how far-reaching the impact of microsporidia infection can be in a host, with changes in the host microbiome due to microsporidia adversely affecting important behaviors like locust swarming.

1.6 Conclusions

In conclusion, exciting progress has been made recently in investigating host responses to microsporidia infection. Many of the studies described above highlight the struggle between host and parasite for control of host defense pathways including innate and cellular immune pathways, cellular clearance and autophagy, and the proteasome. Interactions between host and pathogen manifest across many levels of host biology, ranging from transcriptional changes in the genome, to cytoskeletal and trafficking modifications within cells, and even to alterations in host behavior (Figure 1). Studying these interactions should help us understand infectious disease caused by microsporidia, and more generally the needs of both hosts and parasites.

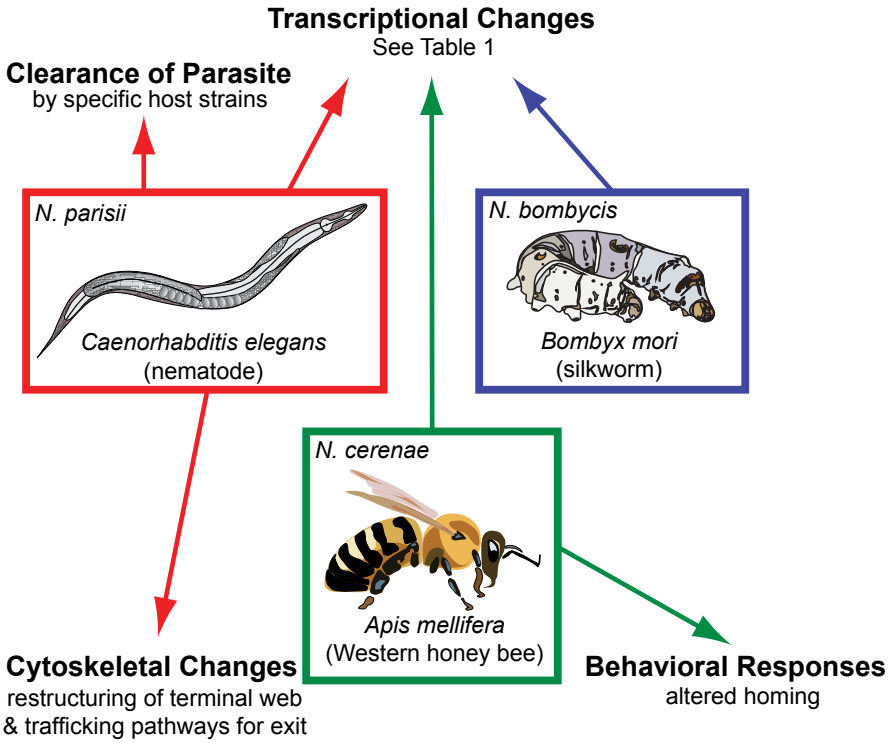

Figure 1-1. Microsporidia-host interactions. Recent studies conducted in nematodes, silkworms, and honeybees have enhanced our understanding of the basic biology of host-parasite interactions by examining how hosts respond to microsporidia infection. Examples of host responses studied in each host-parasite pair discussed in detail in this review are summarized above.

1.7 Additional Acknowledgements

We thank Michael Botts and Lianne Cohen for helpful comments on the manuscript. This work was supported by NIH predoctoral training grant T32 GM008666 and a NSF Predoctoral Fellowship to S.C.S.; and NIAID R01 AI087528, the Searle Scholars Program, Packard Foundation and Burroughs Wellcome Fund fellowships to E.R.T.

Chapter 1, in full, is currently being prepared for submission for publication of the material. The dissertation author was the primary investigator and author of this material.

1.8 References

Andreadis, T.G., Takaoka, H., Otsuka, Y. and Vossbrinck, C.R. (2013). Morphological and molecular characterization of a microsporidian parasite, Takaokaspora nipponicus n. gen., n. sp. from the invasive rock pool mosquito, Ochlerotatus japonicus japonicus. *Journal of Invertebrate Pathology* **114,** 161-172.

Ashfaq, A. and White, A.C., Jr. (2013). Microsporidiasis. *Handbook of Clinical Neurology* **114,** 183-191.

Aufauvre, J., Misme-Aucouturier, B., Vigues, B., Texier, C., Delbac, F. and Blot, N. (2014). Transcriptome analyses of the honeybee response to Nosema ceranae and insecticides. *PloS One* **9,** e91686.

Bakowski, M.A., Desjardins, C.A., Smelkinson, M.G., Dunbar, T.A., Lopez-Moyado, I.F., Rifkin, S.A., Cuomo, C.A. and Troemel, E.R. (2014). Ubiquitin-mediated response to microsporidia and virus infection in C. elegans. *PLoS Pathogens* **10,** e1004200.

Balla, K.M., Andersen, E.C., Kruglyak, L. and Troemel, E.R. (2015). A wild C. elegans strain has enhanced epithelial immunity to a natural microsporidian parasite. *PLoS Pathogens*.

Botias, C., Martin-Hernandez, R., Barrios, L., Meana, A. and Higes, M. (2013). Nosema spp. infection and its negative effects on honey bees (Apis mellifera iberiensis) at the colony level. *Veterinary Reserch* **44,** 25.

Campbell, S.E., Williams, T.A., Yousuf, A., Soanes, D.M., Paszkiewicz, K.H., and Williams, B.A. (2013). The genome of Spraguea lophii and the basis of host-microsporidian interactions. *PLoS Genetics* **9**, e1003676.

Capella-Gutierrez, S., Marcet-Houben, M. and Gabaldon, T. (2012). Phylogenomics supports microsporidia as the earliest diverging clade of sequenced fungi. *BMC Biology* **10,** 47.

Cepero, A., Ravoet, J., Gomez-Moracho, T., Bernal, J.L., Del Nozal, M.J., Bartolome, C., Maside, X., Meana, A., González-Porto, A.V., de Graaf, D.C., Martín-Hernández, R. and Higes, M. (2014). Holistic screening of collapsing honey bee colonies in Spain: a case study. *BMC Research Notes* **7,** 649.

Chen, J., Geng, L., Long, M., Li, T., Li, Z., Yang, D., Ma, C., Wu, H., Ma, Z., Li, C., Pan, G. and Zhou, Z. (2013). Identification of a novel chitin-binding spore wall protein (NbSWP12) with a BAR-2 domain from Nosema bombycis (microsporidia). *Parasitology* **140,** 1394-1402.

Cohen, L.B. and Troemel, E.R. (2014). Microbial pathogenesis and host defense in the nematode C. elegans. *Current Opinion in Microbiology* **23C,** 94-101.

Corradi, N., Pombert, J.F., Farinelli, L., Didier, E.S. and Keeling, P.J. (2010). The complete sequence of the smallest known nuclear genome from the microsporidian Encephalitozoon intestinalis. *Nature Communications* **1,** 77.

Corradi, N. and Selman, M. (2013). Latest progress in microsporidian genome research. *The Journal of Eukaryotic Microbiology* **60,** 309-312.

Cuomo, C.A., Desjardins, C.A., Bakowski, M.A., Goldberg, J., Ma, A.T., Becnel, J.J., Didier, E.S., Fan, L., Heiman, D.I., Levin, J.Z., Young, S., Zeng, Q. and Troemel, E.R. (2012). Microsporidian genome analysis reveals evolutionary strategies for obligate intracellular growth. *Genome Reseach* **22,** 2478-2488.

Dang, X., Pan, G., Li, T., Lin, L., Ma, Q., Geng, L., He, Y. and Zhou, Z. (2013). Characterization of a subtilisin-like protease with apical localization from microsporidian Nosema bombycis. *Journal of Invertebrate Pathology* **112,** 166-174.

Desoubeaux, G., Maakaroun-Vermesse, Z., Lier, C., Bailly, E., Morio, F., Labarthe, F., Bernard, L. and Chandenier, J. (2013). Successful treatment with fumagillin of the first pediatric case of digestive microsporidiosis in a liver-kidney transplant. *Transplant Infectious Disease* **15,** E250-259.

Duncan, A.B., Agnew, P., Noel, V., Demettre, E., Seveno, M., Brizard, J.P. and Michalakis, Y. (2012). Proteome of Aedes aegypti in response to infection and coinfection with microsporidian parasites. *Ecology and Evolution* **2,** 681-694.

Edlind, T.D., Li, J., Visvesvara, G.S., Vodkin, M.H., McLaughlin, G.L. and Katiyar, S.K. (1996). Phylogenetic analysis of beta-tubulin sequences from amitochondrial protozoa. *Molecular Phylogenetics and Evolution* **5,** 359-367.

Estes, K.A., Szumowski, S.C. and Troemel, E.R. (2011). Non-lytic, actin-based exit of intracellular parasites from C. elegans intestinal cells. *PLoS Pathogens* **7,** e1002227.

Favet, J., Lapanje, A., Giongo, A., Kennedy, S., Aung, Y.Y., Cattaneo, A., Davis-Richardson, A.G., Brown, C.T., Kort, R., Brumsack, H.J., Schnetger, B., Chappell, A., Kroijenga, J., Beck, A., Schwibbert, K., Mohamed, A.H., Kirchner, T., de Quadros, P.D., Tripplett, E.W., Broughton, W. J. and Gorbushina, A.A. (2013). Microbial hitchhikers on intercontinental dust: catching a lift in Chad. *Isme Journal* **7,** 850-867.

Felix, M.A. and Barkoulas, M. (2012). Robustness and flexibility in nematode vulva development. *Trends in Genetics* **28,** 185-195.

Friedrich, N., Hagedorn, M., Soldati-Favre, D., and Soldati, T. (2012). Prison break: pathogens' strategies to egress from host cells. *Microbiology and molecular biology reviews : MMBR* **76**, 707-720.

Goblirsch, M., Huang, Z.Y. and Spivak, M. (2013). Physiological and behavioral changes in honey bees (Apis mellifera) induced by Nosema ceranae infection. *PloS One* **8,** e58165.

Harkness, J.E., Guselle, N.J. and Speare, D.J. (2013). Demonstrated efficacy of a pilot heterologous whole-spore vaccine against Microsporidial gill disease in rainbow trout. *Clinical and Vaccine Immunology* **20,** 1483-1484.

Kotkova, M., Sak, B., Kvetonova, D. and Kvac, M. (2013). Latent microsporidiosis caused by Encephalitozoon cuniculi in immunocompetent hosts: a murine model demonstrating the ineffectiveness of the immune system and treatment with albendazole. *PloS One* **8,** e60941.

Kumar, G., Saleh, M., Abdel-Baki, A.A., Al-Quraishy, S. and El-Matbouli, M. (2014). In vitro cultivation model for Heterosporis saurida (Microsporidia) isolated from lizardfish, Saurida undosquamis (Richardson). *Journal of Fish Diseases* **37,** 443-449.

Lom, J., and Dykova, I. (2005). Microsporidian xenomas in fish seen in wider perspective. *Folia Parasitol (Praha)* **52**, 69-81.

Ma, Z., Li, C., Pan, G., Li, Z., Han, B., Xu, J., Lan, X., Chen, J., Yang, D., Chen, Q., Sang, Q., Ji, X., Li, T., Long, M. and Zhou, Z. (2013). Genome-wide transcriptional response of silkworm (Bombyx mori) to infection by the microsporidian Nosema bombycis. *PloS One* **8,** e84137.

Mc, C.S., Sheppard, J., Wright, G.M. and Speare, D.J. (2014). Development of the microsporidian parasite, Loma salmonae, in a rainbow trout gill epithelial cell line (RTG-1): evidence of xenoma development in vitro. *Parasitology***,** 1-6.

McDonnell, C.M., Alaux, C., Parrinello, H., Desvignes, J.P., Crauser, D., Durbesson, E., Beslay, D. and Le Conte, Y. (2013). Ecto- and endoparasite induce similar chemical and brain neurogenomic responses in the honey bee (Apis mellifera). *BMC Ecology* **13,** 25.

Meng, X., Zheng, J., Gao, Y., Zhang, Y. and Jia, H. (2014). Evaluation of spore wall protein 1 as an alternative antigen for the diagnosis of Encephalitozoon cuniculi infection of farmed foxes using an enzyme-linked immunosorbent assay. *Veterinary Parasitology* **203,** 331-334.

Morsy, K., Bashtar, A.R., Abdel-Ghaffar, F. and Al-Quraishy, S. (2013). Morphological and phylogenetic description of a new xenoma-inducing microsporidian, Microsporidium aurata nov. sp., parasite of the gilthead seabream Sparus aurata from the Red Sea. *Parasitology Research* **112,** 3905-3915.

Natsopoulou, M.E., McMahon, D.P., Doublet, V., Bryden, J. and Paxton, R.J. (2015). Interspecific competition in honeybee intracellular gut parasites is asymmetric and favours the spread of an emerging infectious disease. *Proceedings of the Royal Society B: Biological Sciences* **282,** 20141896.

Naug, D. and Gibbs, A. (2009). Behavioral changes mediated by hunger in honeybees infected with Nosema ceranae. *Apidologie* **40,** 595-599.

Sak, B., Brady, D., Pelikanova, M., Kvetonova, D., Rost, M., Kostka, M., Tolarova, V., Huzova, Z. and Kvac, M. (2011a). Unapparent microsporidial infection among immunocompetent humans in the Czech Republic. *Journal of Clinical Microbiology* **49,** 1064-1070.

Sak, B., Kvac, M., Kucerova, Z., Kvetonova, D. and Sakova, K. (2011b). Latent microsporidial infection in immunocompetent individuals - a longitudinal study. *PLoS Neglected Tropical Diseases* **5,** e1162.

Saleh, M., Kumar, G., Abdel-Baki, A.A., Dkhil, M., El-Matbouli, M. and Al-Quraishy, S. (2014a). Development of a novel in vitro method for drug development for fish; application to test efficacy of antimicrosporidian compounds. *Veterinary Record* **175,** 561.

Sanders, J.L., Watral, V. and Kent, M.L. (2012). Microsporidiosis in zebrafish research facilities. *Ilar Journal* **53,** 106-113.

Sapir, A., Dillman, A.R., Connon, S.A., Grupe, B.M., Ingels, J., Mundo-Ocampo, M., Levin, L.A., Baldwin, J.G., Orphan, V.J. and Sternberg, P.W. (2014). Microsporidia-nematode associations in methane seeps reveal basal fungal parasitism in the deep sea. *Frontiers in Microbiology* **5,** 43.

Senderskiy, I.V., Timofeev, S.A., Seliverstova, E.V., Pavlova, O.A. and Dolgikh, V.V. (2014). Secretion of Antonospora (Paranosema) locustae proteins into infected cells suggests an active role of microsporidia in the control of host programs and metabolic processes. *PloS One* **9,** e93585.

Shi, W., Guo, Y., Xu, C., Tan, S., Miao, J., Feng, Y., Zhao, H., St. Leger, R.J. and Fang, W. (2014). Unveiling the mechanism by which microsporidian parasites prevent locust swarm behavior. *Proceedings of the National Academy of Sciences of the United States of America* **111,** 1343-1348.

Stentiford, G.D., Feist, S.W., Stone, D.M., Bateman, K.S. and Dunn, A.M. (2013). Microsporidia: diverse, dynamic, and emergent pathogens in aquatic systems. *Trends in Parasitology* **29,** 567-578.

Szumowski, S.C., Botts, M.R., Popovich, J.J., Smelkinson, M.G. and Troemel, E.R. (2014). The small GTPase RAB-11 directs polarized exocytosis of the intracellular pathogen N. parisii for fecal-oral transmission from C. elegans. *Proceedings of the National Academy of Sciences of the United States of America* **111,** 8215-8220.

Troemel, E.R., Felix, M.A., Whiteman, N.K., Barriere, A. and Ausubel, F.M. (2008). Microsporidia are natural intracellular parasites of the nematode Caenorhabditis elegans. *PLoS Biology* **6,** 2736-2752.

van den Heever, J.P., Thompson, T.S., Curtis, J.M., Ibrahim, A. and Pernal, S.F. (2014). Fumagillin: an overview of recent scientific advances and their significance for apiculture. *Journal of Agricultural and Food Chemistry* **62,** 2728-2737.

Vidau, C., Panek, J., Texier, C., Biron, D.G., Belzunces, L.P., Le Gall, M., Broussard, C., Delbac, F. and El Alauoi, H. (2014). Differential proteomic analysis of midguts from Nosema ceranae-infected honeybees reveals manipulation of key host functions. *Journal of Invertebrate Pathology* **121,** 89-96.

Wang, Y., Dang, X., Ma, Q., Liu, F., Pan, G., Li, T. and Zhou, Z. (2014). Characterization of a novel spore wall protein NbSWP16 with proline-rich tandem repeats from Nosema bombycis (microsporidia). *Parasitology***,** 1-9.

Wolf, S., McMahon, D.P., Lim, K.S., Pull, C.D., Clark, S.J., Paxton, R.J., and Osborne, J.L. (2014). So near and yet so far: harmonic radar reveals reduced homing ability of Nosema infected honeybees. *PloS One* **9**, e103989.

Yang, D., Dang, X., Peng, P., Long, M., Ma, C., Qin, J.J., Wu, H., Liu, T., Zhou, X., Pan, G. and Zhou, Z. (2014). NbHSWP11, a microsporidia Nosema bombycis protein, localizing in the spore wall and membranes, reduces spore adherence to host cell BME. *Journal of Parasitology* **100,** 623-632.

Yue, Y.J., Tang, X.D., Xu, L., Yan, W., Li, Q.L., Xiao, S.Y*.,* Fu, X.L., Wang, W., Li, N. and Shen, Z.Y. (2015). Early responses of silkworm midgut to microsporidium infection - A Digital Gene Expression analysis. *Journal of Invertebrate Pathology* **124,** 6-14.

Zhu, F., Shen, Z., Hou, J., Zhang, J., Geng, T., Tang, X., Xu, L. and Guo, X. (2013). Identification of a protein interacting with the spore wall protein SWP26 of Nosema bombycis in a cultured BmN cell line of silkworm. *Infection, Genetics, and Evolution* **17,** 38-45.

2 Introduction: Preparing a discreet escape: microsporidia reorganize host cytoskeleton prior to non-lytic exit from *C. elegans* intestinal cells

COMMENTARY

Worm 1:4, 207–211; October/November/December 2012; © 2012 Landes Bioscience

Preparing a discreet escape

Microsporidia reorganize host cytoskeleton prior to non-lytic exit from *C. elegans* intestinal cells

Suzannah C. Szumowski, Kathleen A. Estes and Emily R. Troemel*

Division of Biological Sciences; Section of Cell and Developmental Biology; University of California San Diego; La Jolla, CA USA

Intracellular pathogens commonly invade and replicate inside of intestinal cells and exit from these cells is a crucial step in pathogen transmission. For convenience, studies of intracellular pathogens are often conducted using in vitro cell culture systems, which unfortunately lack important features of polarized, intact intestinal epithelial cells. The nematode *C. elegans* provides a tractable system to study intracellular pathogens in vivo, where features of differentiated epithelial cells are easily visualized. In a recent paper, we used *C. elegans* as a host organism to study the exit strategy of *Nematocida parisii*, a naturally occurring intracellular pathogen in the microsporidia phylum. We showed that *N. parisii* remodels the *C. elegans* host cytoskeleton, and then exits host cells in an actin-dependent, non-lytic fashion. These findings illuminate key details about the transmission of microsporidia, which are poorly understood but ubiquitous pathogens. More generally, these findings have implications for exit strategies used by other intracellular pathogens that also infect epithelial cells.

Keywords: actin, intermediate filaments, terminal web, host-pathogen interactions, intracellular pathogen, host cell exit, intestinal infection, microsporidia, *C. elegans*

Submitted: 04/19/12

Accepted: 04/24/12

http://dx.doi.org/10.4161/worm.20501

*Correspondence to: Emily R. Troemel; Email: etroemel@ucsd.edu

Commentary to: Estes KA, Szumowski SC, Troemel ER. Non-lytic, actin-based exit of intracellular parasites from *C. elegans* intestinal cells. PLoS Pathog 2011; 7:e1002227; PMID:21949650; http://dx.doi.org/10.1371/journal.ppat.1002227

Introduction

By residing inside of host cells, intracellular pathogens have the advantages of protection from extracellular antimicrobials and access to host nutrients and energy stores. However, intracellular replication requires that pathogens eventually exit from their host cell in order to spread to new cells or to new hosts. While some intracellular pathogens such as *Toxoplasma gondii*, Leishmania species and *Plasmodium falciparum* exit by lysing host cells (**Fig. 1A**), other intracellular pathogens have evolved strategies that maintain host cell integrity during exit.[4] Understanding the mechanisms of host cell exit could aid in the development of treatments to prevent intracellular pathogen transmission. In a recent study, we showed that microsporidia, a phylum of pathogens closely related to fungi, exits the *C. elegans* gut epithelia in a non-lytic manner involving actin.[5]

Actin and pathogen egress. Many intracellular pathogens exploit host actin in order to exit.[6] For example, Listeria and Rickettsiae species both secrete actin-nucleation promoting factors that interact with host Arp2/3 actin polymerization machinery. Actin polymerization forms comet-like actin "tails" on the pathogens that are used for motility and jetting between and exiting from host cells. Shigella species exit host cells by activating formin-mediated actin polymerization to generate protrusions from the host cell, which are engulfed by neighboring cells to facilitate pathogen exit and spreading (**Fig. 1B**).[7] Another actin-dependent exit strategy is employed by Mycobacterium species and involves an actin-rich structure called an "ejectosome," which is a pore-like structure in the host membrane through which pathogens can exit the host cell (**Fig. 1C**).[1] In addition to the above-mentioned bacteria, the eukaryotic pathogen *C. neoformans* also uses actin to non-lytically exit from host cells. The exit

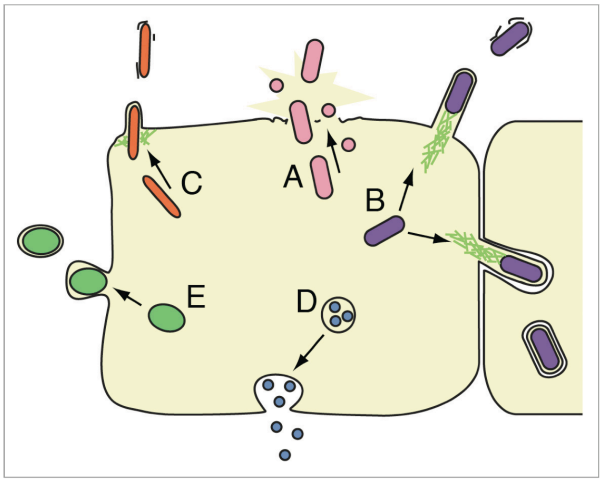

Figure 1. Exit strategies of intracellular pathogens. (**A**) Lytic exit from host cells through activation of "pyroptosis," secretion of membrane pore-forming toxins, or secretion of proteases. (e.g., *S. flexneri, Salmonella* spp, *L. pneumophila, L. monocytogenes, F. tularensis, Chlamydia* spp, *P. falciparum, Leishmania* spp, *T. gondii).* (**B**) Exit by actin "comet tails," which protrude into host membrane to induce engulfment by neighboring cells, sometimes resulting in a double membrane (used by *L. monocytogenes, S. flexneri, R. rickettsii, R. conorii,* Burkholderia, Pseudomallei*).* (**C**) Exit through an actin-rich, pore-like "ejectosome" that is inserted in the host membrane (used by *M. marinum*[1]). (**D**) Exit by exocytosis (used by *C. neoformans, C. albicans*[2]). (**E**) Exit by budding out of the host cell coated in host membrane, leaving the host cell intact (used by *Chlamydia* spp, *O. tsutsugamushi, P. berghei*[3]) (adapted with permission from Hybiske and Stephens, 2008[4]).

process used by *C. neoformans,* as well as *C. albicans* (another pathogenic yeast), appears similar to exocytosis, although the underlying mechanisms are poorly understood (**Fig. 1D**).[2,8,9] A summary of these five major pathogen exit mechanisms is illustrated in **Figure 1**. Based on the prevalence of actin-related exit strategies used by the diverse microbes shown in this figure, host actin appears to be an ideal resource exploited by pathogens to facilitate exit.[6]

The lysis or preservation of host membrane can have important implications for virulence of the exiting pathogen. In particular, a pathogen that lyses its host cell inflicts damage on its host, thus harming the host's ability to support future pathogen growth. In the case of organisms with non-renewing tissues, such as *C. elegans*, and especially with unicellular organisms, cell lysis can have a substantial impact on host survival. It has been hypothesized that over time intracellular pathogens evolve reduced virulence in order to maximize replication.[10,11] Thus, it would be expected that pathogens that have coevolved with their hosts would trend toward non-lytic exit strategies.

Microsporidia are natural pathogens of *C. elegans* and provide a convenient in vivo system for the study of intracellular pathogens. Most studies of intracellular pathogen exit have been conducted in tissue culture cells or in unicellular hosts that lack important features of in vivo metazoan tissue structure. As such, findings in tissue culture may differ from findings in vivo, as exemplified by a recent study of Listeria infection by Nikitas et al.[12] The authors performed microscopy of whole-tissue mounts to characterize Listeria intracellular trafficking through intestinal cells. Surprisingly, they found that in vivo trafficking differs substantially from the well-studied in vitro pathway mentioned above, in which Listeria escapes from the internalization vacuole and then induces actin tail polymerization to force its way into new host cells.[13-16] In vivo, the authors found that Listeria remains membrane-bound as it transits from the apical to the basolateral side of intestinal epithelial cells, and then exits via exocytosis at the basolateral side of cells to disseminate systematically.[12] Interestingly, this in vivo transcytosis pathway does not require the well-described Listeria factors identified by in vitro studies. These contrasting results from in vitro vs. in vivo studies highlight the importance of studying intestinal infections in vivo.

A key feature of metazoan intestinal epithelial cells is their apical-basolateral polarity, which is not necessarily maintained in in vitro studies.[17] The apical surface of these cells is decorated with actin-rich microvilli that protrude into the intestinal lumen where they can absorb nutrients. These microvilli are anchored into a cytoskeletal structure called the terminal web (**Fig. 2A**). Although the terminal web is a prominent feature that was noted long ago in electron micrograph (EM) images of vertebrate intestinal cells, little is known about how this structure is first assembled and then remodeled to allow for vesicle passage.[18-24] A major challenge in addressing these questions is the relative inaccessibility of this tissue in vertebrate systems. Fortunately, key features of intestinal cells are shared between humans and the nematode *C. elegans*, including actin-rich microvilli anchored into a terminal web made of actin and intermediate filaments (**Fig. 2A**). This conservation, together with the convenience and transparency of nematodes, make *C. elegans* an excellent in vivo model system to study the exit of intracellular pathogens from intestinal cells.

In 2008, we discovered the first intracellular pathogen of *C. elegans* through identification of a natural pathogen that infects the intestinal cells. We named this pathogen *N. parisii*, or "nematode killer from Paris," and found it defines a new genus and species of microsporidia.[25] Microsporidia comprise a large phylum of over 1,200 species of eukaryotic intracellular pathogens.[26-28] The phylogenetic placement of microsporidia is controversial, but their closest relatives are fungi. Microsporidia can infect a wide variety of animal hosts, commonly infecting the intestine. Fourteen species of microsporidia can infect humans and some can lead to lethal diarrhea in AIDS patients. Due to

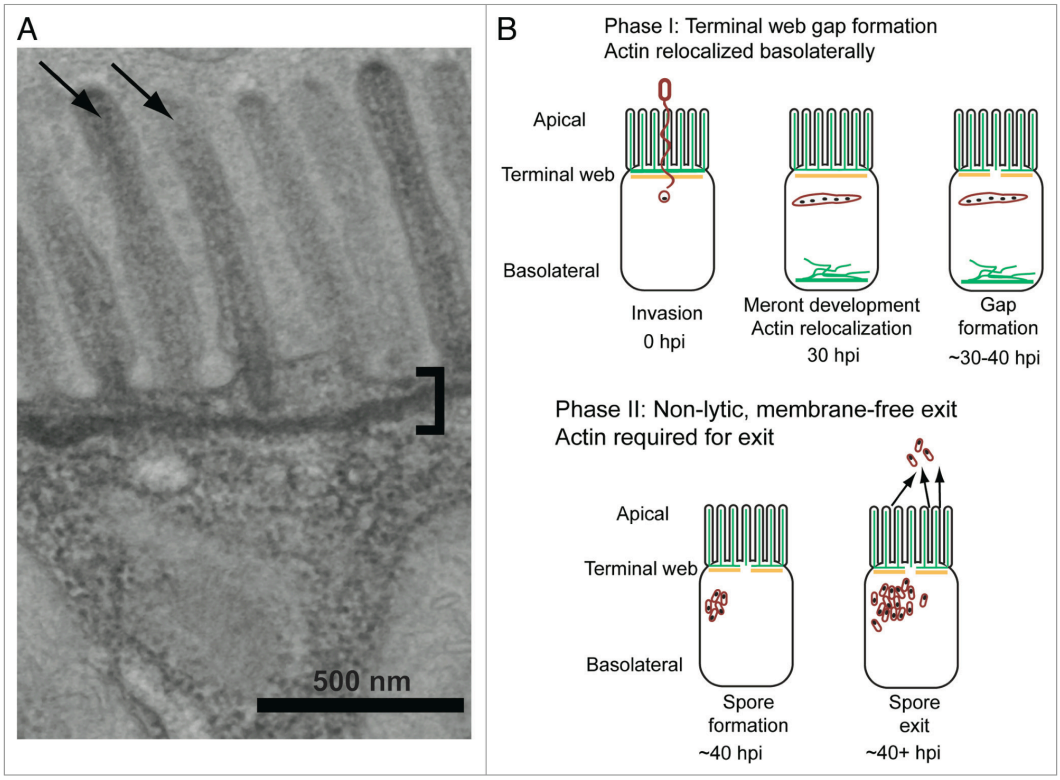

Figure 2. Intestinal cell morphology and microsporidia life cycle. (**A**) Electron micrograph of *C. elegans* intestinal epithelial cell. The microvilli brush border (arrows) lining the lumen is prominent on the apical surface of the cell. Microvilli are anchored to the cell with the terminal web (bracket), which is visible as a line below the microvilli. Both of these morphological features are conserved with human intestinal cells. (**B**) Phases of *N. parisii* exit strategy from *C. elegans* host intestinal cells. Green is ACT-5 and orange is IFB-2. Pathogen cells are depicted in red and nuclei depicted in black. During Phase I of infection, microsporidia spores fire their polar tubes, and inject their nucleus and sporoplasm into the host cell. This material develops into a multinucleated meront, and ACT-5 appears basolaterally, where it can form filament-like structures. During the final step of Phase I, gaps form in IFB-2 expression along the apical part of the cell. During Phase II, spores mature at approximately 40hpi and exit in a non-lytic, actin-dependent fashion from the host cell into the intestinal lumen.

the problems they cause in immunocompromised patients and the lack of treatments, microsporidia have been deemed priority pathogens by the US National Institutes of Health.[29] Microsporidia also cause significant agricultural problems in fisheries and have been implicated in colony collapse disorder in honeybees.[30-33] These obligate intracellular pathogens are challenging to study because they can only replicate inside of host cells.

Figure 2B illustrates the *N. parisii* life cycle within *C. elegans* intestinal cells, which is similar to the life cycle of microsporidia species that infect other hosts. Upon ingestion, microsporidia spores germinate and pierce the host cell membrane with a polar tube, through which the spore nucleus and sporoplasm are injected into the host cell. Once inside the cell, the pathogen produces multinucleated structures called meronts, which then replicate and redifferentiate into mature spores. In *C. elegans*, microsporidian spores then exit from the apical side of cells into the lumen, and are defecated out to transmit the infection to new hosts. *N. parisii* infection in *C. elegans* offers a unique system to obtain insights into these poorly understood pathogens. In addition, it provides the rare opportunity to leverage the powerful tools of the *C. elegans* model system on co-evolved host-pathogen interactions in polarized epithelial cells in vivo.

Microsporidia Infection Causes Reorganization of the Host Cytoskeletal Terminal Web

We had previously observed in EM images that the terminal web was restructured in *N. parisii*-infected animals, resulting in terminal web "gaps."[25] The *C. elegans* terminal web is comprised of an intestinal-specific actin isoform called ACT-5, and several intermediate filament proteins, including IFB-2. In uninfected animals these proteins are apically localized within

intestinal cells, with ACT-5 localized to both the terminal web and microvilli, and IFB-2 localized exclusively to the terminal web. By infecting a *C. elegans* strain expressing *YFP::ACT-5* and *IFB-2::CFP*, we were able to track IFB-2 localization in live animals to determine when the host terminal web is remodeled during *N. parisii* infection, and how this relates to ACT-5 localization. During the replicative, or "meront," phase of infection, we found that ACT-5 relocalizes to the basolateral side of the cell, where it is not normally found in uninfected animals. After this relocalization, we observed gaps in *IFB-2::CFP* expression, which appears similar to the restructuring of the terminal web observed by EM (**Fig. 2B**). Interestingly, we found that *IFB-2::CFP* gap formation precedes spore exit and that all contagious animals have *IFB-2::CFP* gaps. Furthermore, after the initial bout of gap formation, the number of gaps does not increase over the course of infection. These results imply that terminal web gap formation is part of an orchestrated exit strategy, rather than damage that occurs as the spores exit from the apical side of the cell.

Because terminal web gaps form after ACT-5 relocalization to the basolateral side of cells, we hypothesized that depletion of ACT-5 from the apical side might trigger gap formation. To test this idea, we reduced ACT-5 levels with RNA interference and found that this knock-down was sufficient to induce gaps in *IFB-2::CFP* expression in the absence of infection. This result suggests that depletion of ACT-5 at the apical side promotes terminal web weakening in preparation for microsporidia exit. Terminal web weakening occurs immediately prior to spore formation, which would be the ideal time to remove a potential barrier to exit. We have termed this actin-mediated preparation for spore exit "Phase I" to provide contrast to a different role for actin later in infection that is part of "Phase II," described below (**Fig. 2B**). Such seemingly careful preparation for spore exit implies the existence of precisely timed molecular interactions between *N. parisii* and *C. elegans*, as might be expected in a host/pathogen pair that has co-evolved. Indeed, Nematocida strains have been found infecting wild-caught Caenorhabditis nematodes in many parts of the world, consistent with this possibility of co-evolution (Fèlix MA, unpublished data).[25]

Thousands of Microsporidia Spores Exit Host Cells in a Process that Requires ACT-5

If ACT-5 relocalization induces terminal web gap formation to facilitate exit, we would expect that depleting ACT-5 in infected animals would increase gap number and increase pathogen exit. To test this hypothesis, we developed an assay to measure the number of spores exiting from the intestinal cells of infected animals. We found that a single infected animal could produce thousands of spores in one hour, and this production rate could continue for dozens of hours. This finding is especially striking considering that *C. elegans* has a total of only 20 intestinal cells! With this assay, we compared wild-type animals to those defective for *act-5*, either caused by treatment with RNAi or by being heterozygous for an *act-5* deletion allele (*act-5* homozygous mutants are dead). Unexpectedly, we found that a reduction of ACT-5 resulted in a dose-dependent reduction in spore excretion. This observation indicated a complex role for *act-5* and led to our two-phase pathogen exit model. In Phase I of this model, actin inhibits exit by maintaining terminal web integrity, and in Phase II, actin promotes exit by an unknown mechanism (**Fig. 2B**). A further test of Phase I in this model would be to determine whether IFB-2 gaps are required for exit, but we have not yet identified a method to block gap formation. In any case, our results indicate that actin plays a multi-faceted role in the microsporidian exit strategy, with many outstanding questions to address (see below).

N. parisii Exits into the Lumen Free of Host Plasma Membrane, and Without Causing Lysis

Our results indicated that *C. elegans* intestinal cells produce large numbers of *N. parisii* spores while animals are still alive, suggesting that host membranes are left intact. To investigate membrane topology during *N. parisii* exit, we visualized host apical plasma membrane in a strain expressing a *PGP-1::GFP* membrane marker, which localizes to the apical side of intestinal cells. We found that spores exited into the lumen free of *PGP-1::GFP*, indicating that microsporidia do not take host plasma membrane with them while exiting the cell. Furthermore, we tested for cell lysis upon spore exit by feeding contagious animals propidium iodide, a dye that cannot diffuse freely into intact cells. Using this assay, we found that host cell integrity was maintained and thus *N. parisii* exit is non-lytic, as perhaps would be expected for an obligate intracellular pathogen of an animal with non-renewing cells.

Outlook

Our findings indicate that *C. elegans* host cell restructuring is precisely coordinated with *N. parisii* pathogen development so that physical barriers are removed at the proper time to enable non-lytic exit. These findings highlight key events of the infection cycle that would not be observed in less natural experimental systems. Similar themes emerged in studies of the bacterial pathogen Listeria as mentioned above, as well as studies of the eukaryotic pathogen *Toxoplasma gondii*. In human fibroblasts, it was shown that *T. gondii* exits host cells using a different mechanism when exit occurs naturally than when exit is artificially stimulated by permeabilization of the host cell, which is a common experimental technique in the field.[34] By studying *N. parisii* infection in its natural host, which is a powerful model organism, we expect to uncover meaningful host-pathogen interactions for a group of obligate intracellular pathogens that have been historically very difficult to study.

In future studies, we aim to determine how *N. parisii* spores exit without lysing the host cell. Orchestrating a non-lytic exit with membrane-free spores released into the lumen likely requires that some membrane surrounds spores prior to exit (**Fig. 1**). However, EM images show that *N. parisii* appears to be in direct contact with the cytoplasm during its early replicative stage.[25] Therefore, it is possible that *N. parisii* steals intracellular host membrane as it forms spores in order to

enter host trafficking pathways. These membrane-coated spores could then fuse with the plasma membrane to exit the cell free of membrane. It will be interesting to determine which host proteins regulate this process and the level at which *N. parisii* directs this regulation.

In future studies, it will also be interesting to investigate whether terminal web remodeling is a conserved exit strategy used by other species of microsporidia, such as the human-infecting species *Encephalitozoon intestinalis*, *Encephalitozoon cuniculi* and *Enterocytozoon bieneusi*. And beyond the microsporidia phylum, it seems certain that other intracellular pathogens must cross terminal web barriers to exit. The terminal web is found not only in intestinal cells but also in many differentiated epithelial cells, such as those found in lung and urogenital epithelia, which are also subject to intracellular infection by a variety of pathogens. Deciphering how intracellular pathogens remodel host tissues in vivo to make a discreet exit will lead to a better understanding of pathogen transmission.

Disclosure of Potential Conflicts of Interest

No potential conflicts of interest were disclosed.

Acknowledgments

We would like to thank Andrew Chisholm, Robert Luallen, and Kevin Hybiske for reading earlier drafts and providing helpful suggestions. This work was supported by NIH predoctoral training grant T32 GM008666 to S.C.S. and NIAID R01 AI087528, the Searle Scholars Program, Ray Thomas Edwards Foundation, David and Lucille Packard Foundation fellowship to E.R.T.

References

1. Hagedorn M, Rohde KH, Russell DG, Soldati T. Infection by tubercular mycobacteria is spread by nonlytic ejection from their amoeba hosts. Science 2009; 323:1729-33; PMID:19325115; http://dx.doi.org/10.1126/science.1169381.
2. Bain JM, Lewis LE, Okai B, Quinn J, Gow NA, Erwig LP. Non-lytic expulsion/exocytosis of Candida albicans from macrophages. Fungal Genet Biol 2012; In press; PMID:22326419; http://dx.doi.org/10.1016/j.fgb.2012.01.008.
3. Sturm A, Amino R, van de Sand C, Regen T, Retzlaff S, Rennenberg A, et al. Manipulation of host hepatocytes by the malaria parasite for delivery into liver sinusoids. Science 2006; 313:1287-90; PMID:16888102; http://dx.doi.org/10.1126/science.1129720.
4. Hybiske K, Stephens RS. Exit strategies of intracellular pathogens. Nat Rev Microbiol 2008; 6:99-110; PMID:18197167; http://dx.doi.org/10.1038/nrmicro1821.
5. Estes KA, Szumowski SC, Troemel ER. Non-lytic, actin-based exit of intracellular parasites from C. elegans intestinal cells. PLoS Pathog 2011; 7:e1002227; PMID:21949650; http://dx.doi.org/10.1371/journal.ppat.1002227.
6. Stevens JM, Galyov EE, Stevens MP. Actin-dependent movement of bacterial pathogens. Nat Rev Microbiol 2006; 4:91-101; PMID:16415925; http://dx.doi.org/10.1038/nrmicro1320.
7. Heindl JE, Saran I, Yi CR, Lesser CF, Goldberg MB. Requirement for formin-induced actin polymerization during spread of Shigella flexneri. Infect Immun 2010; 78:193-203; PMID:19841078; http://dx.doi.org/10.1128/IAI.00252-09.
8. Chrisman CJ, Alvarez M, Casadevall A. Phagocytosis of Cryptococcus neoformans by, and nonlytic exocytosis from, Acanthamoeba castellanii. Appl Environ Microbiol 2010; 76:6056-62; PMID:20675457; http://dx.doi.org/10.1128/AEM.00812-10.
9. Johnston SA, May RC. The human fungal pathogen Cryptococcus neoformans escapes macrophages by a phagosome emptying mechanism that is inhibited by Arp2/3 complex-mediated actin polymerisation. PLoS Pathog 2010; 6:e1001041; PMID:20714349; http://dx.doi.org/10.1371/journal.ppat.1001041.
10. Anderson RM, May RM. Coevolution of hosts and parasites. Parasitology 1982; 85:411-26; PMID:6755367; http://dx.doi.org/10.1017/S0031182000055360.
11. Frank SA. Models of parasite virulence. Q Rev Biol 1996; 71:37-78; PMID:8919665; http://dx.doi.org/10.1086/419267.
12. Nikitas G, Deschamps C, Disson O, Niault T, Cossart P, Lecuit M. Transcytosis of Listeria monocytogenes across the intestinal barrier upon specific targeting of goblet cell accessible E-cadherin. J Exp Med 2011; 208:2263-77; PMID:21967767; http://dx.doi.org/10.1084/jem.20110560.
13. Tilney LG, DeRosier DJ, Tilney MS. How Listeria exploits host cell actin to form its own cytoskeleton. I. Formation of a tail and how that tail might be involved in movement. J Cell Biol 1992; 118:71-81; PMID:1618908; http://dx.doi.org/10.1083/jcb.118.1.71.
14. Myers JT, Tsang AW, Swanson JA. Localized reactive oxygen and nitrogen intermediates inhibit escape of Listeria monocytogenes from vacuoles in activated macrophages. J Immunol 2003; 171:5447-53; PMID:14607950.
15. Kocks C, Hellio R, Gounon P, Ohayon H, Cossart P. Polarized distribution of Listeria monocytogenes surface protein ActA at the site of directional actin assembly. J Cell Sci 1993; 105:699-710; PMID:8408297.
16. Henry R, Shaughnessy L, Loessner MJ, Alberti-Segui C, Higgins DE, Swanson JA. Cytolysin-dependent delay of vacuole maturation in macrophages infected with Listeria monocytogenes. Cell Microbiol 2006; 8:107-19; PMID:16367870; http://dx.doi.org/10.1111/j.1462-5822.2005.00604.x.
17. Pukkila-Worley R, Ausubel FM. Immune defense mechanisms in the Caenorhabditis elegans intestinal epithelium. Curr Opin Immunol 2012; 24:3-9; PMID:22236697; http://dx.doi.org/10.1016/j.coi.2011.10.004.
18. Bossinger O, Fukushige T, Claeys M, Borgonie G, McGhee JD. The apical disposition of the Caenorhabditis elegans intestinal terminal web is maintained by LET-413. Dev Biol 2004; 268:448-56; PMID:15063180; http://dx.doi.org/10.1016/j.ydbio.2004.01.003.
19. Fath KR, Burgess DR. Microvillus assembly. Not actin alone. Curr Biol 1995; 5:591-3; PMID:7552163; http://dx.doi.org/10.1016/S0960-9822(95)00117-5.
20. Hirokawa N, Tilney LG, Fujiwara K, Heuser JE. Organization of actin, myosin, and intermediate filaments in the brush border of intestinal epithelial cells. J Cell Biol 1982; 94:425-43; PMID:7202010; http://dx.doi.org/10.1083/jcb.94.2.425.
21. Ku NO, Zhou X, Toivola DM, Omary MB. The cytoskeleton of digestive epithelia in health and disease. Am J Physiol 1999; 277:G1108-37; PMID:10600809.
22. Mooseker MS. Organization, chemistry, and assembly of the cytoskeletal apparatus of the intestinal brush border. Annu Rev Cell Biol 1985; 1:209-41; PMID:3916317; http://dx.doi.org/10.1146/annurev.cb.01.110185.001233.
23. Takemura R, Masaki T, Hirokawa N. Developmental organization of the intestinal brush-border cytoskeleton. Cell Motil Cytoskeleton 1988; 9:299-311; PMID:3292061; http://dx.doi.org/10.1002/cm.970090403.
24. Thomas GH. Spectrin: the ghost in the machine. Bioessays 2001; 23:152-60; PMID:11169588; http://dx.doi.org/10.1002/1521-1878(200102)23:2<152::AID-BIES1022>3.0.CO;2-1.
25. Troemel ER, Félix MA, Whiteman NK, Barrière A, Ausubel FM. Microsporidia are natural intracellular parasites of the nematode Caenorhabditis elegans. PLoS Biol 2008; 6:2736-52; PMID:19071962; http://dx.doi.org/10.1371/journal.pbio.0060309.
26. Keeling PJ, Fast NM. Microsporidia: biology and evolution of highly reduced intracellular parasites. Annu Rev Microbiol 2002; 56:93-116; PMID:12142484; http://dx.doi.org/10.1146/annurev.micro.56.012302.160854.
27. Texier C, Vidau C, Viguès B, El Alaoui H, Delbac F. Microsporidia: a model for minimal parasite-host interactions. Curr Opin Microbiol 2010; 13:443-9; PMID:20542726; http://dx.doi.org/10.1016/j.mib.2010.05.005.
28. Williams BA. Unique physiology of host-parasite interactions in microsporidia infections. Cell Microbiol 2009; 11:1551-60; PMID:19673893; http://dx.doi.org/10.1111/j.1462-5822.2009.01362.x.
29. Didier ES, Weiss LM. Microsporidiosis: current status. Curr Opin Infect Dis 2006; 19:485-92; PMID:16940873; http://dx.doi.org/10.1097/01.qco.0000244055.46382.23.
30. Bromenshenk JJ, Henderson CB, Wick CH, Stanford MF, Zulich AW, Jabbour RE, et al. Iridovirus and microsporidian linked to honey bee colony decline. PLoS One 2010; 5:e13181; PMID:20949138; http://dx.doi.org/10.1371/journal.pone.0013181.
31. Higes M, Martín-Hernández R, Botías C, Bailón EG, González-Porto AV, Barrios L, et al. How natural infection by Nosema ceranae causes honeybee colony collapse. Environ Microbiol 2008; 10:2659-69; PMID:18647336; http://dx.doi.org/10.1111/j.1462-2920.2008.01687.x.
32. Shaw RWKM. Fish Microsporidia. In: Wittner M WL, ed. The Microsporidia and Microsporidiosis: ASM, 1999.
33. Troemel ER. New models of microsporidiosis: infections in Zebrafish, C. elegans, and honey bee. PLoS Pathog 2011; 7:e1001243; PMID:21379567; http://dx.doi.org/10.1371/journal.ppat.1001243.
34. Lavine MD, Arrizabalaga G. Exit from host cells by the pathogenic parasite Toxoplasma gondii does not require motility. Eukaryot Cell 2008; 7:131-40; PMID:17993573; http://dx.doi.org/10.1128/EC.00301-07.

2.1 Additional Acknowledgements

Chapter 2, in full, is reprinted from Worm, 1, Szumowski, S.; Estes, K.; Troemel, E., Preparing a discreet escape: Microsporidia reorganize host cytoskeleton prior to non-lytic exit from *C. elegans* intestinal cells, 207-211, (2012), with permission from Landes Bioscience. The dissertation author was the primary investigator and author of this material.

3 Non-lytic, actin-based exit of intracellular parasites from *C. elegans* intestinal cells

OPEN ACCESS Freely available online PLoS PATHOGENS

Non-Lytic, Actin-Based Exit of Intracellular Parasites from *C. elegans* Intestinal Cells

Kathleen A. Estes, Suzannah C. Szumowski, Emily R. Troemel*

Division of Biological Sciences, University of California, San Diego, La Jolla, California, United States of America

Abstract

The intestine is a common site for invasion by intracellular pathogens, but little is known about how pathogens restructure and exit intestinal cells *in vivo*. The natural microsporidian parasite *N. parisii* invades intestinal cells of the nematode *C. elegans*, progresses through its life cycle, and then exits cells in a transmissible spore form. Here we show that *N. parisii* causes rearrangements of host actin inside intestinal cells as part of a novel parasite exit strategy. First, we show that *N. parisii* infection causes ectopic localization of the normally apical-restricted actin to the basolateral side of intestinal cells, where it often forms network-like structures. Soon after this actin relocalization, we find that gaps appear in the terminal web, a conserved cytoskeletal structure that could present a barrier to exit. Reducing actin expression creates terminal web gaps in the absence of infection, suggesting that infection-induced actin relocalization triggers gap formation. We show that terminal web gaps form at a distinct stage of infection, precisely timed to precede spore exit, and that all contagious animals exhibit gaps. Interestingly, we find that while perturbations in actin can create these gaps, actin is not required for infection progression or spore formation, but actin is required for spore exit. Finally, we show that despite large numbers of spores exiting intestinal cells, this exit does not cause cell lysis. These results provide insight into parasite manipulation of the host cytoskeleton and non-lytic escape from intestinal cells *in vivo*.

Citation: Estes KA, Szumowski SC, Troemel ER (2011) Non-Lytic, Actin-Based Exit of Intracellular Parasites from *C. elegans* Intestinal Cells. PLoS Pathog 7(9): e1002227. doi:10.1371/journal.ppat.1002227

Editor: Robin Charles May, University of Birmingham, United Kingdom

Received March 27, 2011; **Accepted** July 6, 2011; **Published** September 15, 2011

Funding: This work was supported by NIH Training in Immunology Grant 5T32AI060536 to KAE; NIH Genetics Training Program Grant T32GM008666 to SCS, NIH grant AI087528 (http://www.niaid.nih.gov), funds from the Searle Scholars Program (http://www.searlescholars.net/), Packard Foundation (http://www.packard.org/), Ray Thomas Edwards Foundation (http://www.edwardsfoundation.org/) and a Center for AIDS Research Developmental Grant (http://cfar.ucsd.edu/) to ERT. The funders had no role in study design, data collection and analysis, decision to publish, or preparation of the manuscript.

Competing Interests: The authors have declared that no competing interests exist.

* E-mail: etroemel@ucsd.edu

Introduction

Intracellular pathogens have a life cycle that includes three major steps: invasion of the host cell, replication, and exit out of the host cell. While the question of how pathogens invade cells has been intensively studied, much less is known about how pathogens exit cells, although this process appears to be highly regulated [1]. Even when pathogen exit causes lysis of host cells, this lysis is often due not simply to mechanical stress, but is part of a regulated process controlled by the pathogen. For example, the intracellular bacterium *Chlamydia* uses a cysteine protease to lyse host cells at the proper time as a mechanism of escape [2]. In addition to lytic escape, there are also less destructive modes of pathogen exit. One example of non-lytic pathogen exit comes from the Gram-positive bacterium *Listeria*, which polymerizes host actin to force its way into neighboring cells, which then engulf the bacterium to allow cell-to-cell spread [3]. Another example of non-lytic pathogen exit involving actin is used by *Mycobacterium* [4,5]. In contrast to *Listeria*, *Mycobacterium* appears to break through the host plasma membrane as it is exiting, and the membrane reseals behind the pathogen such that the host cell is not lysed. Acquiring a better understanding of the mechanisms of pathogen exit *in vivo* could lead to better treatments in a variety of settings, since the process of exit is critical for the propagation and spread of intracellular pathogens of all types.

Many intracellular pathogens invade their host and progress through infection in the intestine. However, most studies of pathogen exit have been performed in tissue culture cells or single-celled hosts, such as the studies described above. Unfortunately, these model hosts lack the connectivity, differentiated structures, and polarity of intact intestinal cells. The *Caenorhabditis elegans* intestinal tract provides an excellent system to study intestinal pathogens as it is composed of 20 epithelial cells that share many morphological properties with human intestinal epithelial cells [6]. In both humans and worms, the intestine contains polarized epithelial cells decorated with apical, finger-like microvilli anchored into a cytoskeletal structure called the terminal web, which is composed of actin and intermediate filaments. Because *C. elegans* intestinal cells share these structural similarities with human intestinal epithelial cells and because nematodes are transparent, *C. elegans* provides a very useful whole-animal model for study of host/pathogen interactions in intestinal epithelial cells [7,8].

Recently, we described the first natural intracellular pathogen of *C. elegans* and found that it defines a new species of microsporidia [9,10]. Microsporidia are obligate intracellular parasites that can infect virtually all animal phyla, as well as a few protists [11,12,13]. These parasites comprise a phylum that is either part of the fungal kingdom or is a sister group to the fungi [14,15,16,17]. The Microsporidia phylum contains over 1200 species, 14 of which can cause infection in humans. These infections most commonly afflict AIDS patients and other immunocompromised patients where they can cause persistent and lethal diarrhea [18]. Because so little is known about these microbes and few treatments are available,

Author Summary

The intestine is a common site for invasion by pathogens, but little is known about how pathogens exit out of live intestinal cells in order to spread and propagate. One group of parasites that often invades the intestine is the microsporidia, which comprise a phylum of over 1200 fungal-like species that can cause disease in humans, as well as in agriculturally significant organisms such as fish, silkworm and honey bee. Here, we investigated a natural microsporidian infection in live intestinal cells of the roundworm *C. elegans*. We discovered a novel exit strategy used by microsporidia to restructure the cytoskeleton of intestinal cells, involving relocalization of actin and reorganization of a structure called the terminal web, which may be a barrier to exit. In addition, we found that despite large numbers of parasites exiting out of intestinal cells, this process does not cause cells to burst. Our findings indicate that microsporidia, which are completely dependent on their hosts for replication, have evolved a regulated and non-damaging mechanism of exit that shares similarities with strategies used by evolutionarily distant bacterial pathogens. This study provides new insights into the methods by which pathogens restructure live intestinal cells to facilitate their spread and propagation.

they have been deemed priority pathogens by the U.S. National Institutes of Health. Microsporidia are also considered microbial contaminants of concern by the U.S. Environmental Protection Agency and can plague agriculturally relevant organisms. For example, microsporidia have been responsible for the collapse of fisheries and have also been implicated in honey bee colony collapse disorder [19,20,21,22]. We named the *C. elegans*-infecting microsporidia species *Nematocida parisii*, or nematode-killer from Paris, since it was first isolated from a French wild-caught nematode and it eventually kills its host.

The microsporidia are a diverse group of pathogens that can have very complex life cycles. On a general level, the *N. parisii* life cycle appears similar to that of other microsporidia (Figure 1A) [9,13]. *N. parisii* infects the *C. elegans* intestine in its transmissible spore form and is transmitted horizontally, likely via a fecal-oral route. After ingestion, microsporidia invade host cells using a specialized infection apparatus called a polar tube, which is coiled inside of the spore and then "fires" to pierce the host cell. The polar tube can inject the nuclei and sporoplasm of the parasite directly into host cells, thereby avoiding extracellular defenses of the host. This injected parasite material develops intracellularly in a replicating cellular structure called a meront. These meronts go through several stages of development and eventually re-differentiate to generate mature spores that somehow must exit the cell and continue the parasite life cycle. *N. parisii* ultimately kills

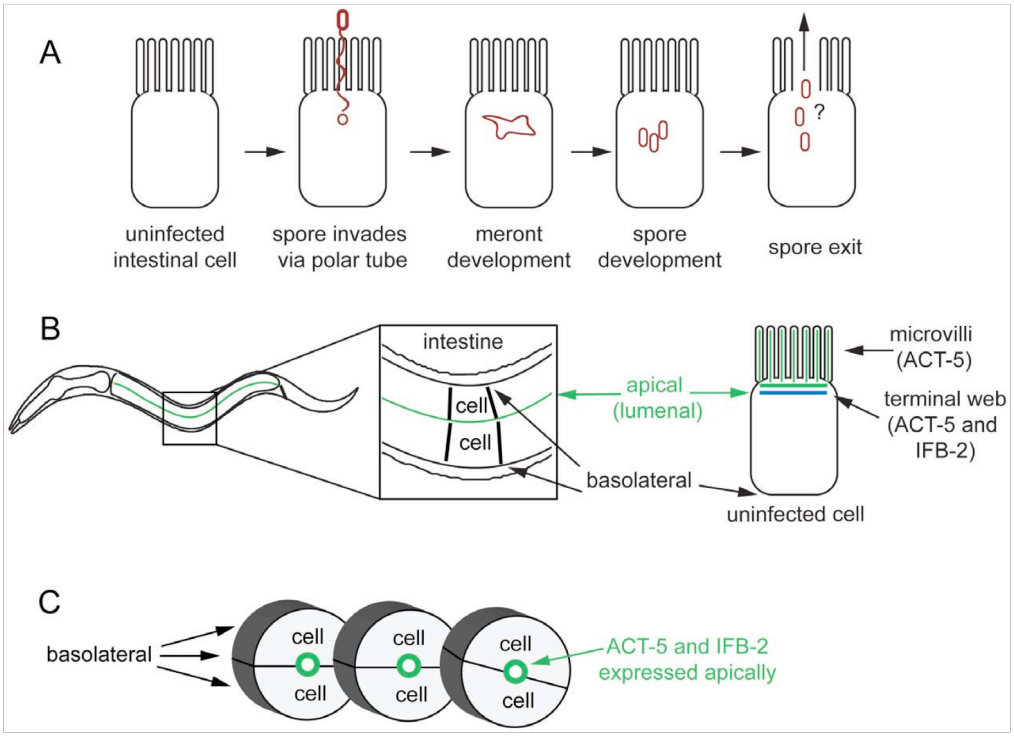

Figure 1. Microsporidian lifecycle and anatomy of *C. elegans* intestinal cells. (A) Generalized microsporidian life cycle inside a host cell. (B) Two dimensional (2D) view of the *C. elegans* intestine. The intestine is formed of polarized epithelial cells, mostly in rings of 2 cells each. On the apical (lumenal) side of these cells are actin-rich microvilli that are anchored into the terminal web, which is composed of actin (ACT-5) and intermediate filaments (IFB-2). (C) Three dimensional (3D) view of three rings of the *C. elegans* intestine (int2, 3, 4), two cells in each ring (other rings not shown for simplicity).
doi:10.1371/journal.ppat.1002227.g001

its host, but *C. elegans* can sustain a large spore burden before death. Indeed, live animals can be contagious to their neighbors, indicating that there is a mechanism of exit that does not cause severe damage to the host. Previously, we had observed gaps in the intermediate filaments of the terminal web in infected animals and hypothesized that they may be part of a regulated exit strategy of *N. parisii* [9]. However, we did not know what initiated these gaps, nor how they related to pathogen development and exit.

Here we show that *N. parisii* infection causes dramatic rearrangement of intestinal actin that is part of a novel two-phase, non-lytic exit strategy. The first phase involves restructuring of the terminal web, which is a barrier that pathogens must cross to exit cells. During this phase the subcellular localization of actin is altered, with the apically-restricted actin appearing ectopically on the basolateral side of host cells and forming networks. Subsequently, gaps appear in the terminal web, as assessed by IFB-2, an intermediate filament component of the terminal web. We hypothesize that actin redistribution away from the apical membrane may trigger these gaps in the terminal web, since lowering actin levels causes terminal web gaps in the absence of infection. Soon after the appearance of gaps, the parasite enters the second phase of the exit strategy. During this phase *N. parisii* spores are able to exit the cell. Interestingly, we find that host actin promotes spore exit and that decreasing the levels of actin impairs spore exit. Our analyses of cell integrity indicate that despite very large numbers of spores exiting *C. elegans* intestinal cells, these cells do not lyse. We propose that a novel, two-phase, non-lytic exit strategy allows *N. parisii* to escape from host intestinal cells while minimizing damage to its host, thus increasing parasite transmission.

Results

C. elegans Actin Ectopically Relocalizes in Intestinal Cells during *N. parisii* Infection

N. parisii infection proceeds through distinct stages in *C. elegans* intestinal cells, starting with the meront stage when the parasite is actively replicating (Figure 1A). *N. parisii* meronts appear to develop in direct contact with the host cytoplasm, essentially creating "parasite organelles", which eventually develop into mature spores [9]. Both meronts and spores form inside *C. elegans* intestinal cells, which are polarized epithelial cells that are found in rings of two to four cells that form a tube [6]. Like mammalian intestinal cells, these cells are decorated on the apical (lumenal) side with microvilli that are anchored into a cytoskeletal structure called the terminal web. The *C. elegans* terminal web contains a specialized actin isoform called ACT-5 and an intermediate filament component called IFB-2 (Figure 1B, C). ACT-5 is restricted mostly to microvilli-containing cells and is localized to both the microvilli and the terminal web [23], whereas IFB-2 is restricted to the terminal web [24,25]. To examine how *N. parisii* infection modifies the intestinal cytoskeleton, we generated a strain that expresses *YFP::ACT-5* as well as *IFB-2::CFP* in the intestine to track both of these cytoskeletal components simultaneously. In uninfected animals, we found that *YFP::ACT-5* colocalized with *IFB-2::CFP* at the apical side of intestinal cells (Figure 2A), consistent with previous reports [24,25].

We next imaged these cytoskeletal components during infection with *N. parisii*. Because *N. parisii* cannot be propagated outside of host cells, we prepare infectious spores by mechanically disrupting infected animals and purifying the spores away from other material. By adding a preparation of these spores onto plates regularly used to maintain *C. elegans*, the animals become infected by simply ingesting the spores. Once ingested, the spores then presumably fire their polar tubes, injecting *N. parisii* sporoplasm and nuclei into the *C. elegans* intestinal cells. We investigated cytoskeletal protein localization as *N. parisii* infection progressed and found that infection with *N. parisii* caused dramatic changes in ACT-5 localization without concomitant changes in IFB-2. The first relocalization of ACT-5 occurred during *N. parisii* meront development, which is the first stage of parasite development. At this point, we found that ACT-5 localization no longer remained restricted to the apical side of intestinal cells, but appeared ectopically on the basolateral side of cells (Figure 2B). Coinciding with this ectopic basolateral localization that appeared as an unbranched line, we also observed more complex networks of ACT-5 expression (Figure 2C). These networks exhibited branches that varied in number and length, and also appeared basolaterally. The exact molecular nature of these structures is unknown, so we refer to them generally as "actin networks". They may be part of the same basolateral relocalization phenomenon shown in Figure 2B, but are more easily visualized in the plane of focus shown in Figure 2D because of the orientation of the animal on the slide. In both cases, actin still remained apically localized, although often at lower levels. Videos S1 and S2 show a Z-series of *YFP::ACT-5* localization in the intestine to provide a three-dimensional view of this actin relocalization phenomenon. In general, we did not observe IFB-2 relocalizing with ACT-5 (Figure 2B and 2C), indicating that *N. parisii* infection directs a specific relocalization of actin.

To determine whether these ectopic patterns of ACT-5 localization were general responses to pathogen infection or were specific to *N. parisii* infection, we analyzed *YFP::ACT-5* localization in animals infected with other intestinal pathogens. The Gram-negative bacterial pathogens *Pseudomonas aeruginosa* and *Salmonella enterica* also cause lethal intestinal infections in *C. elegans* [26,27,28,29]. We did not observe ectopic actin basolateral localization or networks in animals infected with *P. aeruginosa* (n = 55 animals), or *S. enterica* (n = 154 animals), indicating that the previously described localization patterns are somewhat specific to infection by the natural intracellular parasite *N. parisii*. We also examined a larger number of uninfected animals and saw only one out of 200 animals that had a single ectopic actin structure without obvious branching, further supporting our finding that this dramatic actin relocalization is specific to *N. parisii* infection.

Actin Relocalization Precedes Restructuring of Intermediate Filaments in the Terminal Web

To further characterize this actin relocalization in infected animals, we examined the kinetics of ACT-5 ectopic localization with respect to changes in IFB-2 and to progression of *N. parisii* development. We infected a synchronized population of *YFP::ACT-5;IFB-2::CFP* animals and tracked both *N. parisii* parasite development and changes in these cytoskeletal markers in a population over time (Figure 3). The stages of parasite development are shown in Figure 3A–D. We subdivided the meront stage into "early meront" (Figure 3B), where there was only a small area of gut granule clearing in the intestine, and "late meront" (Figure 3C), where there was more extensive clearing throughout the intestine. Following meront development, spores become visible (Figure 3D). Early meronts appeared by 16 hours post-inoculation (hpi), late meronts appeared by 30 hpi and spores appeared by 40 hpi (Figure 3E). The first obvious change in the cytoskeleton was the ectopic localization of *YFP::ACT-5* (Figure 3E), appearing as a line on the basolateral side of intestinal cells (as shown in Figure 2B). This pattern was observed in all animals of a population during the late meront stage, at 30 hpi. In addition to this linear basolateral relocalization, there was also

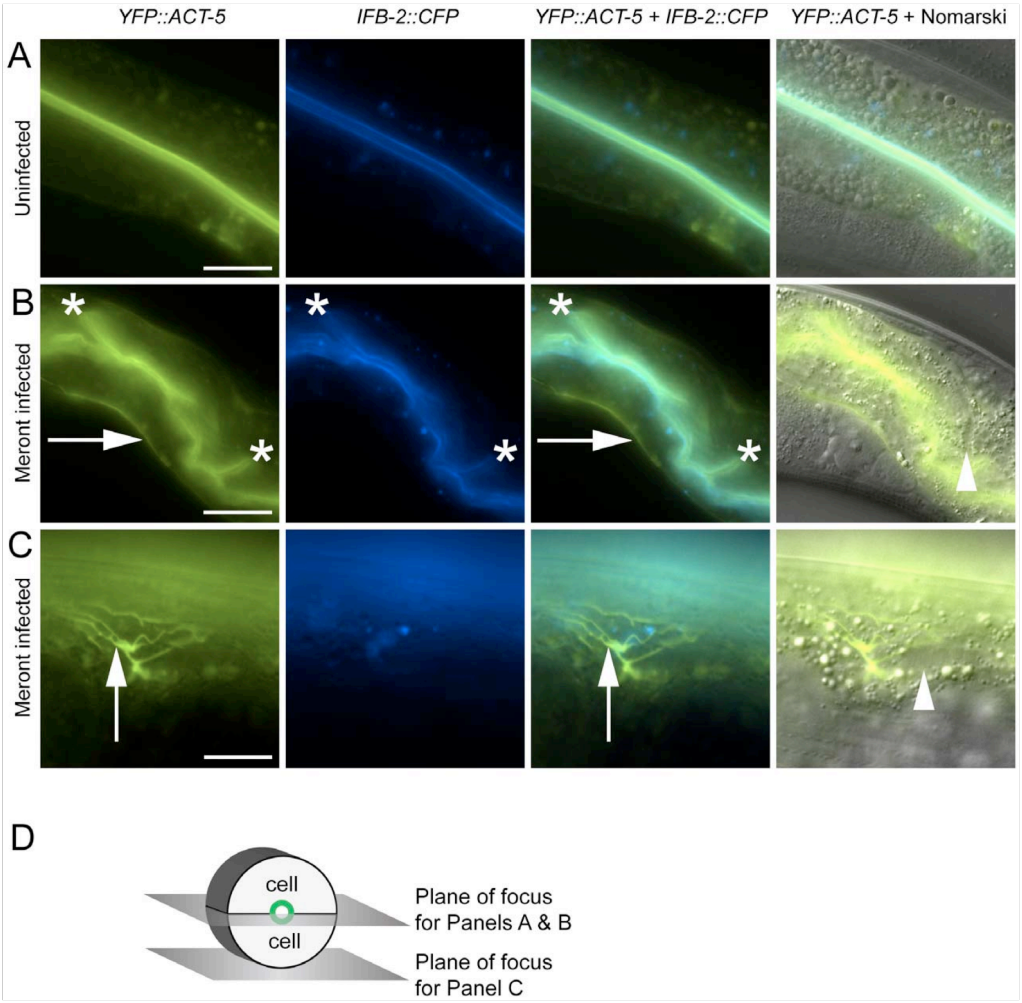

Figure 2. Host intestinal actin relocalizes basolaterally during *N. parisii* meront development. (A) Uninfected animals have apical colocalization of *YFP::ACT-5* and *IFB-2::CFP*. (B) Meront-infected animals exhibit ectopic basolateral localization of *YFP::ACT-5* (indicated by rightward arrows), without concomitant *IFB-2::CFP*. Infected animals often exhibit additional involutions of the lumen as indicated by asterisks, and later during infection exhibit gut distension (not shown). (C) Meront-infected animals exhibit ectopic *YFP::ACT-5* networks (upward-pointing arrows), again in the absence of *IFB-2::CFP*. Meronts are observed as clearings of gut granules, as indicated by arrowheads in Nomarski overlays of (B) and (C). Scale bar for (A, B) is 20 µm, for (C) is 10 µm. (D) Diagram of the 2D planes of focus for (A–C) shown in the context of 3D intestinal cell rings.
doi:10.1371/journal.ppat.1002227.g002

evidence of ACT-5 networks at this time (Figure 2C and Video S2), continuing at a low level until 40 hpi when all animals contained spores.

We also examined how this ectopic actin localization correlates with restructuring of the terminal web by assessing IFB-2 localization in these same animals. Previously, we had identified gaps in the terminal web of infected animals using transmission electron microscopy (TEM) and gaps in IFB-2 localization using anti-IFB-2 antibodies [9]. Here, we found very similar-appearing gaps in infected animals using CFP-tagged IFB-2 (*IFB-2::CFP)* (compare uninfected animals in Figure 3F to heavily infected animals in Figure 3G). We first observed these gaps in 13% of animals infected at 30 hpi, the late meront stage of infection (Figure 3E). At 40 hpi, when all animals were infected at the spore stage, gaps were found in the terminal web of 100% of animals (Figure 3E). Based on these observations, it appears that actin relocalization occurs before IFB-2 restructuring during infection. We saw a similar pattern of IFB-2 restructuring with respect to parasite development in single *IFB-2::CFP* transgenic animals, indicating that the presence of the *YFP::ACT-5* transgene did not affect *IFB-2::CFP* expression or localization (Figure S1).

The studies described above were performed with a population of animals, which is informative, but does not provide insight into the progression of symptoms within an individual animal. To determine whether the trends we observed in a population (e.g. ACT-5 is relocalized before IFB-2 localization is disrupted) were

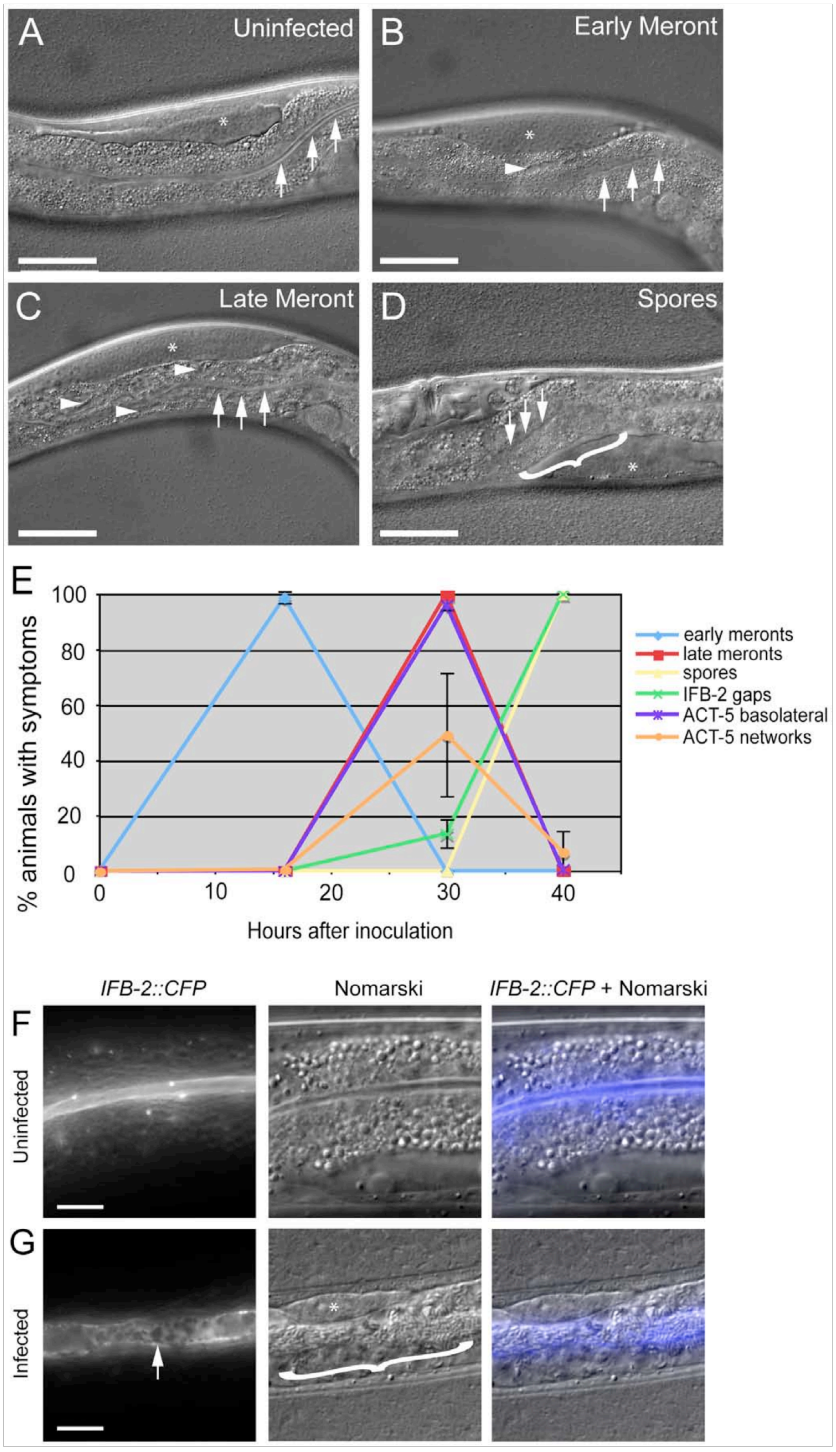
A
Uninfected
B
Early Meront
C
Late Meront
D
Spores
E
% animals with symptoms
100
80
60
40
20
0
0
10
20
30
40
Hours after inoculation
early meronts
late meronts
spores
IFB-2 gaps
ACT-5 basolateral
ACT-5 networks
IFB-2::CFP
Nomarski
IFB-2::CFP + Nomarski
F
Uninfected
G
Infected

Figure 3. Actin relocalization occurs before terminal web restructuring. (A–D) Stages of *N. parisii* development during infection of *C. elegans* intestine. Three arrows indicate the intestinal lumen and asterisk indicates the germ line. Scale bar is 50 μm. (A) Uninfected animal. (B) Animal infected at early meront stage. Small number of meronts indicated with arrowhead. (C) Animal infected at late meront stage. Meronts are found throughout the intestine; three examples are indicated with arrowheads. (D) Animal infected with spores. Bracket in D indicates region of intestine filled with spores. (E) Kinetics of cytoskeletal restructuring and parasite development in a population of animals infected at time = 0 hours. ACT-5 ectopic localization basolaterally and in branched networks occurs before the appearance of gaps in IFB-2 localization, which occur before and in conjunction with *N. parisii* spore formation. Data shown are the average of three independent experiments with 50 animals scored at each timepoint in each experiment (for a total of at least 150 animals scored at each timepoint). Error bars are SD. (see Table S1 for separate longitudinal infection studies of ACT-5 and IFB-2 in individual animals over time). (F) Uninfected animals exhibit uniform expression of *IFB-2::CFP* in the terminal web on the apical side of intestinal cells. (G) *N. parisii* infection causes gaps in *IFB-2::CFP* expression in the terminal web. Arrow indicates gaps in *IFB-2::CFP,* bracket indicates *N. parisii* spores. Scale bars in (F, G) are 10 μm.
doi:10.1371/journal.ppat.1002227.g003

also true in an individual, we performed longitudinal studies. Individual animals were mounted on slides at varying timepoints for viewing, and then recovered onto plates in between these timepoints to allow them to recover and to allow the infection to progress (Table S1). Consistent with the population studies, these experiments showed that *YFP::ACT-5* basolateral relocalization occurred first, followed by gaps in *IFB-2::CFP* localization.

Our previous studies with IFB-2 antibodies had suggested that terminal web gaps were specific to *N. parisii* infection – we did not observe them in animals infected with other pathogens that cause lethal intestinal infections, such as *P. aeruginosa* and *Staphylococcus aureus* [9]. Using the *IFB-2::CFP* transgene we also analyzed the terminal web in animals infected with the bacterial pathogen *S. enterica*, but did not find evidence that infection caused gap formation in the terminal web (n = 154 animals). To further confirm that terminal web gaps were a *N. parisii*-induced phenotype, we used the *IFB-2::CFP* transgenic animals and performed a thorough inspection of IFB-2 localization in uninfected animals (n = 200 animals). We found that only one animal exhibited a gap, and this was a single, isolated gap. For our analyses of *N. parisii* infected animals, we only scored animals as positive for gap formation if we observed multiple gaps. Thus, similar to the ACT-5 relocalization phenotype, the gaps observed in *IFB-2::CFP* localization appear to be specific to *N. parisii* infection.

Perturbations in Actin Can Cause Terminal Web Gaps in the Absence of Infection

Since relocalization of ACT-5 during *N. parisii* infection preceded the appearance of gaps in IFB-2 localization, we hypothesized that reduced levels of ACT-5 in the apical membrane might cause IFB-2 terminal web gaps. To test this hypothesis we reduced ACT-5 expression with feeding RNA interference (RNAi) against *act-5*. We observed a substantial reduction in *YFP::ACT-5* expression in *act-5* RNAi-treated animals compared to control-treated animals, confirming the efficacy of *act-5* RNAi (Figure 4A, B). Interestingly, when we analyzed the terminal web in *act-5* RNAi-treated animals we found gaps in *IFB-2::CFP* that appeared in the absence of infection (Figure 4B). Therefore, we speculate that infection-induced reduction of ACT-5 at the apical membrane may be a triggering event that results in the disruption of the terminal web.

All Contagious Animals Have Terminal Web Gaps, Which Form during a Discrete Stage of Infection

Our studies of *N. parisii* parasite development and host cell restructuring suggested that terminal web gap formation is an important stage of the infection cycle. Therefore, we investigated whether terminal web gaps have a functional role by examining how they relate to spore exit. As a functional read-out for spore exit, we tested the contagiousness of individual infected animals: in order for an animal to be contagious, spores must exit intestinal cells, leave the intestinal tract (likely through normal defecation), and then be consumed by a neighboring animal. To measure contagiousness, uninfected "recipient" animals were exposed to individual infected "donor" animals for a defined length of time. Each individual donor animal was then removed and examined for stage of infection and whether it had gaps in *IFB-2::CFP* localization. Several days later, recipient animals were examined to determine whether they had become infected, thus implying that the donor animal had shed spores and was contagious. After testing 164 individual donor animals for contagiousness, we found 87 animals that were contagious and all of these animals had spores, consistent with previous studies. Strikingly, we found that 100% of these contagious animals exhibited terminal web gaps (Figure 5A), consistent with the model that gaps are functionally related to spore exit. Of the animals that were non-contagious, 12% of them exhibited a small number of spores (and gaps). In previous studies we had found that animals infected with only a small number of spores are not always contagious, likely due to a low amount of spores being shed before the donors were removed from the plate [9]. There were also 9% of non-contagious animals that exhibited gaps but only meronts (no spores), consistent with population studies that indicated gaps appear slightly before spore formation (Figure 3E). The remaining 79% of animals that were non-contagious exhibited no gaps and only meronts (no spores). Since all contagious animals exhibit terminal web gaps, these data support the model that terminal web gaps may be a necessary part of spore exit from the intestinal cells.

We next sought to determine whether new gaps are continually being made during the course of infection, or whether gap formation is a discrete event that occurs only once during infection. In general, gaps first appeared in the region of the intestine exhibiting the heaviest *N. parisii* infection and gaps were always present in the region of intestine that had spores (Table S1 and data not shown). To quantify the number of gaps over time we chose a plane of focus with the largest number of gaps from *N. parisii* spore-infected animals and counted the number of gaps at 40 hpi, when they first are visible in all animals, and again at 63 hpi. With this analysis, we found that the number of gaps per unit area remained similar as the infection proceeded, suggesting that new gaps are not made after their initial formation at 40 hpi (Figure 5B). Next, we quantified the size of gaps at 40 hpi and 63 hpi (see Figure legend and Experimental Procedures for more detail on quantification). With this analysis, we found that gaps became larger as the infection proceeded, suggesting that once a gap is made it becomes larger over time (Figure 5C). This effect may be due to the lumenal distention that is observed as infection progresses, or it may be due to a more active process. In any case, these data indicate that the formation of gaps appears to be a discrete, regulated event that is orchestrated by the parasite at a particular stage in infection.

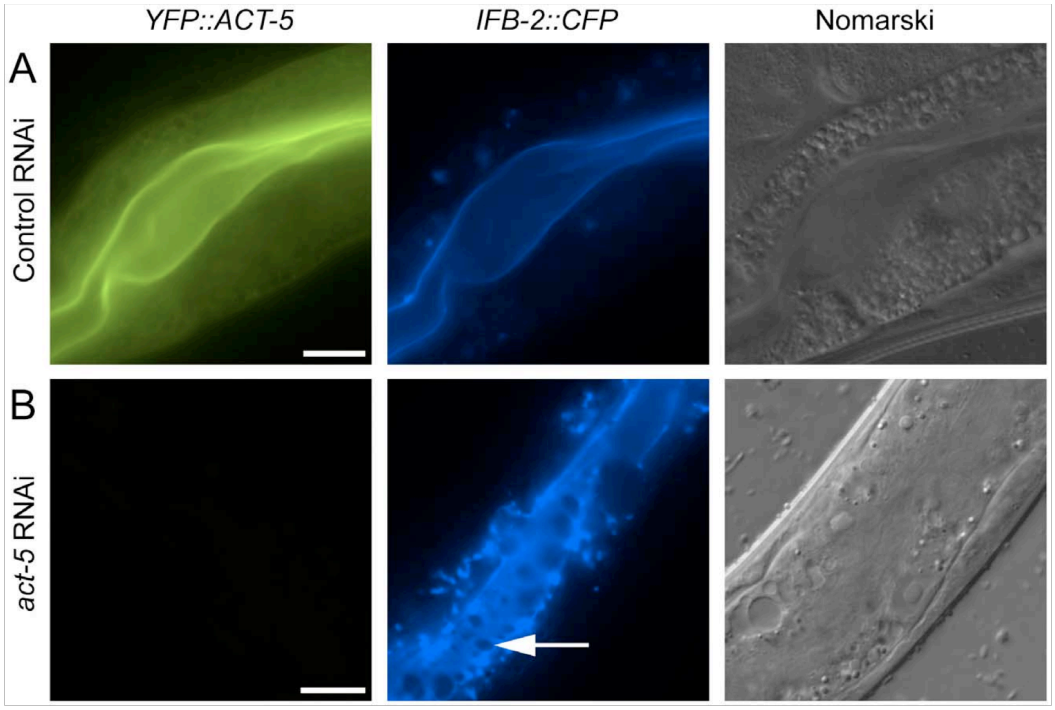

Figure 4. Reducing expression of actin causes terminal web gaps in the absence of infection. (A) Expression of *YFP::ACT-5* and *IFB-2::CFP* in control (L4440 vector alone) RNAi-treated animals. (B) *act-5* RNAi reduces expression of *YFP::ACT-5* and causes gaps in *IFB-2::CFP* expression in the absence of infection, as indicated by arrow. Exposure times were the same between (A) and (B). Scale bar is 20 μm.
doi:10.1371/journal.ppat.1002227.g004

Reducing Levels of Host Actin Impairs *N. parisii* Spore Exit

The extensive relocalization of ACT-5 during infection and the induction of gaps in IFB-2 localization upon RNAi against *act-5* led us to investigate the functional role of ACT-5 during infection. First, we assessed whether reducing levels of actin would affect the development of *N. parisii* infection inside intestinal cells. We measured the progression of *N. parisii* infection in animals fed with bacteria expressing dsRNA against *act-5*. Because feeding undiluted *act-5* dsRNA-expressing bacteria can slow the growth of animals, we titrated back the dose of RNAi to allow animals to develop more normally. Diluting *act-5* RNAi bacteria 1:25 and 1:50 with control bacteria allowed worms to develop relatively normally, but still caused reduced *act-5* levels (as assessed by imaging *YFP::ACT-5*, Figure S2). We found that meronts and spores appeared in *act-5* RNAi-treated animals at a similar rate to control-treated animals (Figure 6A). Therefore, despite the changes induced in actin localization upon infection, reduction of *act-5* expression had no obvious effect on progression of *N. parisii* infection or formation of spores within the host cells.

Since reducing actin in the absence of infection caused gaps in the terminal web, which could be a barrier for exit, we speculated that reducing actin might cause animals to shed more spores. Thus, we sought to measure spore exit in *act-5*-defective animals. Previously, we used single animal contagiousness assays to measure spore exit (Figure 5A). However, these assays are labor-intensive and categorical (animals are binned as either contagious or non-contagious). Therefore, we developed a more quantitative "spore shedding" assay to measure the number of spores shed by a population of animals. Fifty infected animals were placed in liquid media containing *E. coli* (the normal food source of *C. elegans*) and allowed to shed spores into the media. After defined periods of time, the number of spores shed was quantified. Animals appeared to shed spores throughout the assay, as we found increasing numbers of spores were shed with increasing amounts of time (Figure 6B). Under these assay conditions we found that a single infected worm could produce thousands of spores per hour. However, the number of spores shed per animal had significant animal-to-animal variability (data not shown), so we performed assays with populations of animals. Using this assay, we tested whether reducing ACT-5 levels would increase *N. parisii* spore shedding. Surprisingly, we found that spore shedding was almost completely blocked in 1:25 *act-5* RNAi-treated animals and was substantially blocked in 1:50 *act-5* RNAi-treated animals compared to control-treated (L4440) animals (Figure 6C). These findings suggest that reduction of ACT-5 impairs spore exit, in contrast to our original hypothesis. Altogether, our experiments indicate that proper levels of host actin are not important for *N. parisii* development inside cells, but are critical for promoting spore exit from those cells.

To further test the hypothesis that actin promotes spore exit we examined two other *C. elegans* strains that have differing levels of *act-5* expression. First, we examined the *YFP::ACT-5* transgene, which likely overexpresses actin. Our experiments indicated that *YFP::ACT-5* had no effect on the levels of spore shedding in our assays compared to wild-type animals (Figure 6D). Next we examined the *act-5(ok1397)* deletion mutant, which is likely a null mutation, as it deletes half of the 5′ translated region of *act-5* as

A

	% with gaps and with spores	% with gaps and meronts only	% without gaps and with spores	% without gaps and meronts only	n (animals)
contagious animals	100	0	0	0	87
non-contagious animals	12	9	0	79	77

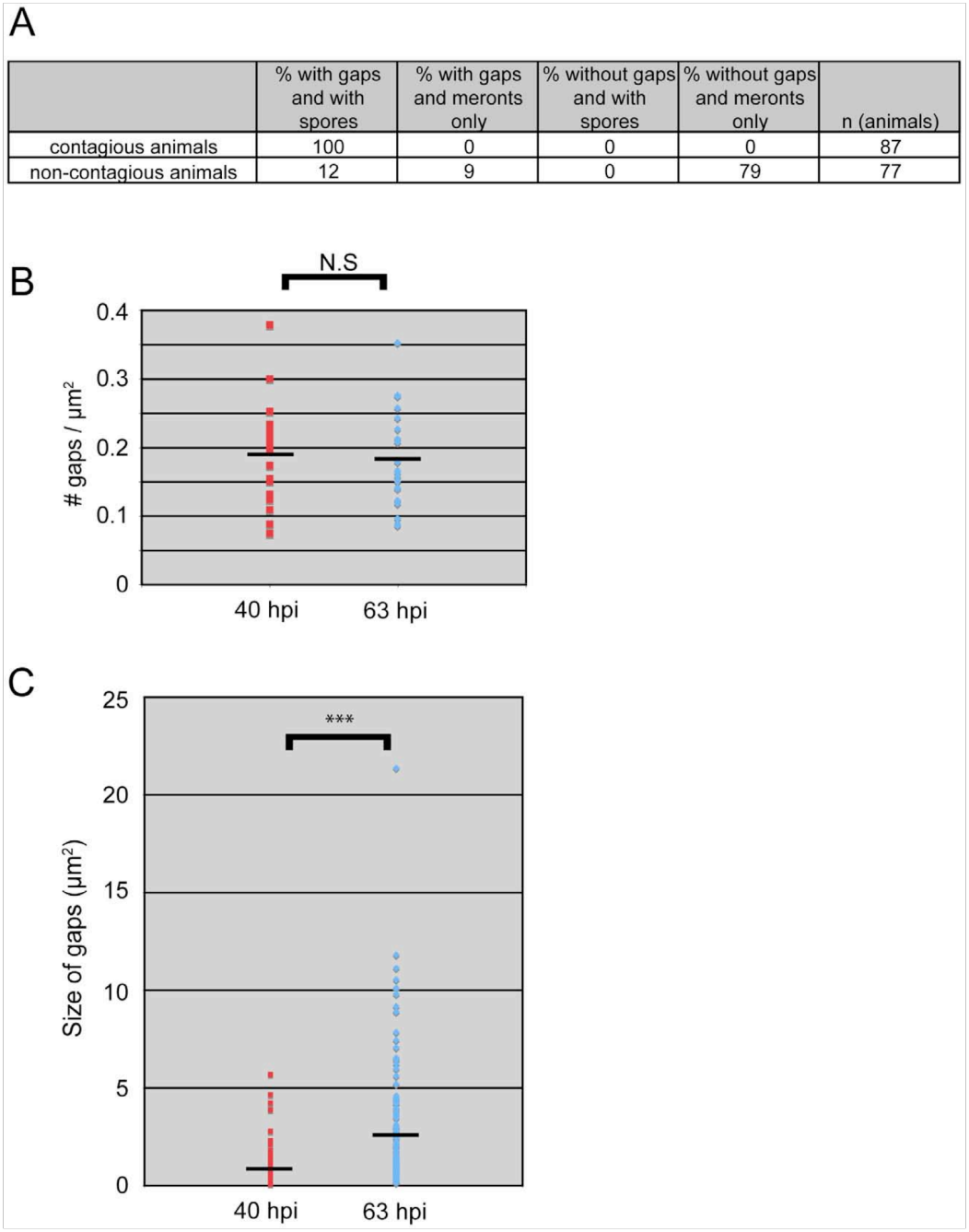

Figure 5. All contagious animals have *IFB-2::CFP* terminal web gaps, which do not increase in number over time but increase in size. (A) Single animal contagiousness assays. Individual ''donor'' infected *IFB-2::CFP* animals were tested for contagiousness by exposing them to ''recipient'' uninfected animals. Donors were examined for *IFB-2::CFP* terminal web gaps and scored for stage of infection. 100% of contagious animals exhibited gaps in *IFB-2::CFP* localization and *N. parisii* spores. (B) The number of gaps in *IFB-2::CFP* localization does not change over time. Each datapoint represents one animal (n = 20 animals at each timepoint) where the number of gaps was counted in a defined region of the intestine to calculate the number of gaps/µm^2. Average number of gaps at 40 hpi is 0.19 gaps/µm^2 and at 63 hpi is 0.18 gaps/µm^2 (difference is not significant, p = 0.64, two-tailed *t*-test). (C) The size of gaps in *IFB-2::CFP* localization increases with time. Each datapoint represents the area of one gap, with

several gaps quantified per infected animal. At 40 hours post-inoculation (hpi) n = 119 gaps and n = 20 animals; at 63 hpi n = 144 gaps and n = 20 animals. Average gap size at 40 hpi is 0.87 μm^2 and at 63 hpi is 2.45 μm^2 (*** difference is significant, $p<10^{-7}$, two-tailed *t*-test). See Materials and Methods for more details on the quantitation method. Data graphed in Figure 5B and C are the combination of two independent experiments: 1) A population study examining two different sets of animals at each timepoint (Table S2), and 2) A longitudinal experiment where we followed single animals at two time points during infection and quantified the gaps in each animal (Table S3). We saw very similar trends within individual animals as we saw within a population of animals in that the number of gaps did not change over time, but gaps increased in size.
doi:10.1371/journal.ppat.1002227.g005

well as the upstream untranslated region. Because the *act-5(ok1397)* mutation is lethal when homozygous, we examined spore shedding in *act-5(ok1397)*/+ heterozygote mutants, which develop normally. We infected these animals with *N. parisii* and found that spore development proceeded at a similar pace as in wild-type animals (data not shown). Interestingly, in *act-5* heterozygote mutants where *act-5* expression should be reduced to half of wild-type levels, we found that spore shedding was approximately half of wild-type levels (Figure 6D), consistent with our hypothesis that actin promotes exit. This result suggests that there is a dose-dependent effect of actin on spore shedding, and that proper levels of actin are critical for efficient *N. parisii* spore exit from host cells.

Spores Exit Apically from Intestinal Cells and Appear to be Free of *C. elegans* Membrane

The spore shedding and contagiousness assays described above measure the spores that have left the animal, presumably through defecation. Before these spores are shed through defecation, they must first exit the intestinal cells into the lumen. Our previous studies indicated that spores are only found in intestinal cells, and spores are therefore unlikely to exit out of cells basolaterally to enter the rest of the animal (e.g. into the gonad). To more closely examine that spores only exit apically as opposed to basolaterally, we performed transmission electron microscopy (TEM) to analyze the location of spores in the whole animal. The only tissue in which we conclusively found spores was the intestine (Figure 7A);

A

Treatment	% animals with meronts at 24 hours	n (animals)	% animals with spores at 48 hours	n (animals)
Control RNAi	93	30	100	30
act-5 RNAi (1:50)	93	30	100	30

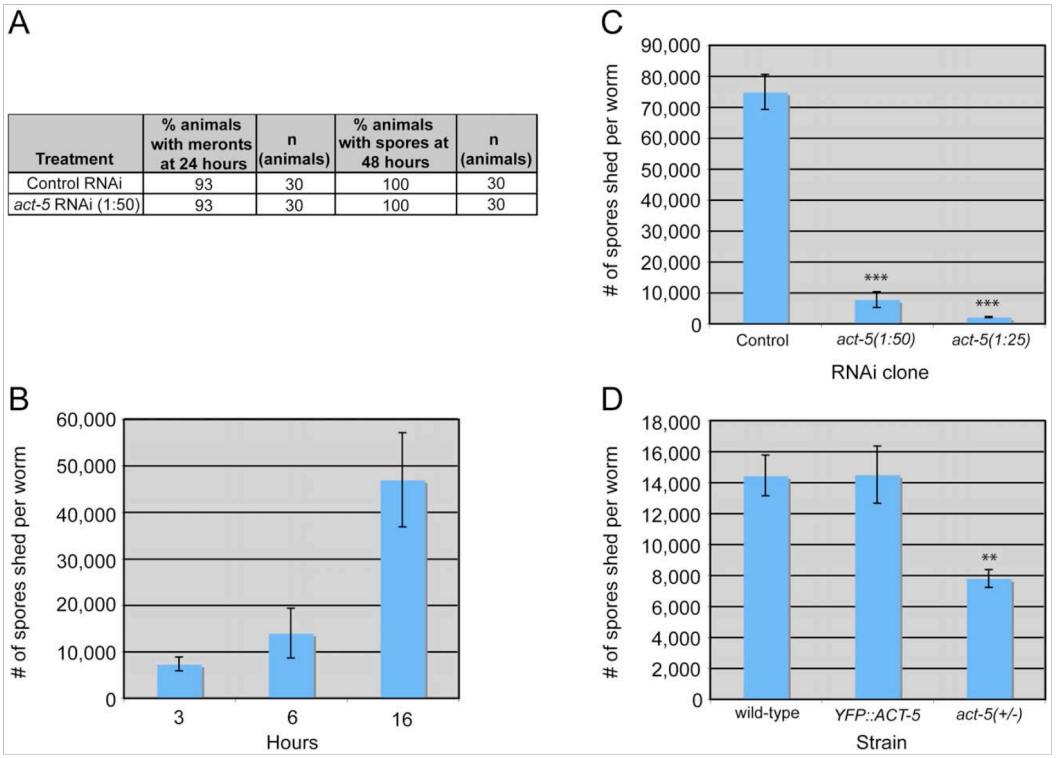

Figure 6. Host actin is required for spore shedding. (A) Infection kinetics in RNAi-treated animals. *N. parisii* development proceeds similarly in control (L4440) and *act-5* RNAi-treated animals. Results are representative of three independent experiments, with at least 25 animals in each condition of each experiment. (B) Spore shedding assay shows increasing number of spores shed by animals over time. Error bars are SD to show variance in assay. (C) *act-5* RNAi inhibits spore shedding, compared to control (L4440) treated animals. 1:25 diluted *act-5* RNAi inhibits shedding more than 1:50 diluted *act-5* RNAi. Animals shed spores for 16 hours in this assay. (D) *YFP::ACT-5* animals shed the same number of spores as wild-type animals, while *act-5(ok1397)/mT1[dpy-10(e128)]* heterozygote mutants shed 50% fewer spores than wild-type animals. Animals shed for 13 hours in this assay. (C-D) Number of spores shed per worm is the average of three replicates in a single experiment (with 50 animals tested in each replicate), error bars are SEM. Results are representative of three independent experiments. (*** indicates $p<0.0005$, ** indicates $p<0.002$, two-tailed *t*-test).
doi:10.1371/journal.ppat.1002227.g006

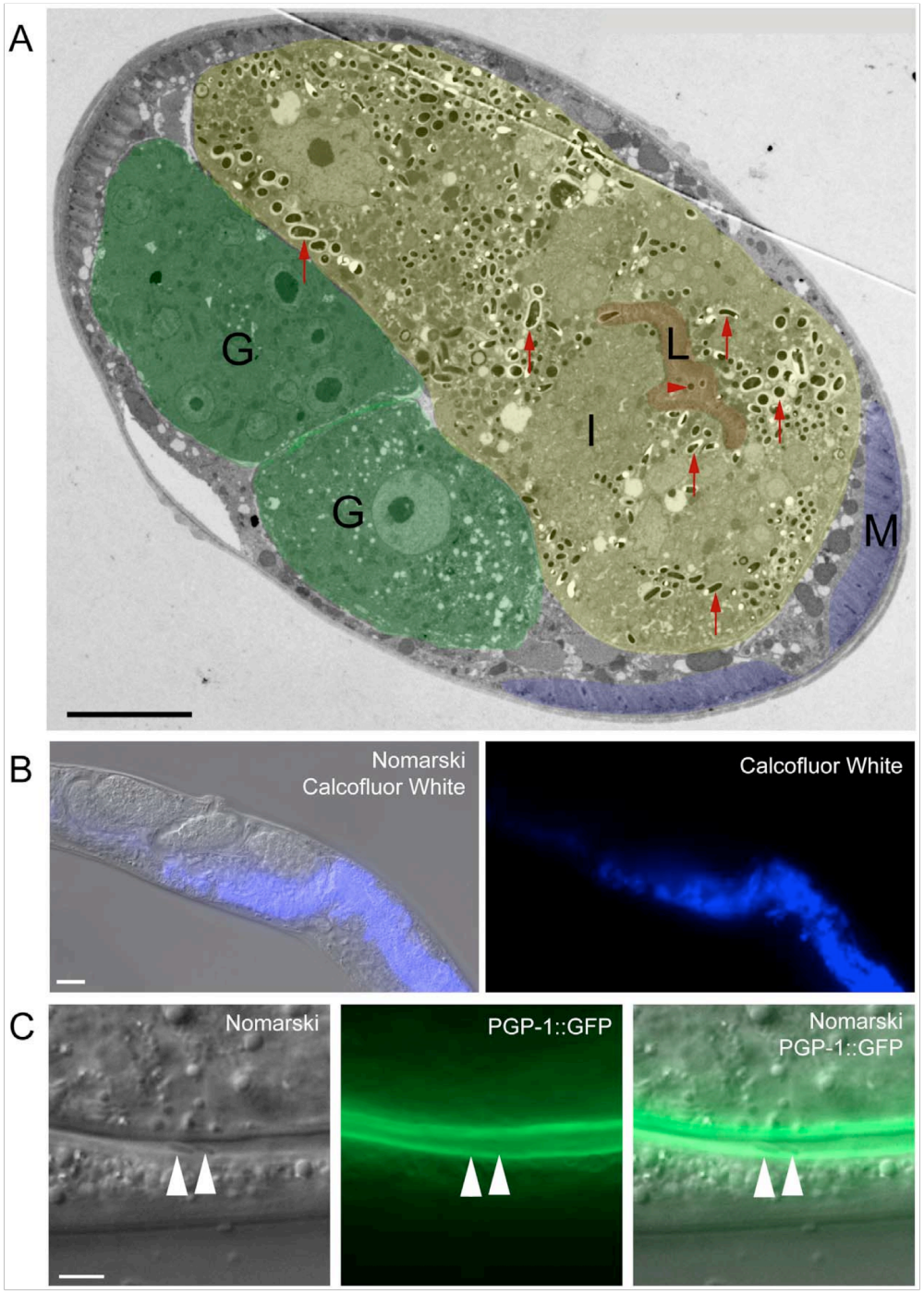

Figure 7. *N. parisii* spores exit apically out of intestinal cells and are not labeled with a *C. elegans* membrane marker. (A) TEM indicating *N. parisii* spores inside intestinal cells and the intestinal lumen. Intestinal cells are false colored yellow (labeled I), the intestinal lumen and microvilli are false colored red (labeled L), the gonad is false colored green (labeled G) and body wall muscle is false colored purple (labeled M). Examples of

intracellular spores in the intestinal cells are indicated with red upward arrows and an example of a lumenal extracellular spore is indicated with red rightward arrowhead. Spores were only observed inside intestinal cells and in the intestinal lumen, suggesting that they only exit apically from intestinal cells (not basolaterally). Scale bar is 10 μm. (B) *N. parisii* infected animal fixed and stained with Calcofluor White to label *N. parisii* spores inside intestinal cells. Scale bar is 20 μm. (C) *N. parisii* spores in the intestinal lumen of *PGP-1::GFP* animals are free of GFP, suggesting that they did not take *C. elegans* membrane upon exit into the lumen. Two spores in lumen are indicated with arrowheads. *PGP-1::GFP* labels the apical (lumenal) side of two intestinal cells. Scale bar is 5 μm.
doi:10.1371/journal.ppat.1002227.g007

we did not see evidence of spores in any other tissue (e.g. hypodermis, muscle or gonad). In order to further examine spore location throughout the animal, we also fixed animals and stained with Calcofluor White, a dye that binds to the chitin found in *N. parisii* spores. Again, we only found evidence of *N. parisii* spores in the intestine, not in other regions of the animal (Figure 7B).

Because *N. parisii* spores have to cross the *C. elegans* apical plasma membrane of intestinal cells to exit into the lumen, we investigated whether spores in the lumen may have acquired *C. elegans* plasma membrane upon exit. To address this question we infected transgenic animals expressing *PGP-1::GFP*, which is a GFP-tagged ATP binding-cassette (ABC) transporter that localizes to the apical side of intestinal cells [30]. After infecting worms, we transferred them repeatedly away from spores onto fresh plates, so that any spores in the lumen were likely the result of exit and not the result of consumption (see Materials and Methods for details). We did not find any lumenal *N. parisii* spores that were labeled with GFP (Figure 7C, n = 50 spores examined), suggesting that spores do not take *C. elegans* membrane with them when they exit into the lumen.

N. parisii Spores Can Exit Intestinal Cells without Causing Lysis

It is clear that *N. parisii* spores are exiting while animals are still alive, as live animals are contagious to other animals ([9] and Figure 5A) and animals are alive at the end of spore shedding assays (Figure 6). However, it is unclear whether this process of spore exit causes tissue damage that leads to cell lysis. To address this question, we next examined whether *N. parisii* spore exit and/or terminal web restructuring cause disruption of cellular integrity of the intestinal cells. To assay cellular integrity, we used the cell-impermeable dye propidium iodide (PI), which can be fed to *C. elegans*. When intestinal cells are intact, PI does not enter cells after short incubation periods, but instead remains restricted to the intestinal lumen. As a positive control for PI entry into cells that have lost integrity, we used animals that were exposed to the *Bacillus thuringiensis* pore-forming toxin Cry5B, which creates nanometer-sized holes in the plasma membrane. A recent study demonstrated that Cry5B treatment of *C. elegans* creates pores in intestinal cells that allow PI to enter intracellularly [31]. Consistent with these studies, we found that animals fed *E. coli* that expresses Cry5B had intracellular PI staining whereas animals fed normal *E. coli* did not (compare Figure 8A and B). Strikingly, animals infected with *N. parisii* (also fed on *E. coli*) did not exhibit intracellular PI, indicating that cellular integrity was not compromised (Figure 8C and G). These animals were infected with *N. parisii* spores (Figure 8H), and exhibited gaps in *IFB-2::CFP* localization (Figure 8I). In order to quantify this effect, we scored the percentage of animals with intracellular PI in 100 animals of each condition, only choosing animals that were infected throughout the intestine with spores for the *N. parisii* infection condition. From single-animal contagiousness assays with animals at a similar stage of infection (Figure 5A), we estimate that 80-90% of these animals were contagious. In these studies we found that almost all Cry5B-treated animals exhibited intracellular PI, whereas virtually none of the *N. parisii*-infected animals did (Figure 8J). Thus, while *N. parisii* infection causes gaps in the terminal web and results in the passage of 1 μm-wide *N. parisii* spores (much larger than Cry5B-induced pores) across the membrane in order to exit into the lumen, these events do not appear to cause lysis of *C. elegans* intestinal cells. These data support the hypothesis that cytoskeletal rearrangements and spore exit are highly regulated processes that maintain the integrity of the host cell during infection.

Discussion

Intracellular pathogens have privileged access to host cell components that they can exploit in order to survive, replicate, and then exit to infect new hosts. The studies presented here provide insight into parasite-directed cellular reorganization that occurs *in vivo* in order to exit cells but minimize damage to the host. We find that the intestinal parasite *N. parisii* redirects host actin in order to non-lytically exit from intestinal cells and propose a two-phase model for this exit, with terminal web restructuring occurring during Phase I and non-lytic exit occurring during Phase II (Figure 8K). Phase I takes place after invasion (step 1), when *N. parisii* is developing as a metabolically active meront, a stage that essentially forms a new organelle within the host cell. At this time, the intestinal-specific actin isoform ACT-5 ectopically relocalizes to the basolateral side of intestinal cells, often forming network-like structures (step 2). Soon after this relocalization of ACT-5, gaps appear in localization of IFB-2, an intermediate filament component of the terminal web (step 3). We speculate that relocalization of ACT-5 may trigger these gaps, since reducing the level of ACT-5 expression causes gaps in the terminal web in the absence of infection. We show that all contagious animals exhibit gaps in localization of IFB-2, and that formation of gaps occurs during a discrete stage of the infection cycle, suggesting that gap formation is a highly regulated process. Phase II of the exit strategy begins after *N. parisii* develops into spores and these spores exit out of cells into the lumenal space (step 4). Surprisingly, we found that reducing levels of ACT-5 impairs spore shedding, indicating that host actin is required for proper exit of *N. parisii* spores at this stage, even though the infection and parasite development can proceed normally within the cell. Interestingly, *N. parisii* spore exit is non-lytic, since extracellular dyes continue to be excluded from the intracellular space of intestinal cells (step 5). This finding is striking, as a single infected animal can shed thousands of spores (Figure 6).

Our functional analyses of host intestinal actin during *N. parisii* infection indicate that there are two distinct roles for actin, with opposing effects in each of the two phases of exit. As described above, it appears that host actin impairs exit during Phase I, since a reduction of actin leads to gaps in the terminal web, which may present a barrier to exit. However, we found that a reduction of actin levels led to an overall reduction in spore exit. Thus, one explanation is that host actin impairs spore exit during Phase I, but promotes spore exit during Phase II. A caveat to this interpretation is that the function of terminal web gaps (and thus the role of actin in Phase I) is unclear since we do not yet have a method to block gap formation during infection: it is possible that gaps serve a purpose other than facilitating exit. Our proposed role of actin in Phase II to promote exit also requires further investigation. One possibility is that actin provides motor force to drive spores out of

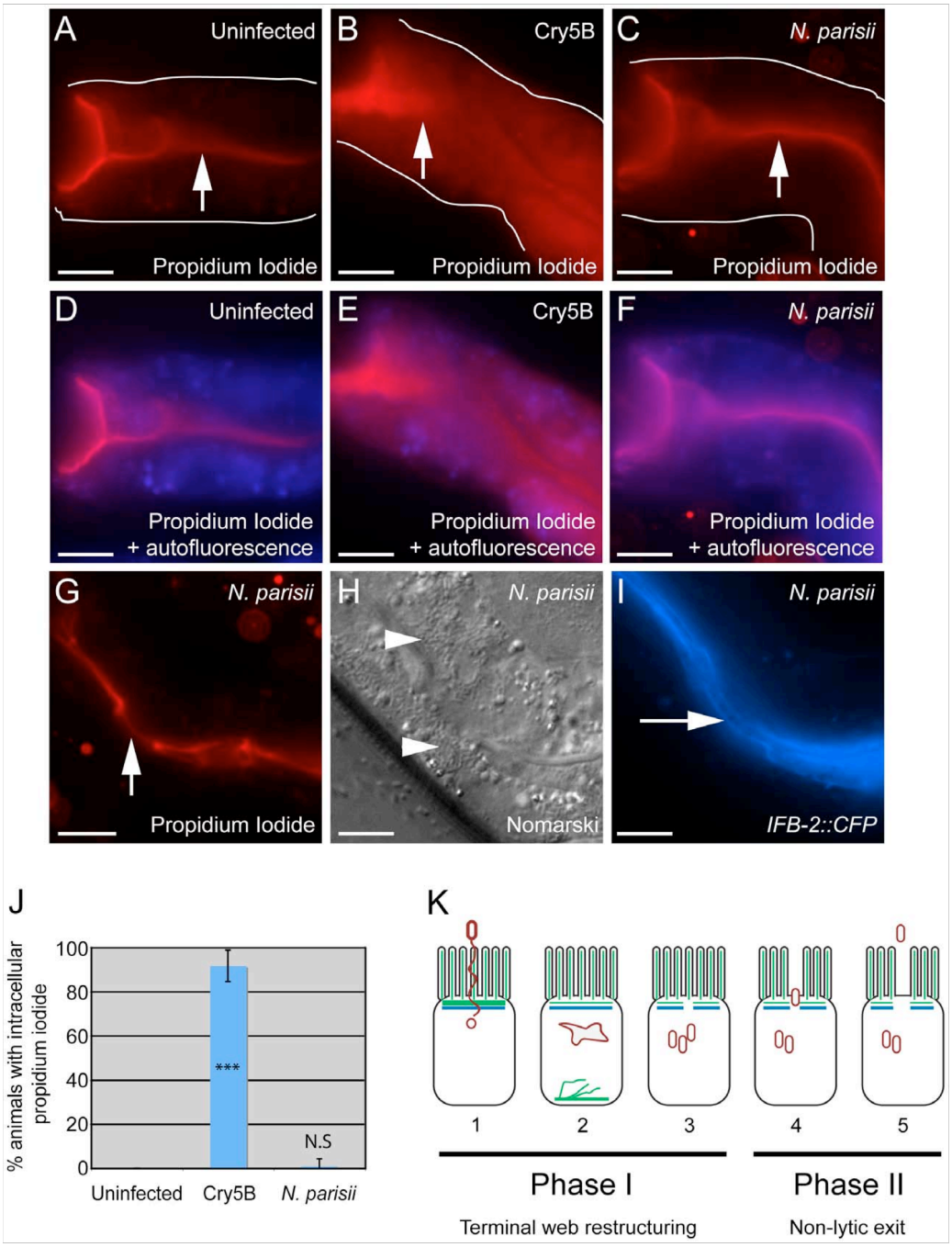

Figure 8. Animals infected with *N. parisii* spores do not take up the extracellular dye propidium iodide. Propidium iodide staining in uninfected animal (A, D), animal treated with Cry5B pore-forming toxin (B, E), and animal infected with *N. parisii* spores (C, F). Intestinal cells encompass the entire space between the lumen (indicated with upward arrows) and the basolateral side of intestinal cells (indicated with outlines). Outlines were drawn based on Nomarski images, which are shown in Figure S3 in order to better illustrate intestinal cell morphology. The intracellular region is also indicated with an overlay the autofluorescence in the blue channel to indicate intracellular regions of intestinal cells (D–F). Note the

extensive propidium iodide staining filling up the intracellular region in Panels B and E. (G) Propidium iodide staining in an *N. parisii* infected animal with upward arrow indicating lumen. (H) Nomarski image of animal shown in G, arrowheads indicate *N. parisii* spores; (I) *IFB-2::CFP* of animal shown in G and H, rightward-pointing arrow indicates gaps in the terminal web; Scale bar is 20 μm in A–I. (J) Percentage of animals with intracellular propidium iodide shown as the average of 4 independent experiments, n = 100 animals total for each condition, error bars are SD. The difference between uninfected and Cry5B treated animals is significant, *** indicates $p<10^{-6}$ with a two-tailed *t*-test. The difference between uninfected and *N. parisii*-infected animals is not significant (p = 0.36). (K) Model for actin-based, non-lytic *N. parisii* spore exit from *C. elegans* intestinal cells has two phases in five steps: 1) *N. parisii* spores invade *C. elegans* intestinal cells, likely with polar tube. 2) *N. parisii* meronts develop and ACT-5 ectopically localizes to the basolateral side of cell and in branched networks. This may lead to less expression on the apical side. 3) Gaps appear in the terminal web, then *N. parisii* spores form. 4) Spores exit the cells, causing worms to be contagious. 5) Exit is non-lytic, because the extracellular dye propidium iodide is unable to enter cells.
doi:10.1371/journal.ppat.1002227.g008

the cell. The nature of this actin polymerization and its relocalization at the proper time may be the key to orchestrating the complex events that enable large numbers of microsporidian spores to egress out of *C. elegans* intestinal cells in a manner that minimizes damage to its host.

Understanding how *N. parisii* is able to exit the host cell necessitates understanding what barriers it must cross and the mechanism it employs to cross them. In Phase I of the *N. parisii* exit strategy, the terminal web is restructured. Our studies indicate that terminal web gaps appear right before spore formation (Figures 3E and 5A), implying that gaps are not caused by the mechanical process of spore exit, but rather by a regulated signaling event that is precisely timed to precede spore formation and the need to exit. The terminal web is a conserved structure found in microvilli-containing cells from *C. elegans* to humans, but surprisingly little is known about its assembly and dynamics [32,33,34,35]. The terminal web presumably represents a barrier that host vesicles must traffic through during normal endocytosis and exocytosis events. Do intracellular vesicles need to dissolve the terminal web in order to cross this barrier? Electron microscopy studies indicate there are tiny gaps in the *C. elegans* terminal web that are too small to allow for vesicle passage, but are associated with vesicular elements and could represent a system of regulated passage [36]. Perhaps *N. parisii* is exploiting this vesicle passage system to create gaps in the terminal web, but in a way that does not result in resealing of these gaps. It will be interesting to perform live imaging of the kinetics of these structures in uninfected animals to examine what is the basal level of movement and restructuring of this conserved structure in intestinal cells. It will also be interesting to further examine the mechanism by which *N. parisii* spores cross the plasma membrane, as our studies indicate that they do not acquire *C. elegans* membrane as they exit into the lumenal space of the intestine (Figure 7C).

In spite of the terminal web restructuring described above, and the passage of 1 μm-wide spores out of cells into the digestive tract, cellular integrity assays indicate that actin-based exit of *N. parisii* spores does not cause lysis of *C. elegans* intestinal cells (Figure 8). This finding is intriguing, since bacterial pathogens such as *Listeria* and *Mycobacterium* also use actin-based, non-lytic forms of exit, suggesting a common evolutionary strategy for exit between eukaryotic and prokaryotic pathogens. Several bacterial virulence factors have been identified that direct these actin-based processes within host cells [4,37], but comparatively little has been explored about eukaryotic intracellular pathogens and the factors they use to exploit host cells. And almost nothing is known about virulence factors in the Microsporidia phylum. One of the few characterized examples of microsporidian virulence factors is a class of ATP transporters that can "steal" ATP from the host cell [14,38]. These transporters are expressed on the plasma membrane of the parasite while it is living inside the host cell and act to import ATP directly into the parasite. In addition to this method of host exploitation, it is likely that microsporidia also secrete factors from the meront into the host cytoplasm to facilitate other kinds of nutrient acquisition, as well as to direct the cytoskeletal changes we have observed. The *N. parisii* genome has recently been sequenced (E.R.T. and the Broad Institute, as part of the Microsporidian Genomes Consortium, unpublished data, http://www.broadinstitute.org/files/shared/genomebio/Microsporidia_wp.pdf) and may provide clues into which parasite components are secreted into the host cell to direct this restructuring.

We have isolated microsporidia-infected nematodes from a wide variety of geographical locations, including multiple regions in France (the *N. parisii* strain used in this study was isolated near Paris), Portugal, India, Colombia and Cape Verde ([9] and Marie-Anne Félix, personal communication). Thus, *Caenorhabditis* nematodes have likely co-evolved with *Nematocida* and other microsporidia species. Over time, co-evolution of host/parasite pairs is thought to lead to a reduction in virulence [39,40]. This pressure is likely to be especially great in obligate intracellular parasites such as microsporidia, which cannot grow in the absence of host cells. Microsporidian species that infect fish appear to have adopted a strategy of minimal virulence in order to maximize parasite production: they often form "spore factories" called xenomas in the fish nervous system that can produce large numbers of spores without substantial impact on the health of the fish [20]. Perhaps the non-lytic exit of *N. parisii* is part of a strategy similar to the xenomas found in fish that serves to maximize spore production and transmission, but minimize virulence.

N. parisii likely has an intimate relationship with the *C. elegans* intestinal cell during the meront stage, since it essentially creates a parasite organelle that develops in direct contact with the host cytoplasm [9]. The human-infecting microsporidian pathogen *Enterocytozoon bieneusi* also develops in direct contact with the host cytoplasm during the meront stage [41]. *E. bieneusi* infection in humans is restricted to intestinal cells, and is the most common cause of microsporidian disease in humans, being responsible for lethal diarrhea in AIDS patients [18]. Effective treatments are lacking for *E. bieneusi* infection [15,42] and it has not been possible to propagate *E. bieneusi* in tissue culture cells, perhaps because these cells lack some aspect of differentiated intestinal cells that is needed for the infection cycle. While *E. bieneusi* and *N. parisii* are in distinct clades of the microsporidia, their similar developmental life cycle in the cytoplasm of intestinal cells may involve similar pathogenic strategies. The *C. elegans*/*N. parisii* host/parasite system may thus provide insights into the mechanisms employed by medically relevant but intractable microsporidian species such as *E. bieneusi* to further understand how they cause disease and potentially how to treat the infections they cause.

Materials and Methods

Strains

C. elegans were maintained on NGM plates seeded with OP50-1, as described [43]. We used N2 wild-type animals. BJ49 *kcIs6[IFB-2::CFP]* was kindly provided by Olaf Bossinger. JM125 caIs*[ges-1p::YFP::ACT-5]* was kindly provided by James McGhee [24].

ERT38 caIs *[YFP::ACT-5;IFB-2::CFP]* was made by crossing BJ49 and JM125 strains. A separately made *YFP::ACT-5* strain, IN4000 dtIs2298, was kindly provided by James Waddle and used for Videos S1 and S2. VC971 *+/mT1 II; act-5(ok1397)/mT1[dpy-10(e128)] III* was provided by the *C. elegans* Reverse Genetics Core Facility at UBC via the *Caenorhabditis* Genetics Center (CGC). The presence of the *act-5(ok1397)* deletion was confirmed by PCR genotyping. GK288 *GFP::PGP-1* and *E. coli* (OP50)-Cry5B strains were kindly provided by Ferdinand Los and Raffi Aroian. *N. parisii* strain ERTm1 (isolated originally from Franconville, France, near Paris) was used for all microsporidia infection experiments.

N. parisii Spore Preps

N. parisii infected animals were disrupted with silicon beads as described [9]. This lysate was then filtered through a 5 µm filter (Millipore) attached to a 10 ml syringe, to eliminate undisrupted *C. elegans* eggs, larvae and other debris. The filtrate containing *N. parisii* spores was frozen at −80°C and then thawed right before use. *N. parisii* spores were quantitated by staining with Calcofluor White (Fluka) and counting with a hemocytometer (Cell-Vu).

Infection Assays and Microscopy

In general, synchronized L1 larvae were grown for 24 hours on 10 cm NGM plates seeded with OP50 at 20°C until approximately L3 stage, when they were infected with 3×10^7 *N. parisii* spores and then incubated at 25°C. Symptoms of infection were tracked by mounting approximately 50 animals on agarose pads and then viewing animals with Nomarski optics and/or fluorescence on a Zeiss AxioImager at 630X magnification. Images were captured with Axiovision software. *P. aeruginosa* PA14 infection assays and *S. enterica* SL1344 infection assays were performed as described [44], except that *S. enterica* infection assays included a pre-treatment with *bec-1* RNAi to knock down the autophagy pathway, as described [29]. Transmission electron microscopy was performed as described [9]. Calcofluor White staining on infected animals was performed by fixing and staining with a 1:1 mix of 1M NaOH and Calcofluor White. In order to examine spores that had newly exited into the intestinal lumen (as shown in Figure 7C), animals were repeatedly washed to reduce exposure to external spores they might ingest. Specifically, at 24 hpi (prior to spore formation) animals were washed four times in M9, added to fresh NGM plates seeded with OP50, and incubated at 25°C until 40 hpi when this process was repeated. To reduce the probability of animals consuming spores shed by their neighbors, worms were replated at a low density of approximately 45 worms per 6 cm plate. Lumen-localized spores were then imaged in animals at 42 hpi.

Contagiousness Assays

Donor BJ49 *[IFB-2::CFP]* animals were generated for contagiousness assays as follows. Synchronized L1 larvae were grown on 6 cm NGM plates seeded with OP50 for 24 hours at 20°C, then infected with 1.5×10^5, 4.7×10^5 or 9.3×10^5 spores diluted in 500 µl of M9 and placed at 20°C or 25°C for 20 hours in order to generate animals at a variety of infection stages. These animals were picked to new NGM/OP50 plates without spores and incubated for 4 hours, washed off the plate with M9, rinsed three times to remove spores attached to the cuticle and then added to a new plate. Next, these infected donor animals were individually placed onto 6 cm NGM plates seeded with OP50 as well as 200 L1 recipient animals. The donor and recipient animals were co-incubated for 16 hours and the donor animal was then removed to assess infection level by mounting the animal on a slide and scoring for meronts or spores using Nomarski optics, as well as scored for gaps using fluorescence microscopy, at 630X. Recipient animals were scored for infection similarly 7 days later. If no infection was observed, plates were kept and then scored again for infection 3 days later.

Characterization of Gaps in *IFB-2::CFP* Localization

Animals at 40 and 63 hours post-inoculation (hpi) were analyzed. A 10 µm length of the intestine was chosen such that the wall of the intestine was in a single plane of view. The width of this 10 µm long section was measured and the total number of gaps in *IFB-2::CFP* localization was counted to calculate the number of gaps per μm^2. This area was then divided into 4 quadrants. In a single, randomly chosen quadrant, the area of each individual gap within the quadrant was quantified using the measure tool in AxioImager in order to calculate the average size of gaps. Statistical comparisons of data at 40 hpi and 63 hpi were done with a two-tailed *t*-test in Excel.

Longitudinal Infection Assays

ERT38 *[IFB-2::CFP; YFP::ACT-5]* synchronized L1 animals were plated on NGM OP50 plates and infected with 3.6×10^6 spores 24 hours later. In order to perform longitudinal analysis of infection symptoms in the same animal over time, animals were anesthetized with levamisole and mounted onto agarose slides for scoring of symptoms, and then recovered onto NGM/OP50 plates until the next timepoint.

RNA Interference Assays

Feeding RNAi was performed as described. Briefly, RNAi bacterial clones were streaked onto LB agar plates with ampicillin and tetracycline. A single colony was inoculated into LB with ampicillin, grown overnight and then seeded on RNAi plates (essentially nematode growth media with IPTG and ampicillin – usually 6 cm plates). Plates were incubated for at least one day before being seeded with a synchronized population of L1 *C. elegans. act-5* RNAi was either used undiluted, or diluted 1:25 or 1:50 with L4440 (vector alone) control RNAi bacteria. We performed *act-5* RNAi experiments either with a clone from the Ahringer RNAi library or a clone that was a gift from James Waddle [23]. RNAi clones were confirmed by sequencing. Similar results were obtained with both clones, but in general, the Ahringer clone caused more severe phenotypes.

Spore-Shedding Assays

Animals were infected with 4.5×10^5 or 9.3×10^5 *N. parisii* spores on NGM plates seeded with *E. coli* OP50 and placed at 25°C. At 24 hpi, animals were washed with M9 and transferred to new NGM OP50 plates (except when performing RNAi). Then at 48 hpi animals were washed several times and then transferred to a fresh NGM/OP50 plate to remove external spores. Next, 50 animals were picked off of this plate into a microfuge tube with M9 and concentrated OP50, and rotated on a nutator for 16 hours. The microfuge tube was removed from the nutator and incubated without shaking for 10 minutes to allow the *C. elegans*, but not the spores, to pellet to the bottom of the tube. Then the supernatant was transferred to a new microfuge tube and the spores were pelleted by spinning at high speed in a microfuge. The supernatant was removed after this spin and the spores in the pellet were stained with Calcofluor White and quantified with a hemocytometer. The absolute number of spores shed per worm varied from experiment to experiment. The viability of animals was confirmed at the end of the assays and assays were performed in triplicate for each experiment. Statistical comparisons of data were done with a two-tailed *t*-test in Excel.

Cellular Integrity Assays

Assays for integrity of intestinal cells was performed with a propidium iodide assay, as described [31]. Briefly, *YFP::ACT-5; IFB-2::CFP* animals were infected with 9.3×10^5 spores on an OP50-seeded 6cm NGM plate. Approximately 40 hours later, animals were washed off the plate and put in a solution of 5-HT at 5 mg/ml for 15 minutes in order to force feed dye into animals – Cry5B treatment causes animals to cease feeding. Animals were then stained in a 20 µg/ml solution of propidium iodide for 30 minutes, washed twice with M9 to remove background excess dye, and imaged using fluorescence microscopy at 630X. We scored only animals that were at the "full spore" stage and therefore were very likely contagious and actively shedding spores. Negative control animals were treated similarly except they were not infected with spores. Positive control Cry5B-treated animals were plated as synchronized L1 larvae on NGM OP50 plates until they reached the L4 stage. They were then washed onto NGM/Ampicillin/IPTG plates seeded with OP50-Cry5B and incubated at 25°C for 30 minutes. They were then washed off the plates and treated as detailed above. In order to quantify the percentage of animals exhibiting propidium iodide staining intracellularly, we imaged animals with a defined exposure time and then measured the maximum fluorescence intensity in the lumen and intracellularly using ImageJ software from the NIH (http://rsb.info.nih.gov/ij/). If the maximum fluorescence intensity was greater intracellularly than in the lumen, the animal was binned as exhibiting intracellular propidium iodide. Statistical comparisons of data were done with a two-tailed *t*-test in Excel.

Accession Numbers

Accession numbers for the genes and gene products mentioned in this paper are given for Wormbase, a publically available database that can be accessed at http://www.wormbase.org.

These accession numbers are: *act-5 (T25C8.2), ifb-2 (F10C1.7), bec-1 (T19E7.3), pgp-1 (K08E7.9).*

Supporting Information

Figure S1 Terminal web restructuring in *IFB-2::CFP* single transgenic animals. Kinetics of terminal web restructuring and parasite development in a population of animals infected at time = 0 hours. Data shown are the average of two independent experiments with 50 animals scored at each timepoint in each experiment (for a total of at least 100 animals scored at each timepoint). Error bars are SD.
(TIF)

Figure S2 Diluted RNAi against *act-5* causes reduction in *YFP::ACT-5* expression. *YFP::ACT-5; IFB-2::CFP* animals treated with control RNAi (A), 1:50 dilution of *act-5* RNAi (B) and 1:25 dilution of *act-5* RNAi (C). First column on left is images in the YFP channel, second column is CFP channel, third column is Nomarski bright-field and fourth column is an overlay of all three channels. Images in YFP and CFP channels were taken with same exposure time: note decreased level of *YFP::ACT-5* signal with 1:50 *act-5* RNAi and further decreased level with 1:25 *act-5* RNAi. Scale bar is 20 µm.
(TIF)

Figure S3 Nomarski images of animals analyzed for cellular integrity. In order to illustrate intestinal cell morphology, the same animals shown in Figure 8 A–F are shown in this figure with Nomarski bright-field imaging in A–C and Nomarski overlay with propidium iodide in red and autofluorescence in blue D–F. Upward arrows in D–F indicate lumen. Arrowheads in C indicate two examples of clusters of *N. parisii* spores, which are false-colored green. Scale bar is 20 µm.
(TIF)

Table S1 Longitudinal studies of ACT-5 and IFB-2 changes in individual animals throughout infection.
(XLS)

Table S2 Analysis of *IFB-2::CFP* terminal web gap number and size in a population of animals.
(XLS)

Table S3 Analysis of *IFB-2::CFP* terminal web gap number and size in a longitudinal study of individual animals.
(XLS)

Video S1 Relocalization of intestinal actin upon infection. Uninfected IN4000 *YFP::ACT-5* animal: note the restriction of *YFP::ACT-5* to the apical membrane. Anterior is down, pharynx is just outside of the field of view. Video plays through a Z-stack of 35 images taken every 0.5 µm in a single animal. Video starts at the plane of focus toward the outside of the animal (similar to the plane of focus in Figure 2C), and end at the plane of focus inside the animal (similar to the plane of focus in Figure 2B). See Figure 2D for more anatomical information.
(MOV)

Video S2 Relocalization of intestinal actin upon infection. *N. parisii* meront-infected IN4000 *YFP::ACT-5* animal. Note the extensive branched networks of ectopic *YFP::ACT-5* in basolateral regions. Lumen is slightly distended in this animal. Anterior is to the right, pharynx is just outside of the field of view. Video plays through a Z-stack of 35 images taken every 0.5 µm in a single animal. Video starts at the plane of focus toward the outside of the animal (similar to the plane of focus in Figure 2C), and end at the plane of focus inside the animal (similar to the plane of focus in Figure 2B). See Figure 2D for more anatomical information.
(MOV)

Acknowledgments

Some of the strains used in this work were provided by the *Caenorhabditis* Genetics Center, which is funded by National Institutes of Health Research Resources. The *act-5* mutant strain VC971 was provided by the *C. elegans* Reverse Genetics Core Facility at the University of British Columbia, which is part of the International *C. elegans* Gene Knockout Consortium. We thank F. Los and R. Aroian for help with propidium iodide assays, O. Bossinger, J. McGhee and J. Waddle for strains and M. Bakowski for help in quantifying spore number and preparing figures. We thank R. Aroian, M. Bakowski, E. Bier, A. Chisholm, T. Dunbar, M. Hansen, F. Los, R. Luallen, A. Ma, and S. Wasserman for helpful comments on the manuscript.

Author Contributions

Conceived and designed the experiments: ERT KAE SCS. Performed the experiments: ERT KAE SCS. Analyzed the data: ERT KAE SCS. Wrote the paper: ERT KAE.

References

1. Hybiske K, Stephens RS (2008) Exit strategies of intracellular pathogens. Nat Rev Microbiol 6: 99–110.
2. Hybiske K, Stephens RS (2007) Mechanisms of host cell exit by the intracellular bacterium Chlamydia. Proc Natl Acad Sci U S A 104: 11430–11435.

3. Hamon M, Bierne H, Cossart P (2006) Listeria monocytogenes: a multifaceted model. Nat Rev Microbiol 4: 423–434.
4. Hagedorn M, Rohde KH, Russell DG, Soldati T (2009) Infection by tubercular mycobacteria is spread by nonlytic ejection from their amoeba hosts. Science 323: 1729–1733.
5. Stamm LM, Pak MA, Morisaki JH, Snapper SB, Rottner K, et al. (2005) Role of the WASP family proteins for Mycobacterium marinum actin tail formation. Proc Natl Acad Sci U S A 102: 14837–14842.
6. McGhee JD (2007) The C. elegans intestine. WormBook. pp 1–36.
7. Gravato-Nobre MJ, Hodgkin J (2005) Caenorhabditis elegans as a model for innate immunity to pathogens. Cell Microbiol 7: 741–751.
8. Irazoqui JE, Urbach JM, Ausubel FM (2010) Evolution of host innate defence: insights from Caenorhabditis elegans and primitive invertebrates. Nat Rev Immunol 10: 47–58.
9. Troemel ER, Felix MA, Whiteman NK, Barriere A, Ausubel FM (2008) Microsporidia are natural intracellular parasites of the nematode Caenorhabditis elegans. PLoS Biol 6: 2736–2752.
10. Hodgkin J, Partridge FA (2008) Caenorhabditis elegans meets microsporidia: the nematode killers from Paris. PLoS Biol 6: 2634–2637.
11. Texier C, Vidau C, Vigues B, El Alaoui H, Delbac F (2010) Microsporidia: a model for minimal parasite-host interactions. Curr Opin Microbiol 13: 443–449.
12. Williams BA (2009) Unique physiology of host-parasite interactions in microsporidia infections. Cell Microbiol 11: 1551–1560.
13. Keeling PJ, Fast NM (2002) Microsporidia: biology and evolution of highly reduced intracellular parasites. Annu Rev Microbiol 56: 93–116.
14. Katinka MD, Duprat S, Cornillot E, Metenier G, Thomarat F, et al. (2001) Genome sequence and gene compaction of the eukaryote parasite Encephalitozoon cuniculi. Nature 414: 450–453.
15. Didier ES, Maddry JA, Brindley PJ, Stovall ME, Didier PJ (2005) Therapeutic strategies for human microsporidia infections. Expert Rev Anti Infect Ther 3: 419–434.
16. Keeling PJ, Luker MA, Palmer JD (2000) Evidence from beta-tubulin phylogeny that microsporidia evolved from within the fungi. Mol Biol Evol 17: 23–31.
17. Lee SC, Corradi N, Byrnes EJ, 3rd, Torres-Martinez S, Dietrich FS, et al. (2008) Microsporidia evolved from ancestral sexual fungi. Curr Biol 18: 1675–1679.
18. Didier ES, Weiss LM (2006) Microsporidiosis: current status. Curr Opin Infect Dis 19: 485–492.
19. Higes M, Martin-Hernandez R, Botias C, Bailon EG, Gonzalez-Porto AV, et al. (2008) How natural infection by Nosema ceranae causes honeybee colony collapse. Environ Microbiol 10: 2659–2669.
20. Shaw RWKM (1999) Fish Microsporidia. In: Wittner MWL, ed. The Microsporidia and Microsporidiosis: ASM. pp 418–446.
21. Troemel ER (2011) New Models of Microsporidiosis: Infections in Zebrafish, C. elegans, and Honey Bee. PLoS Pathog 7: e1001243.
22. Bromenshenk JJ, Henderson CB, Wick CH, Stanford MF, Zulich AW, et al. (2010) Iridovirus and Microsporidian Linked to Honey Bee Colony Decline. PLoS One 5: e13181.
23. MacQueen AJ, Baggett JJ, Perumov N, Bauer RA, Januszewski T, et al. (2005) ACT-5 is an essential Caenorhabditis elegans actin required for intestinal microvilli formation. Mol Biol Cell 16: 3247–3259.
24. Bossinger O, Fukushige T, Claeys M, Borgonie G, McGhee JD (2004) The apical disposition of the Caenorhabditis elegans intestinal terminal web is maintained by LET-413. Dev Biol 268: 448–456.
25. Husken K, Wiesenfahrt T, Abraham C, Windoffer R, Bossinger O, et al. (2008) Maintenance of the intestinal tube in Caenorhabditis elegans: the role of the intermediate filament protein IFC-2. Differentiation 76: 881–896.
26. Tan MW, Mahajan-Miklos S, Ausubel FM (1999) Killing of Caenorhabditis elegans by Pseudomonas aeruginosa used to model mammalian bacterial pathogenesis. Proc Natl Acad Sci U S A 96: 715–720.
27. Aballay A, Yorgey P, Ausubel FM (2000) Salmonella typhimurium proliferates and establishes a persistent infection in the intestine of Caenorhabditis elegans. Curr Biol 10: 1539–1542.
28. Labrousse A, Chauvet S, Couillault C, Kurz CL, Ewbank JJ (2000) Caenorhabditis elegans is a model host for Salmonella typhimurium. Curr Biol 10: 1543–1545.
29. Jia K, Thomas C, Akbar M, Sun Q, Adams-Huet B, et al. (2009) Autophagy genes protect against Salmonella typhimurium infection and mediate insulin signaling-regulated pathogen resistance. Proc Natl Acad Sci U S A 106: 14564–14569.
30. Sato T, Mushiake S, Kato Y, Sato K, Sato M, et al. (2007) The Rab8 GTPase regulates apical protein localization in intestinal cells. Nature 448: 366–369.
31. Los FC, Kao CY, Smitham J, McDonald KL, Ha C, et al. (2011) RAB-5- and RAB-11-Dependent Vesicle-Trafficking Pathways Are Required for Plasma Membrane Repair after Attack by Bacterial Pore-Forming Toxin. Cell Host Microbe 9: 147–157.
32. Grimm-Gunter EM, Revenu C, Ramos S, Hurbain I, Smyth N, et al. (2009) Plastin 1 binds to keratin and is required for terminal web assembly in the intestinal epithelium. Mol Biol Cell 20: 2549–2562.
33. Takemura R, Masaki T, Hirokawa N (1988) Developmental organization of the intestinal brush-border cytoskeleton. Cell Motil Cytoskeleton 9: 299–311.
34. Keller TC, 3rd, Conzelman KA, Chasan R, Mooseker MS (1985) Role of myosin in terminal web contraction in isolated intestinal epithelial brush borders. J Cell Biol 100: 1647–1655.
35. Keller TC, 3rd, Mooseker MS (1982) Ca++-calmodulin-dependent phosphorylation of myosin, and its role in brush border contraction in vitro. J Cell Biol 95: 943–959.
36. Carberry K, Wiesenfahrt T, Windoffer R, Bossinger O, Leube RE (2009) Intermediate filaments in Caenorhabditis elegans. Cell Motil Cytoskeleton 66: 852–864.
37. Bhavsar AP, Guttman JA, Finlay BB (2007) Manipulation of host-cell pathways by bacterial pathogens. Nature 449: 827–834.
38. Tsaousis AD, Kunji ER, Goldberg AV, Lucocq JM, Hirt RP, et al. (2008) A novel route for ATP acquisition by the remnant mitochondria of Encephalitozoon cuniculi. Nature 453: 553–556.
39. Anderson RM, May RM (1982) Coevolution of hosts and parasites. Parasitology 85(Pt 2): 411–426.
40. Frank SA (1996) Models of parasite virulence. Q Rev Biol 71: 37–78.
41. Chalifoux LV, MacKey J, Carville A, Shvetz D, Lin KC, et al. (1998) Ultrastructural morphology of Enterocytozoon bieneusi in biliary epithelium of rhesus macaques (Macaca mulatta). Vet Pathol 35: 292–296.
42. Conteas CN, Berlin OG, Ash LR, Pruthi JS (2000) Therapy for human gastrointestinal microsporidiosis. Am J Trop Med Hyg 63: 121–127.
43. Brenner S (1974) The genetics of Caenorhabditis elegans. Genetics 77: 71–94.
44. Powell JR, Ausubel FM (2008) Models of Caenorhabditis elegans infection by bacterial and fungal pathogens. Methods Mol Biol 415: 403–427.

3.1 Supplemental Figures and Tables

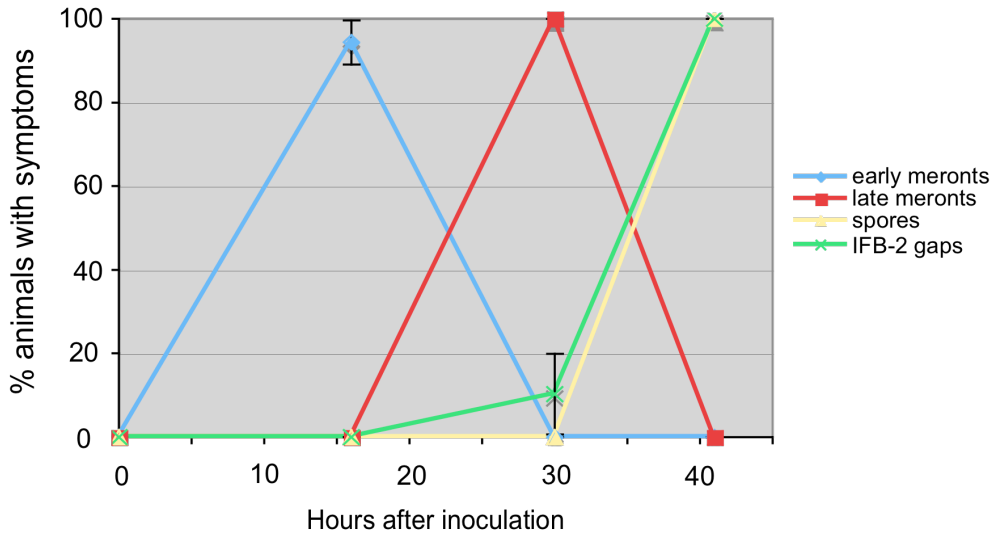

Figure 3-S1. Terminal web restructuring in *IFB-2::CFP* single transgenic animals. Kinetics of terminal web restructuring and parasite development in a population of animals infected at time = 0 hours. Data shown are the average of two independent experiments with 50 animals scored at each timepoint in each experiment (for a total of at least 100 animals scored at each timepoint). Error bars are SD.

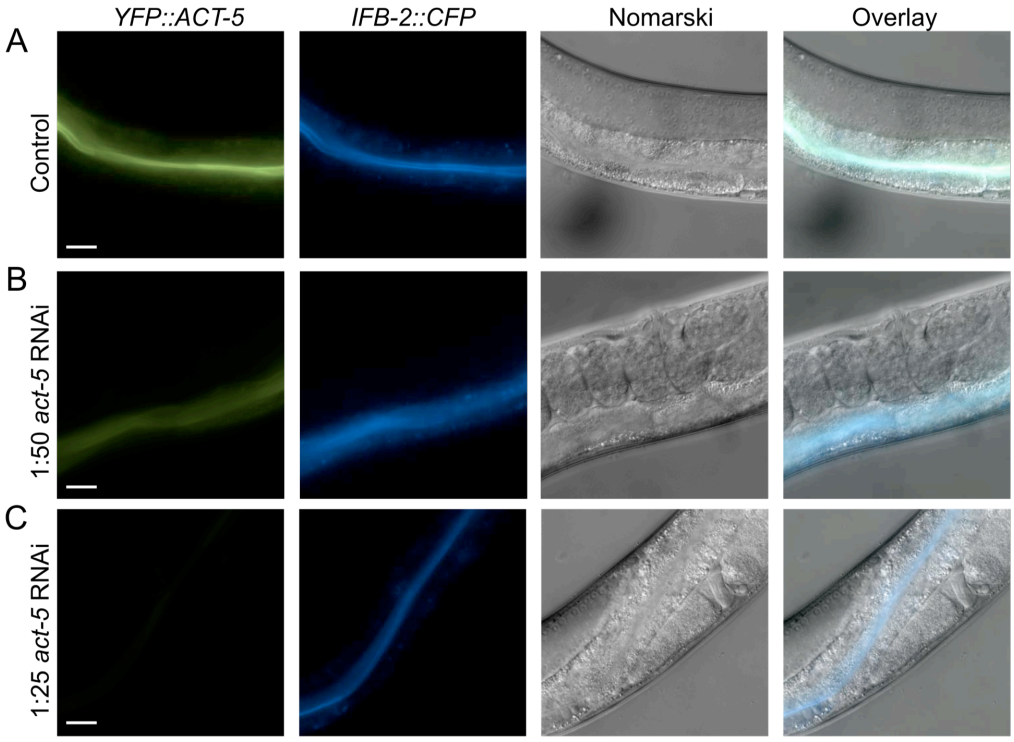

Figure 3-S2. Diluted RNAi against *act-5* causes reduction in *YFP::ACT-5* expression. *YFP::ACT-5*; *IFB-2::CFP* animals treated with control RNAi (A), 1:50 dilution of *act-5* RNAi (B) and 1:25 dilution of *act-5* RNAi (C). First column on left is images in the YFP channel, second column is CFP channel, third column is Nomarski brightfield and fourth column is an overlay of all three channels. Images in YFP and CFP channels were taken with same exposure time: note decreased level of *YFP::ACT-5* signal with 1:50 *act-5* RNAi and further decreased level with 1:25 *act-5* RNAi. Scale bar is 20 mm.

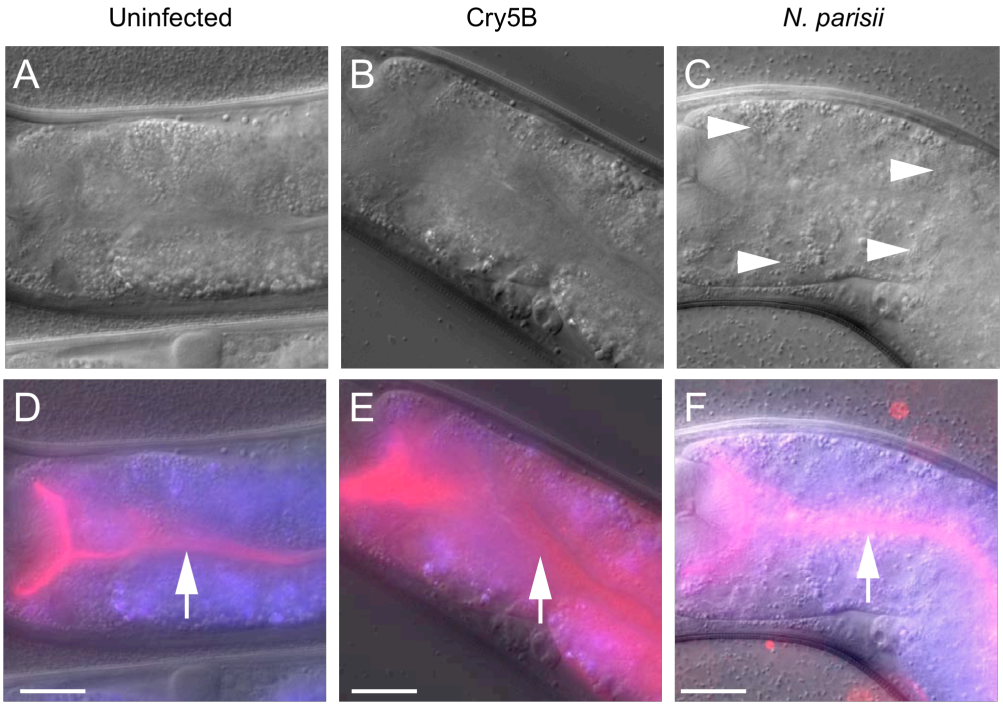

Figure 3-S3. Nomarski images of animals analyzed for cellular integrity. In order to illustrate intestinal cell morphology, the same animals shown in Figure 3-8 A–F are shown in this figure with Nomarski brightfield imaging in A–C and Nomarski overlay with propidium iodide in red and autofluorescence in blue D–F. Upward arrows in D–F indicate lumen. Arrowheads in C indicate two examples of clusters of *N. parisii* spores, which are false-colored green. Scale bar is 20 mm.

Table 3-S1. Longitudinal studies of ACT-5 and IFB-2 changes in individual animals throughout infection.

Study #1

Worm #	16.5 hpi	23 hpi	28 hpi	40 hpi
1	2 circular meronts in mid-intestine	full of meronts all over, no ACT-5 phenotype, no IFB-2 gaps	heavy meronts, basolateral ACT-5, no IFB-2 gaps	spores, 1 small ACT-5 ectopic structure, IFB-2 gaps
2	circular meronts near posterior of intestine	slightly expanded meronts near posterior of intestine, no ACT-5 phenotype, no IFB-2 gaps	mid-meronts, basolateral ACT-5, no IFB-2 gaps	heavy meronts anterior, spores posterior, no ACT-5 phenotype, IFB-2 gaps by spores, not by meronts.
3	circular meronts posterior of mid-intestine	a few other meronts appeard, still small, no ACT-5 phenotype, no IFB-2 gaps	mid-meronts, some basolateral ACT-5, no IFB-2 gaps	heavy meronts anterior, spores posterior, no ACT-5 phenotype, IFB-2 gaps posterior
4	2 small meronts near posterior	meronts expanded in good portion of body, no ACT-5 phenotype, no IFB-2 gaps	heavy meronts in tail, basolateral ACT-5, no IFB-2 gaps	heavy meronts anterior, spores posterior, no ACT-5 phenotype, IFB-2 gaps posterior
5	meront very anterior-next to pharynx, anterior to 1st intestinal nucleus	meront mostly unchanged, no ACT-5 phenotype, no IFB-2 gaps	meronts growing slowly, basolateral ACT-5, no IFB-2 gaps	heavy meronts anterior, spores posterior, ACT-5 branched networks in heavy meronts in midbody, IFB-2 gaps there also
6	uninfected	uninfected	mid-meronts in tail, no ACT-5 phenotype, no IFB-2 gaps	heavy meronts anterior, spores posterior, some branched networks and basolateral ACT-5, IFB-2 gaps by ectopic ACT-5 and spores
7	uninfected	small groove-like meronts, basolateral ACT-5 expression near most pronounced meront, no IFB-2 gaps	posterior-mid meronts, basolateral ACT-5, no IFB-2 gaps	heavy meronts anterior, spores posterior, ACT-5 branched networks, no IFB-2 gaps by ectopic ACT-5 only by spores
8	meronts in posterior-adjacent to a nucleus, 2-3 near various nuclei in posterior of worm	expanded meront, no ACT-5 phenotype, no IFB-2 gaps	tail-heavy meronts, anterior early meronts, no ACT-5 phenotype, no IFB-2 gaps	heavy meronts anterior, spores posterior, no ACT-5 phenotype, IFB-2 gaps
9	oblong-shaped and circular meronts mid-intestine	posterior meront expanded a bit, no ACT-5 phenotype, no IFB-2 gaps	posterior-heavy meronts, basolateral ACT-5 in posterior, no IFB-2 gaps	heavy meronts anterior, spores posterior, no ACT-5 phenotype, IFB-2 gaps by spores
10	some meronts very anterior, some just posterior of mid-intestine, some even further back, most near nuclei	some expanded meronts near mid-intestine, no ACT-5 phenotype, no IFB-2 gaps	posterior-heavy meronts, basolateral ACT-5 by meronts, no IFB-2 gaps,	mostly spores, no ACT-5 phenotype, IFB-2 gaps

Study #2

Worm #	24 hpi	29.5 hpi	34.5 hpi	48 hpi
1	medium meronts posterior, early meronts anterior, no ACT-5 phenotype or IFB-2 gaps	heavy meronts middle of worm, meronts in anterior and posterior, basolateral ACT-5, puncta in/around lumen, no IFB-2 gaps	heavy meronts, basolateral and some ACT-5 branched networks, puncta near lumen in ACT-5, no IFB-2 gaps	IFB-2 gaps
2	oblong medium meronts anterior to but near mid-intestine. Many oblong meronts in posterior, no ACT-5 phenotype, no IFB-2 gaps	heavy meronts, basolateral ACT-5, no IFB-2 gaps	heavy meronts, basolateral and some ACT-5 branched networks, no IFB-2 gaps	IFB-2 gaps
3	oblong meront anterior to mid-intestine, no ACT-5 phenotype, no IFB-2 gaps	heavy meronts, basolateral ACT-5, beginnings of ectopic network no IFB-2 gaps	heavy meronts, basolateral ACT-5, no IFB-2 gaps	IFB-2 gaps
4	circular and oblong meronts in posterior, basolateral ACT-5, no IFB-2 gaps	heavy meronts, basolateral ACT-5, no IFB-2 gaps	heavy meronts, basolateral and ACT-5 around circular meronts, no IFB-2 gaps	IFB-2 gaps
5	mid meronts in posterior, oblong in anterior next to anterior-most nuclei, basolateral ACT-5, no IFB 2 gaps	heavy meronts, basolateral ACT-5, no IFB-2 gaps	heavy meronts, basolateral ACT-5, no IFB-2 gaps	IFB-2 gaps
8	mid meront in middle of worm, ectopic ACT-5	mid meronts, basolateral ACT-5, no IFB-2 gaps	heavy meronts, basolateral and ACT-5 networks, no IFB-2 gaps	dead (due to experimental damage)
9	a few oblong meronts in far anterior and near mid-intestine, hard to see posterior, no ACT-5 phenotype, no IFB-2 gaps	early meronts/mid meronts, basolateral ACT-5, no IFB-2 gaps	heavy meronts posterior, mid meronts anterior, ACT-5 basolateral, no IFB-2 gaps	IFB-2 gaps
10	mid meronts near and anterior to mid-intestine, posterior also, some basolateral ACT-5, overlap of IFB-2 in basolateral staining also, no IFB-2 gaps	very posterior heavy meronts, rest of worm early/mid meronts, basolateral ACT-5, no IFB-2 gaps	heavy meronts, basolateral ACT-5, some basolateral IFB-2? No IFB-2 gaps	IFB-2 gaps

Table 3-S2. Analysis of *IFB-2::CFP* terminal web gap number and size in a population of animals.

Quantitation of gap number. These data contributed to plot in Figure 5B

40hpi

Worm #	Total quadrant size analyzed (μm^2)	# gaps	# gaps/μm^2
1	137.3	15	0.109
2	187.4	14	0.075
3	141.9	28	0.197
4	119.6	18	0.151
5	140.2	28	0.200
6	82.9	17	0.205
7	151.6	20	0.132
8	159.3	34	0.213
9	170.1	39	0.229
10	92.4	35	0.379

62-64hpi

Worm #	Total quadrant size analyzed (μm^2)	# gaps	# gaps/μm^2
11	198.3	17	0.086
12	157.8	22	0.139
13	163.2	20	0.123
14	191.8	27	0.141
15	154.6	35	0.226
16	344.5	33	0.096
17	115.4	28	0.243
18	197.5	31	0.157
19	162.4	29	0.179
20	254.8	30	0.118

Quantitation of gap size, with several gaps counted per worm. These data contributed to plot in Figure 5C

40hpi

Worm #	Quadrant area analyzed for gap size measurements (μm^2)	Gap size (μm^2)
1	34.32	0.79
		0.48
		0.79
		0.13
2	46.85	1.31
		4.23
		1.12
		1.06
		1.72
3	35.47	2.09
		0.36
		0.3
		0.94
		0.28
		0.17
		0.65
4	29.9	0.17
		2.18
		0.33
		0.44
		0.17
		0.98
		2.1
5	35.05	0.55
		0.11
		0.21
		0.55
		0.49
		0.71
		0.38
		0.17
		0.2
		0.15
6	20.7	0.85
		1.47
		1.37
		0.67
7	37.9	4.65
		1.19
		0.83
		0.3
8	39.8	1.15
		0.37
		0.45
		0.62
		0.33
		0.65
		0.44
		0.25
		0.36
9	42.5	1.02
		0.94
		0.63
		0.88
		1.48
		0.41
10	23.1	1.39
		0.41
		0.25
		0.33
		0.66
		0.7
		0.29
		0.61

62-64hpi

Worm #	Quadrant area analyzed for gap size measurements (μm^2)	Gap size (μm^2)
11	49.57	11.8
		2.94
		1.16
		2.46
		2.14
12	39.45	6.52
		1.77
		0.32
		0.7
		5.96
13	40.8	4.17
		3.95
		1.98
		1.35
		2.43
		1.48
		0.71
14	47.95	3.1
		1.03
		2.98
		4.41
		3.68
15	38.65	2.73
		0.71
		2.17
		0.16
		0.28
		0.34
		1.16
		4.38
16	86.12	6.46
		3
		10.09
		0.85
		2.38
		4.17
		0.58
		2.67
		1.04
		0.67
		1.39
		6.21
		7.83
		3.88
		5.18
		1.65
17	28.85	1.43
		1.02
		0.45
		0.88
		0.44
		0.48
		2.03
		2.67
		0.55
18	49.37	7.05
		4.58
		1.11
		0.67
		11.11
		5.59
19	40.6	0.87
		2.73
		1.51
		0.59
		1.73
		1.99
		2.77
20	63.7	4.49
		4.46
		0.55
		10.52
		3.5
		4.19

Table 3-S3. Analysis of *IFB-2::CFP* terminal web gap number and size in a longitudinal study of individual animals.

Quantitation of gap number. These data contributed to plot in Figure 5B

40hpi

Worm #	Total quadrant size analyzed (μm^2)	# gaps	# gaps/μm^2
1	74.1	16	0.216
2	83.1	21	0.253
3	77.7	12	0.154
4	193.4	24	0.124
5	113.1	10	0.088
6	74.9	13	0.174
7	92.8	21	0.226
8	162.5	38	0.234
9	86.1	18	0.209
10	79.9	24	0.300

62-64hpi

Worm #	Total quadrant size analyzed (μm^2)	# gaps	# gaps/μm^2
1	139.8	29	0.207
2	144.9	24	0.166
3	167.2	43	0.257
4	186.9	28	0.150
5	165.9	27	0.163
6	94.8	26	0.274
7	90.6	25	0.276
8	88	31	0.352
9	318.3	28	0.088
10	108.4	23	0.212

Quantitation of gap size, with several gaps counted per worm. These data contributed to plot in Figure 5C

40hpi

Worm #	Quadrant area analyzed for gap size measurements (μm^2)	Gap size (μm^2)
1	18.525	0.81
		0.46
		0.57
		0.99
		0.21
2	20.775	3.87
		0.42
		0.78
		1.35
		0.36
		0.21
3	19.425	0.3
		0.42
		1.15
4	48.35	2.18
		5.68
		2.22
		1.77
		0.42
		1.02
		0.41
5	28.275	0.51
		1.53
		0.37
6	18.725	1.57
		2.77
		2.31
		1.51
7	23.2	0.21
		0.34
		0.25
		0.87
		0.24
8	40.625	1.48
		0.37
		1.29
		0.07
		0.11
		1.48
		0.36
		0.18
		0.26
		0.82
9	21.525	1.06
		0.51
		0.55
		1.27
		0.61
		0.28
10	19.975	0.34
		0.13
		0.24
		0.11
		1.12
		0.5

62-64hpi

Worm #	Quadrant area analyzed for gap size measurements (μm^2)	Gap size (μm^2)
1	34.95	2.14
		1.07
		1.21
		0.77
		0.2
2	36.225	4.25
		0.25
		0.74
		0.82
		1.31
		0.9
3	41.8	0.21
		0.18
		0.4
		0.85
		0.4
		0.17
		0.2
		0.94
		1.81
4	46.725	3.43
		9.15
		8.87
		1.25
		1.35
		0.82
		1.37
		1.65
5	41.475	1.78
		1.51
		1.27
		1.02
		0.55
		0.57
		0.71
		0.74
6	23.7	0.92
		0.94
		0.38
		0.16
		2.80
		0.41
		0.25
		0.25
7	22.65	1.10
		1.15
		1.99
		1.32
		0.55
		0.41
		1.11
8	22	2.54
		1.40
		1.20
		2.14
		1.12
9	79.575	6.42
		9.78
		7.42
		21.35
		3.60
		2.01
		1.25
10	27.1	1.76
		0.91
		1.28
		0.75
		0.42
		0.13
		1.29

3.2 Additional Acknowledgements

Chapter 3, in full, is reprinted from PLoS Pathogens, 7, Estes, K.; Szumowski, S.; Troemel, E., Non-lytic, actin-based exit of intracellular parasites from *C. elegans* intestinal cells, e1002227, (2011), with permission from PLoS. The dissertation author was the second author of this paper. Author contributions to manuscript are as follows: Estes, K.: Figure 1, Figure 2, Figure 3, Figure 4, Figure 5, Figure 6A, 6B, 6C, Figure 8, all Supplemental Figures; Szumowski, S.: Figure 7, all experiments requested for peer review; Troemel, E.: Figure 6D.

4 The small GTPase RAB-11 directs polarized exocytosis of the intracellular pathogen *N. parisii* for fecal-oral transmission from *C. elegans*

The small GTPase RAB-11 directs polarized exocytosis of the intracellular pathogen *N. parisii* for fecal-oral transmission from *C. elegans*

Suzannah C. Szumowski, Michael R. Botts, John J. Popovich, Margery G. Smelkinson, and Emily R. Troemel[1]

Division of Biological Sciences, Section of Cell and Developmental Biology, University of California at San Diego, La Jolla, CA 92093

Edited by Philippe J. Sansonetti, Institut Pasteur, Paris, France, and approved April 25, 2014 (received for review January 13, 2014)

Pathogen exit is a key stage in the spread and propagation of infectious disease, with the fecal-oral route being a common mode of disease transmission. However, it is poorly understood which molecular pathways provide the major modes for intracellular pathogen exit and fecal-oral transmission in vivo. Here, we use the transparent nematode *Caenorhabditis elegans* to investigate intestinal cell exit and fecal-oral transmission by the natural intracellular pathogen *Nematocida parisii*, which is a recently identified species of microsporidia. We show that *N. parisii* exits from polarized host intestinal cells by co-opting the host vesicle trafficking system and escaping into the lumen. Using a genetic screen, we identified components of the host endocytic recycling pathway that are required for *N. parisii* spore exit via exocytosis. In particular, we show that the small GTPase RAB-11 localizes to apical spores, is required for spore-containing compartments to fuse with the apical plasma membrane, and is required for spore exit. In addition, we find that RAB-11–deficient animals exhibit impaired contagiousness, supporting an in vivo role for this host trafficking factor in microsporidia disease transmission. Altogether, these findings provide an in vivo example of the major mode of exit used by a natural pathogen for disease spread via fecal-oral transmission.

After invasion and replication inside of host cells, intracellular pathogens must escape back into the environment to find new hosts and propagate disease. Although pathogen exit is not as well understood as pathogen entry, there are a variety of exit strategies that have been described recently, including both lytic and nonlytic egress from host cells (1, 2). These studies in tissue culture cells have identified a diversity of host pathways and processes in pathogen exit. In some cases, multiple modes of exit have been implicated for the same pathogen, although it is still poorly understood which modes of exit are crucial for disease transmission of any microbial pathogen in a whole animal host.

One of the major sites for pathogen infection in animals is the intestine, which can be invaded by intracellular pathogens that cause food and water-borne disease (3). These pathogens must exit from intestinal cells back into the lumen to be released by defecation for disease transmission. Intestinal pathogens are often studied in tissue culture models, but their life cycles can proceed differently in intact intestinal cells. For example, the bacterial pathogen *Listeria monocytogenes* is initially entrapped in a membrane-bound compartment after entering host cells. When infecting tissue culture cells, *Listeria* escapes from this compartment into the host cytosol, and then spreads between cells by a protrusion mechanism (4). In contrast, it uses a different strategy in vivo. When infecting mice, *Listeria* does not escape from the membrane-bound compartment and instead remains membrane-bound, ultimately exiting basolaterally from intestinal cells by exocytosis to spread systemically into the host (5). However, it is not known how *Listeria* escapes back into the intestinal lumen for transmission to new hosts. These differing results of *Listeria* trafficking in vitro and in vivo highlight the importance of investigating pathogen exit in a whole-animal host.

The nematode *C. elegans* provides an accessible whole-animal host in which to dissect the life cycle and transmission of intestinal pathogens (6, 7). The *C. elegans* intestine consists of 20 nonrenewable epithelial cells that share many morphological similarities with mammalian intestinal epithelial cells (Fig. 1*A*). These cells are polarized, with microvilli on the apical side facing the lumen of the intestinal tract. Like in humans, these microvilli are anchored into a cytoskeletal structure called the terminal web that is composed of actin and intermediate filaments (8). *C. elegans* is transparent, which facilitates analysis of infection in these cells within intact animals. We recently described a natural intracellular pathogen that infects the *C. elegans* intestine and showed that this pathogen defines a new genus and species of microsporidia, which are obligate, fungal-related intracellular pathogens (9, 10). The microsporidia phylum comprises more than 1,400 species of pathogens that can infect a wide variety of animals including humans, where they commonly infect the intestine and can cause lethal diarrhea in immunocompromised hosts (11, 12). We named the *C. elegans*-infecting species of microsporidia *Nematocida parisii*, or nematode killer from Paris, because it was isolated from wild-caught *C. elegans* in a compost pit near Paris and it eventually kills its host. Wild-caught *Caenorhabditis* nematodes infected with microsporidia have been isolated from environmental regions around the globe, indicating that microsporidia are a common cause of infection for *C. elegans* in the wild (9, 13).

Microsporidia are obligate intracellular pathogens, meaning they must be inside of a host cell to replicate. Microsporidia survive outside the host as transmissible spores, which deploy a dramatic invasion mechanism to enter host cells. These spores contain a specialized structure called a polar tube, which "fires"

Significance

Microbial pathogens cause food and water-borne disease through infection of the intestine. Many of these pathogens invade intestinal cells to replicate, but they ultimately need to exit out of these cells to spread to new hosts. We use the transparent nematode *Caenorhabditis elegans* to show that a natural intracellular pathogen called *Nematocida parisii* escapes from intestinal cells by using host trafficking pathways and a host small GTPase protein called RAB-11 for directional exocytosis into the lumen. *N. parisii* belongs to a large phylum of pathogens called microsporidia that can infect all animals, including humans, so our findings may be broadly applicable to understanding how agriculturally and medically relevant diseases are spread.

Author contributions: S.C.S., M.R.B., M.G.S., and E.R.T. designed research; S.C.S., M.R.B., J.J.P., M.G.S., and E.R.T. performed research; S.C.S., M.R.B., M.G.S., and E.R.T. analyzed data; and S.C.S. and E.R.T. wrote the paper.

The authors declare no conflict of interest.

This article is a PNAS Direct Submission.

[1]To whom correspondence should be addressed. E-mail: etroemel@ucsd.edu.

This article contains supporting information online at www.pnas.org/lookup/suppl/doi:10.1073/pnas.1400696111/-/DCSupplemental.

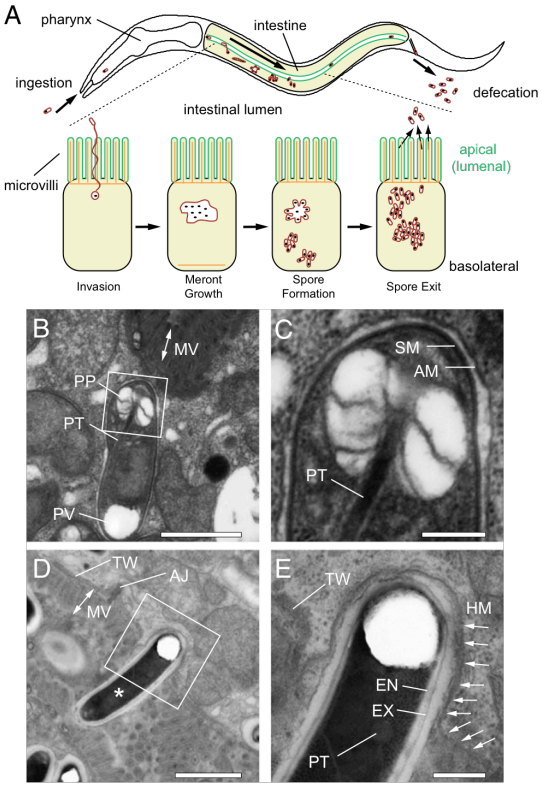

Fig. 1. *N. parisii* spores are contained in an additional membrane-bound compartment inside *C. elegans* intestinal cells. (*A*) The *C. elegans* intestine (in yellow) is comprised of polarized epithelial cells. The apical side (green) faces the lumen and contains actin-rich microvilli anchored into a terminal web (actin labeled orange). Ingested *N. parisii* spores invade intestinal cells by using a polar tube that delivers spore contents directly in host cytosol, where it replicates in the multinucleate meront stage. The pathogen eventually develops back into the spore form, which exits back into the lumen for defecation from the animal. Arrow within intestine indicates the progression of infection over time. (*B*) TEM of an immature *N. parisii* spore. (*C*) Magnification of box from *B* shows the additional membrane (AM) that surrounds the spore membrane (SM). (*D*) A mature spore (asterisk) spanning the luminal membrane. (*E*) Magnification of box from *D*. Arrows indicate continuous host apical membrane (HM) that surrounds the spore. (*B–E*) AJ, apical junction; EN, endospore; EX, exospore; MV, microvilli; PP, polaroplast; PT, polar tube; PV, polar vacuole; TW, terminal web. (Scale bars: *B* and *D*, 1 μm; *C* and *E*, 500 nm.)

to pierce a host cell, and then the parasite nucleus and sporoplasm are injected through this tube directly into the host cytosol (Fig. 1*A*). In the case of *N. parisii* and in most microsporidia species, the pathogen then grows inside the host cell in a replicative meront form that appears to be in direct contact with the host cytosol (9, 14). *N. parisii* meronts become large and multinucleate as they develop and eventually differentiate back into mononucleate cells that become spores, which are shed to transmit the infection (9).

How do *N. parisii* spores exit from host intestinal cells? Previously we showed that extensive cytoskeletal rearrangements occur during the meront stage, with relocalization of *C. elegans* actin from the apical to the basolateral side of intestinal cells (15). This relocalization appears to trigger gap formation in the terminal web as a mechanism to remove this barrier to pathogen exit. We found that *N. parisii* spore exit is nonlytic and that spores do not bud out of the host cell, because spores are released into the lumen free of host membrane. However, the precise exit mechanism was not clear. Our results were consistent with either an exocytic mechanism, which would involve membrane-bound spores fusing with the host plasma membrane, or an ejectosome mechanism, which would involve an actin-rich structure at the plasma membrane that delivers microbes directly from the cytosol into the extracellular environment (16). Here, we show that *N. parisii* spores are in a separate membrane-bound compartment, supporting an exocytic mode of exit. We performed a screen for *C. elegans* small GTPases required for *N. parisii* spore exit and found that components of the endocytic recycling pathway are critical for exit, with the RAB-11 protein acting as a key player in this process. RAB-11 localizes to apically polarized spores, is required for spore-containing compartments to fuse with the apical plasma membrane, and is critical for pathogen exit and for contagiousness. Altogether these studies define endocytic recycling and exocytosis to be key processes for microsporidia exit, and the major mechanism of exit for fecal-oral transmission of an intestinal pathogen in vivo.

Results

***N. parisii* Spores Are Contained in Separate Compartments Inside of Host Intestinal Cells.** As noted above, our previous findings implied that *N. parisii* exit involves either an ejectosome-like mechanism, or an exocytic event in which an intracellular compartment containing a spore fuses with the host apical membrane. To distinguish between these possibilities, we used transmission electron microscopy (TEM) to examine whether there is membrane localization around newly replicated *N. parisii* spores while inside of *C. elegans* intestinal cells. Indeed, we found that intracellular spores were always contained in an additional membrane ($n = 42$ spores examined; immature intracellular spore shown in Fig. 1 *B* and *C* and more mature spores shown in Fig. S1 *A–D*). In addition, we observed plasma membrane surrounding mature spores that appear to be in the process of exiting through host microvilli into the lumen. Occasionally we were able to see that the membrane around these exiting spores is continuous with the host plasma membrane, indicating that the spore-containing compartment (SCC) is fusing with the apical membrane of the host intestine (Fig. 1 *D* and *E*).

***N. parisii* Spore-Containing Compartments Fuse with Host Membrane To Access the Intestinal Lumen.** To confirm that the additional membrane around apically fused *N. parisii* spores was continuous with host-derived membrane, we examined the localization of GFP-tagged *C. elegans* apical membrane markers in infected animals. We infected animals expressing the apical membrane transporter protein *PGP-1::GFP* with *N. parisii* spores, let the infection progress to generate new spores, and then looked at these spores to determine whether they colocalized with the host GFP-tagged membrane (17). Indeed, we found that *PGP-1::GFP* colocalizes with SCCs fused along the apical cell surface that appear to be exiting into the lumen (Fig. 2*A*). Similarly, the apical plasma membrane marker *SID-2::GFP* (18) also localizes to spores along the apical cell surface (Fig. 2*B*). However, we did not observe colocalization of the apical membrane transporter *PEPT-1::DsRed* (19) with *N. parisii* spores (Fig. S1*E*), suggesting that some membrane markers may not mix as easily with the *N. parisii*-containing compartments, or that there is heterogeneity of protein components in the plasma membrane regions where *N. parisii* exits. These experiments suggest that *N. parisii* spores arrive at the apical membrane in compartments that fuse with the apical plasma membrane of *C. elegans* intestinal cells.

After fusion with the plasma membrane, the cargo inside an exocytic vesicle should have access to the luminal environment via the fusion pore. We therefore tested whether spores marked with apical membrane marker were in contact with the intestinal lumen by feeding infected animals the cell-impermeable dye

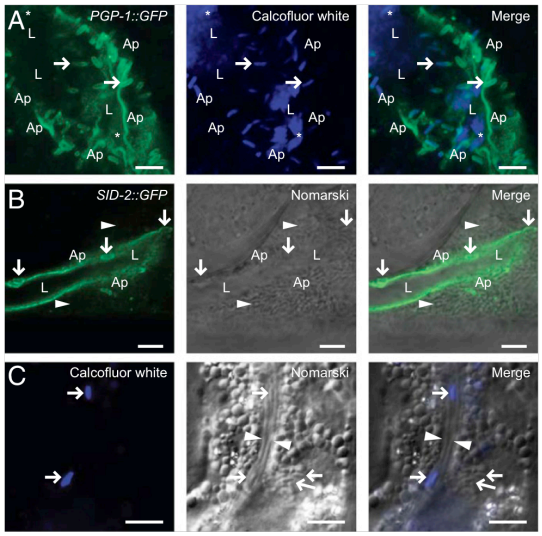

Fig. 2. *N. parisii* spores are surrounded by host apical membrane and have access to the intestinal lumen. (*A*) *PGP-1::GFP* localizes to SCCs fused with host apical membrane. Calcofluor white stains spores in contact with the lumen. Asterisk marks spores free in the lumen, rightward facing arrows mark putative exiting spores that stain with Calcofluor white and *PGP-1::GFP*. (*B*) *SID-2::GFP* surrounds SCCs fused to apical membrane (downward arrows). Arrowheads indicate intracellular spores not stained by Calcofluor white. Ap, apical; L, lumen. (*C*) Calcofluor white does not stain intracellular spores (leftward facing arrows), but does stain spores in lumen (rightward facing arrows). Lumen is indicated by arrowheads. (Scale bars: *A* and *B*, 5 μm; *C*, 10 μm.)

Calcofluor white, which binds chitin found in the spore walls of microsporidia. When fed to *C. elegans*, Calcofluor white only stains spores in contact with the lumen, and not spores inside of intestinal cells (Fig. 2*C*). We found that spores cloaked in the apical membrane marker *PGP-1::GFP* also were marked with Calcofluor white (Fig. 2*A*). Taken together, these results show that intracellular spores are contained in compartments that are able to fuse with the host apical membrane and gain access to the intestinal lumen for exit.

The results described above, together with our previous results (9), indicate that *N. parisii* replicates in direct contact with the cytosol during its meront stage, and then is contained in exocytic compartments at the differentiated spore stage. One likely candidate pathway to mediate this transition from membrane-free to membrane-bound is the autophagy pathway (20). To determine whether the autophagy pathway is important for *N. parisii* exit from the host, we knocked down expression of key host autophagy components using feeding RNAi, infected these animals, and then quantified spore exit. Previously, we demonstrated that an individual infected *C. elegans* animal can shed thousands of *N. parisii* spores per hour, and that spores exit only from the apical side of host cells (15). To measure this exit, we use spore-shedding assays starting at 40 h postinoculation (hpi), when *N. parisii* has differentiated from meronts into spores that are exiting from cells into the lumen and are being defecated out by the host (Fig. S2*A*). Using this assay, we found that RNAi against the autophagy components *atg-18, bec-1,* and *lgg-1* had no significant effect on spore exit (Fig. S2*B*). The RNAi clones appeared to knock down their targets, as assessed by a loss of *GFP::LGG-1* protein in the intestine upon *lgg-1* RNAi treatment (Fig. S2*C*), and a reduction of *GFP::LGG-1* puncta (a standard measure of autophagy) upon *atg-18* and *bec-1* RNAi (Fig. S2*D*). Thus, these results suggest that autophagy is not important for *N. parisii* spore maturation and exit.

Small GTPases Involved in Apical Endocytic Recycling Are Required for Spore Exit. To identify which host factors are required for directional exit of *N. parisii* from intestinal cells, we conducted a feeding RNAi screen of 41 predicted small GTPases (smGTPases) in *C. elegans*, because these factors are involved in many intracellular trafficking events (21). Again we used spore-shedding assays to measure *N. parisii* exit (Fig. S2*A*). Knockdown of genes that caused developmental defects in animals were excluded from analysis (*ran-1, sar-1*) or diluted 10-fold with L4440 empty-vector bacteria (*rab-5, rab-11.1*) to achieve normal development of animals assayed for pathogen exit.

We found that of the 41 genes tested, RNAi knockdown of the smGTPases *rab-2, rab-5*, *rab-10, rab-11.1*, *rab-18, arf-3, arl-5*, and *ral-1* caused significant defects in spore shedding (Fig. S3). These hits from our screen were reanalyzed in independent experiments to confirm the screen results (Fig. 3*A*). Notably, most of these screen hits (*rab-2, rab-5, rab-10, rab-11.1*, and *rab-18*) are implicated in apical recycling pathways, which can direct intracellular cargo up to the apical membrane (22, 23). To ensure that RNAi clones that block spore exit do not simply block *N. parisii* spore development, we examined whether RNAi treatment impaired spore production by using two different methods. First, we examined individual animals semiquantitatively for the amount of intracellular spores produced, and we found no change after any RNAi treatment (Fig. 3*B*) (Friedman's test; ANOVA $P = 0.6081$). In addition, we lysed infected animals to quantitatively assess the number of intracellular spores produced on a population level and again found no difference (Fig. 3*C*). Furthermore, because a defect in spore shedding could also be due to a global disruption of cell polarity, which then could cause a disruption in intracellular trafficking pathways, we also examined whether knocking down these smGTPases affected cell polarity. We analyzed the polarized distribution of the apically localized protein *PGP-1::GFP* and found its localization to be unaffected by any of the RNAi treatments that cause spore shedding defects (Fig. S4). Altogether, these results indicate that blocking expression of these smGTPase proteins does not disrupt spore formation or cell polarity and, instead, disrupts spore exit from the animal.

An additional explanation for reduced spore shedding is that animals are simply defecating less overall volume, which then leads to fewer spores being shed. Accurately measuring the volume defecated by a tiny animal such as *C. elegans* is difficult, and quantifying the number of spores present in the lumen before defecation is challenging and is also confounded by defecation defects. Therefore, to investigate spore exit into the lumen, we developed an assay to measure the density of spores within the contents defecated out of the lumen. We pulse-fed infected animals fluorescent beads and then measured the ratio of spores to fluorescent beads in the defecated material. With this assay, we found a significantly reduced ratio of spores to beads in the contents defecated from *rab-5, rab-10,* and *rab-11.1*-defective animals (Fig. 3 *D* and *E*). Therefore, knockdown of these smGTPases causes a spore shedding defect because of a defect in *N. parisii* spore egress into the lumen, and not simply because of a reduction in defecation volume. In contrast, the spore-shedding defect of *arf-3*–defective animals appears to be solely due to a defecation defect, because the spore density in these defecation contents was similar to that of control animals and the number of defecations per animal was much smaller (Fig. 3*D*). Taken together, these experiments confirm the importance of the apical recycling components RAB-5, RAB-10, and RAB-11 for spore egress from intestinal cells into the intestinal lumen.

RAB-11 Localizes to Spores near the Apical Side of Intestinal Cells. Because endocytic recycling appears to be a pathway required for spore exit, we next examined whether apical endocytic

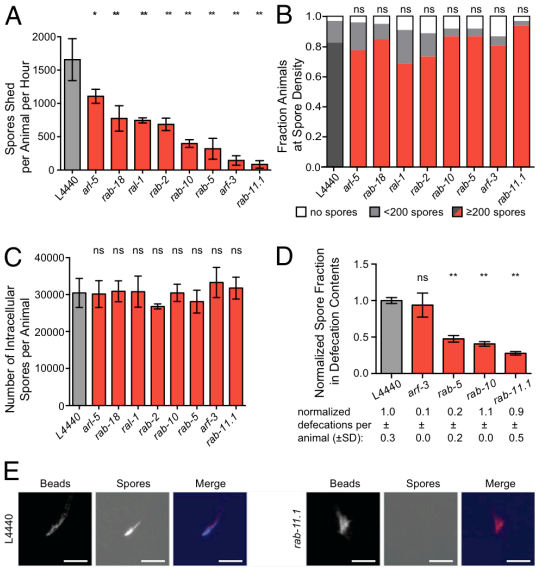

Fig. 3. Host small GTPases in the apical endocytic recycling pathway are required for spore exit. (*A*) Quantification of spore shedding defects in RNAi hits. Average is from three biological replicates; error bars are SD. Experiments were repeated three independent times for *rab-5, rab-10, and rab-11* and two independent times for other genes. (*B*) Spore production in individual assay. Dark gray or red is the fraction of animals with ≥200 spores per animal; light gray with <200 spores per animal; and white with no spores. $n = 40$ animals per treatment group. (*C*) Spore production in population assay. *y* axis indicates the number of intracellular spores per animal after lysis at 44 hpi. Error bars are SD. (*D*) Defecation contents assay. *y* axis indicates the normalized contribution of fluorescent signal from spores in defecated material. Average is from three independent experiments (except for *arf-3*, which was tested twice), error bars are SEM. See *Materials and Methods* for more detail. Number of defecation events is the average from 48 to 96 animals, ± SD. (*E*) Representative images of defecated material quantified in *D* showing fluorescent beads and Calcofluor white spores shed by animals. (Scale bars: 50 μm.)

recycling factors localize to *N. parisii* spores. The Rab11 subfamily comprises Rab11a, Rab11b, and Rab25 in mammals, and they are well-known markers of recycling endosomes, with Rab11a in particular shown to play a key role in targeting endosomes to the apical plasma membrane (24–28). *C. elegans* has two RAB-11 subfamily members called RAB-11.1 and RAB-11.2, which both are most similar to mammalian Rab11a. *C. elegans* RAB-11.1 has been studied in intestinal cell trafficking, where it is apically localized (19, 22) (Fig. 4*A*). Because the *rab-11.1* RNAi clone caused a stronger block in spore shedding than did *rab-11.2*, and because the *rab-11.2* knockdown also reduces RAB-11.1 expression levels (Fig. S5) likely due to the high sequence similarity between these genes, we chose to focus on RAB-11.1. We examined RAB-11.1 localization (hereafter referred to as RAB-11) by infecting transgenic animals expressing *GFP::RAB-11* (19) with *N. parisii*. In the intestinal cells of infected meront-stage animals, we found that *GFP::RAB-11* is still apically enriched, is primarily cytosolic, and is excluded from pathogen tissue (Fig. 4*B*). Strikingly, however, when spores are being shed at approximately 41 hpi, we find that vast numbers of apically localized spores are coated in *GFP::RAB-11* (Fig. 4 *C–E*). These spores are crowded around the lumen in all dimensions, always densest along the apical face of the intestinal cells. To ensure that the localization of RAB-11 to spores was not an artifact of this transgene, we confirmed that a separate *RFP::RAB-11* transgene also localizes to *N. parisii* spores (22) (Fig. 4*F*). In addition, we performed immunohistochemistry by using an antibody directed against endogenous RAB-11 (29) in N2 wild-type animals, and in animals expressing *GFP::RAB-11*. We observed localization of RAB-11 antibody to spores in infected animals, which colocalized with the *GFP::RAB-11* transgene marker (Fig. S6 *A–C*). Interestingly, the vast majority of RAB-11–coated SCCs do not appear to have *PGP-1::GFP* on them, but it appears that some *PGP-1::GFP* SCCs also exhibit RAB-11 staining, suggesting that SCCs may undergo a transition from RAB-11 coats to PGP-1 coats as they fuse with the apical plasma membrane (Fig. 4 *F–H*).

We also investigated the localization of RAB-5 (early endosomes) and RAB-10 (Golgi and recycling endosomes) to *N. parisii* spores by using fluorescently tagged versions of these proteins (22). As in other organisms, RAB-5 and RAB-10 are known to play active roles in intracellular transport in *C. elegans*, including apical recycling in the intestine and neuropeptide secretion in neurons (22, 30). Although both of these proteins are required for *N. parisii* spore egress, we did not find these proteins localized to spores in the intestine (Fig. S7).

RAB-11 Is Required for Spore-Containing Compartment Fusion with the Apical Membrane, and Contagiousness of Infected Animals. The above localization results indicate that RAB-11 acts directly on the *N. parisii* exit process, whereas RAB-5 and RAB-10 act more indirectly. If *N. parisii* spores use RAB-11 membrane compartments to traffic to the apical cell surface, we would expect that blocking RAB-11 function would decrease the number of SCCs fusing with the host apical membrane. To test this hypothesis, we compared the number of apically fused SCCs that are marked

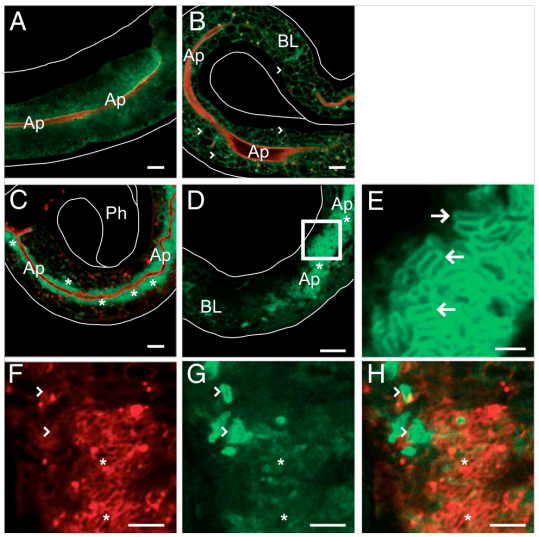

Fig. 4. RAB-11 protein forms coats on apically localized intracellular spores. Uninfected (*A*), meront-infected (*B*), and spore-infected (*C–E*) transgenic animals expressing *GFP::RAB-11* in green and apical marker *mCherry::ACT-5* in red. (*B*) Arrowheads mark examples of meronts, which are dark because of the exclusion of *GFP::RAB-11*. (*C*) *GFP::RAB-11* localizes to spores near the apical cell surface (asterisks). Ph, pharynx. (*D*) Spore-infected animal. Region enclosed by box is expanded in *E*. Ap, apical; BL, basolateral, and white lines outline the animals. (*E*) Arrows point to rod-shaped spores coated in *GFP::RAB-11*. (*F*) Arrowheads mark *RFP::RAB-11* coated spores that are also marked by *PGP-1::GFP* (*G*). Asterisks denote spores with *RFP::RAB-11* but not *PGP-1::GFP*. (*H*) Merged image. (Scale bars: *A–D*, 10 μm; *E*, 2.5 μm; *F–H*, 5 μm.)

with *PGP-1::GFP* (as shown in Fig. 2*A*) in L4440 empty vector control and *rab-11.1* RNAi-treated animals. Indeed, we found that depleting RAB-11 caused a near complete block in the number of SCCs that fused with the apical membrane (Fig. 5*A*). We also quantified the apically fused SCCs as assessed with *PGP-1::GFP* coats in *rab-5* and *rab-10* RNAi-treated animals and found there was not a block in fusion with the apical membrane. Similarly, there was not a substantial block in the formation of *GFP::RAB-11* coats in *rab-5* or *rab-10* RNAi-treated animals (Fig. S6*D*). These results indicate that whereas *N. parisii* relies directly on RAB-11 to achieve apical fusion, RAB-5 and RAB-10 appear to either act in parallel to or downstream of fusion.

We next determined the functional role of RAB-11 on microsporidia disease transmission by conducting contagiousness assays with *rab-11.1* RNAi-treated animals (Fig. S8). These experiments demonstrated that RAB-11–defective animals are less contagious than control animals (Fig. 5*B*). One trivial explanation for this reduced transmission could be that *rab-11.1* RNAi-treated animals die more rapidly than control. However, there was only a slight decrease in survival of *rab-11.1* RNAi-treated animals compared with controls, and this decrease was not caused by infection (Fig. S9). Altogether, these results demonstrate that host RAB-11 is required for fecal-oral transmission of *N. parisii* to new hosts.

Discussion

Our studies indicate that a major mode of *N. parisii* spore exit from intestinal cells is to traffic through RAB-11–marked endocytic recycling compartments, followed by polarized exocytosis into the lumen for fecal-oral transmission (Fig. 5*C*). In particular, we found that RAB-11 is required for SCC fusion with the apical membrane of intestinal cells, whereas RAB-5 and RAB-10 act in parallel to or downstream of fusion. Although RAB-5 and RAB-10 can act upstream of RAB-11 and vesicle fusion in apical recycling events in other systems, they have also been shown to act downstream of vesicle fusion, such as in the *C. elegans* nervous system where they are required for neuropeptide release from dense core vesicles, but are not required for fusion (30). Thus, RAB-5 and RAB-10 may similarly act downstream of fusion for *N. parisii* release, whereas RAB-11 acts upstream of fusion to promote directional exit for fecal-oral transmission of infection.

Rab11 has been well characterized in many systems as the master regulator of endocytic recycling, responsible for directing intracellular cargo to the apical cell surface by acting as an upstream mediator of exocytic trafficking pathways and vesicle fusion (24, 31). Rab11 is apically localized in many polarized epithelial cells, which could aid intracellular pathogens that need to egress from such cells in a directional manner to exit from hosts. Not only intestinal pathogens, but also respiratory and urogenital pathogens, need to egress out the apical side of epithelial cells for transmission to new hosts. Interestingly, a variety of respiratory viruses such as influenza virus have been shown to use host Rab11 for trafficking of viral particles to the plasma membrane (32). Although these viruses ultimately bud from the membrane instead of exiting through exocytosis, trafficking through the host cell by Rab11 could provide apical directionality to viral egress from polarized lung epithelial cells in vivo.

How general is the *N. parisii* polarized exocytosis strategy likely to be for other microbial pathogens? An exocytosis-type process termed "vomocytosis" has been implicated in the exit of fungal pathogens from macrophages (33, 34), although this process is likely distinct from the polarized exocytosis used to escape from epithelial cells. Whereas exocytosis has been shown to contribute to bacterial pathogen exit in mammalian tissue culture systems of epithelial cells (35), multiple modes of exit have been proposed for the same pathogen, and the in vivo significance and contribution of exocytosis to disease transmission has not been clear. In contrast to the *C. elegans* intestine, the mammalian intestine regularly renews and sheds epithelial cells. Exiting through these extruded cells appears to be an exit strategy for *Salmonella* in vivo (36), so it is possible that mammalian pathogens do not need to exit from intact intestinal cells via exocytosis. However, doing so would greatly accelerate their transmission, because intestinal cell shedding occurs on the timescale of days (37), whereas doubling time of many bacterial pathogens occurs on the timescale of minutes. Therefore, pathogens that egress via exocytosis could have a large advantage in terms of doubling time over pathogens that wait for extrusion. Thus, the apical recycling exit process that we have found as critical for exit of *N. parisii* may also be important for exit, and dissemination, of pathogens that use a fecal-oral route of transmission. In particular, *N. parisii* belongs to the microsporidia phylum, which includes a large number of pathogen species that commonly infect and replicate in the intestine. For example, *Enterocytozoon bieneusi*, which has been responsible for lethal diarrhea in AIDS patients, appears to replicate only within human intestinal epithelial cells (38). The mode of exit is unknown for any species of microsporidia, but it is interesting to speculate that other microsporidia species may use exocytosis for egress from host cells.

N. parisii and *C. elegans* are a naturally occurring host–pathogen pair and, by using RAB-11–based exocytosis for productive exit, they appear to have coevolved a compromise between host survival and pathogen propagation. It is likely that facilitating a minimally damaging exit strategy such as exocytosis is beneficial to both the host and the intracellular pathogen: By prolonging the lifespan of the host, the replication environment is preserved for future pathogen generations. Minimizing host damage is likely to be particularly important for *N. parisii,* given that it cannot replicate on its own, and its replication

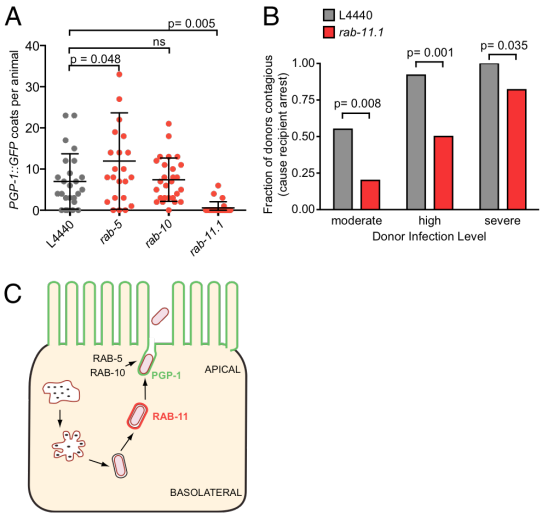

Fig. 5. RAB-11 is required for spore fusion and contagiousness. (*A*) *rab-11.1* RNAi blocks fusion of SCCs with apical plasma membrane, as assessed by *PGP-1::GFP* membrane-coated spores. *rab-5* and *rab-10* RNAi do not significantly impact the number of *PGP-1::GFP*-coated spores. Each point represents the number of *PGP-1::GFP* coats in a single animal. $n = 30$ animals per treatment group. Average is shown with error bars as SD. (*B*) *rab-11.1* RNAi-treated animals are less contagious than control animals. Fraction of infected donor animals causing symptoms of severe infection in recipients is shown for each treatment group. $n = 24$–41 donor animals per infection level per RNAi treatment group ($n = 184$ animals total). (*C*) Model for RAB-11-mediated directional exocytosis of *N. parisii* spores from *C. elegans* intestinal cells.

environment is the nonrenewable epithelial cells of the *C. elegans* intestine. Damage to any of these 20 cells is likely to be detrimental to the host. It will be interesting to investigate how *C. elegans* copes with the demand from this prodigious *N. parisii* spore production, with thousands of spores exiting the host every hour. Presumably this process places a huge increase in demand on *C. elegans* intestinal trafficking pathways.

N. parisii cells appear to initially be in direct contact with the host cytoplasm of intestinal cells (9). How does this pathogen then enter the host vesicle trafficking system to ultimately exit via apical exocytosis? Recently, the autophagy pathway, which can be used to control intracellular pathogen growth, has been implicated as a "recapture" mechanism to return bacterial pathogens that have escaped into the cytoplasm back into a host endosome (39, 40). However, our data indicate that the autophagy pathway is not important for *N. parisii* maturation and exit (Fig. S2). Thus, this pathogen may coopt a distinct pathway to enter the host vesicle trafficking system. Further analyses of host pathways, together with studies of the recently sequenced *N. parisii* genome (10), should help determine how this natural pathogen so efficiently coopts the host intestinal cell for prodigious proliferation and directional exit for fecal/oral transmission.

Materials and Methods

Infection Assays and Microscopy. In general, synchronized *C. elegans* L1 larvae were grown for 24 h on 6-cm NGM plates seeded with OP50 at 20 °C until approximately L3 stage, when they were infected with 2×10^6 *N. parisii* spores and then incubated at 25 °C. Images used for quantifying spores shed and pathogen load were captured with fluorescence on a Zeiss AxioImager at 400× or 630× magnification. Confocal images were acquired on a Zeiss LSM700 at 630× magnification by using ZEN2010 software. Transmission electron microscopy was performed as described (9).

Contagiousness and Survival Assays. Standard infection conditions were used on RNAi-treated donor animals. Contagiousness and survival assays were conducted as in described (9, 15). See Fig. S8 for details. For survival assays, the survival of 40 animals was assessed for each RNAi treatment group, each on three plates for a total of 120 animals per treatment. For each experimental replicate, results from triplicate plates were combined into one dataset. Animals that died because of desiccation on the wall of the plate rather than because of infection were excluded from analysis.

***GFP::RAB-11* and *PGP-1::GFP* Coat Quantification.** To determine whether genes are upstream or downstream of RAB-11 and whether genes are required for SCC fusion with the apical membrane, the number of *GFP::RAB-11.1* or *PGP-1::GFP*-coated SCCs was recorded after RNAi treatment. Animals were fixed in 4% (vol/vol) PFA at 46 hpi, and the anterior-most ring of intestinal cells was imaged in each of 30 animals per treatment group, taking 18 0.8-μm sectional confocal images per animal.

See *SI Materials and Methods* for additional materials and methods.

ACKNOWLEDGMENTS. We thank K. Estes for early characterization of Calcofluor white staining of *N. parisii*; M. Zerial, B. Grant, K. Sato, and D. McEwan for *C. elegans* strains; A. Spang for RAB-11 antibodies; R. Luallen, L. Cohen, and T. Dror for feedback on the manuscript; and M. Wood and N. Olson for TEM assistance. Some strains were provided by the Caenorhabditis Genetics Center, which is funded by National Institutes of Health (NIH) Office of Research Infrastructure Programs Grant P40 OD010440. This work was supported by NIH Predoctoral Training Grant T32 GM008666 and a National Science Foundation Predoctoral Fellowship (to S.C.S.) and National Institute of Allergy and Infectious Diseases Grant R01 AI087528, the Searle Scholars Program, David and Lucile Packard Foundation, and Burroughs Wellcome Fund Fellowship (to E.R.T.).

1. Friedrich N, Hagedorn M, Soldati-Favre D, Soldati T (2012) Prison break: Pathogens' strategies to egress from host cells. *Microbiol Mol Biol Rev* 76(4):707–720.
2. Hybiske K, Stephens RS (2008) Exit strategies of intracellular pathogens. *Nat Rev Microbiol* 6(2):99–110.
3. Gallo RL, Hooper LV (2012) Epithelial antimicrobial defence of the skin and intestine. *Nat Rev Immunol* 12(7):503–516.
4. Hamon M, Bierne H, Cossart P (2006) Listeria monocytogenes: A multifaceted model. *Nat Rev Microbiol* 4(6):423–434.
5. Nikitas G, et al. (2011) Transcytosis of Listeria monocytogenes across the intestinal barrier upon specific targeting of goblet cell accessible E-cadherin. *J Exp Med* 208(11): 2263–2277.
6. Pukkila-Worley R, Ausubel FM (2012) Immune defense mechanisms in the Caenorhabditis elegans intestinal epithelium. *Curr Opin Immunol* 24(1):3–9.
7. Szumowski SC, Estes KA, Troemel ER (2012) Preparing a discreet escape: Microsporidia reorganize host cytoskeleton prior to non-lytic exit from C. elegans intestinal cells. *Worm* 1(4):1–5.
8. McGhee JD (2007) The C. elegans intestine. *WormBook* 1–36.
9. Troemel ER, Félix MA, Whiteman NK, Barrière A, Ausubel FM (2008) Microsporidia are natural intracellular parasites of the nematode Caenorhabditis elegans. *PLoS Biol* 6(12):2736–2752.
10. Cuomo CA, et al. (2012) Microsporidian genome analysis reveals evolutionary strategies for obligate intracellular growth. *Genome Res* 22(12):2478–2488.
11. Didier ES, Weiss LM (2011) Microsporidiosis: Not just in AIDS patients. *Curr Opin Infect Dis* 24(5):490–495.
12. Keeling PJ, Fast NM (2002) Microsporidia: Biology and evolution of highly reduced intracellular parasites. *Annu Rev Microbiol* 56:93–116.
13. Félix MA, Duveau F (2012) Population dynamics and habitat sharing of natural populations of Caenorhabditis elegans and C. briggsae. *BMC Biol* 10:59.
14. Vávra J, Lukeš J (2013) Microsporidia and 'the art of living together' *Adv Parasitol* 82: 253–319.
15. Estes KA, Szumowski SC, Troemel ER (2011) Non-lytic, actin-based exit of intracellular parasites from *C. elegans* intestinal cells. *PLoS Pathog* 7(9):e1002227.
16. Hagedorn M, Rohde KH, Russell DG, Soldati T (2009) Infection by tubercular mycobacteria is spread by nonlytic ejection from their amoeba hosts. *Science* 323(5922): 1729–1733.
17. Sato T, et al. (2007) The Rab8 GTPase regulates apical protein localization in intestinal cells. *Nature* 448(7151):366–369.
18. Winston WM, Sutherlin M, Wright AJ, Feinberg EH, Hunter CP (2007) Caenorhabditis elegans SID-2 is required for environmental RNA interference. *Proc Natl Acad Sci USA* 104(25):10565–10570.
19. Winter JF, et al. (2012) Caenorhabditis elegans screen reveals role of PAR-5 in RAB-11-recycling endosome positioning and apicobasal cell polarity. *Nat Cell Biol* 14(7): 666–676.
20. Huang J, Brumell JH (2014) Bacteria-autophagy interplay: A battle for survival. *Nat Rev Microbiol* 12(2):101–114.
21. Lundquist EA (2006) Small GTPases. *WormBook* 1–18.
22. Chen CC, et al. (2006) RAB-10 is required for endocytic recycling in the Caenorhabditis elegans intestine. *Mol Biol Cell* 17(3):1286–1297.
23. Grant BD, Donaldson JG (2009) Pathways and mechanisms of endocytic recycling. *Nat Rev Mol Cell Biol* 10(9):597–608.
24. Chen W, Feng Y, Chen D, Wandinger-Ness A (1998) Rab11 is required for trans-golgi network-to-plasma membrane transport and a preferential target for GDP dissociation inhibitor. *Mol Biol Cell* 9(11):3241–3257.
25. Casanova JE, et al. (1999) Association of Rab25 and Rab11a with the apical recycling system of polarized Madin-Darby canine kidney cells. *Mol Biol Cell* 10(1):47–61.
26. Hoekstra D, Tyteca D, van IJzendoorn SC (2004) The subapical compartment: A traffic center in membrane polarity development. *J Cell Sci* 117(Pt 11):2183–2192.
27. van Ijzendoorn SC (2006) Recycling endosomes. *J Cell Sci* 119(Pt 9):1679–1681.
28. Takahashi S, et al. (2012) Rab11 regulates exocytosis of recycling vesicles at the plasma membrane. *J Cell Sci* 125(Pt 17):4049–4057.
29. Poteryaev D, Fares H, Bowerman B, Spang A (2007) *Caenorhabditis elegans* SAND-1 is essential for RAB-7 function in endosomal traffic. *Embo J* 26(2):301–312.
30. Sasidharan N, et al. (2012) RAB-5 and RAB-10 cooperate to regulate neuropeptide release in Caenorhabditis elegans. *Proc Natl Acad Sci USA* 109(46):18944–18949.
31. Welz T, Wellbourne-Wood J, Kerkhoff E (2014) Orchestration of cell surface proteins by Rab11. *Trends Cell Biol,* 10.1016/j.tcb.2014.02.004.
32. Bruce EA, Stuart A, McCaffrey MW, Digard P (2012) Role of the Rab11 pathway in negative-strand virus assembly. *Biochem Soc Trans* 40(6):1409–1415.
33. Ma H, Croudace JE, Lammas DA, May RC (2006) Expulsion of live pathogenic yeast by macrophages. *Curr Biol* 16(21):2156–2160.
34. Nicola AM, Robertson EJ, Albuquerque P, Derengowski LdaS, Casadevall A (2011) Nonlytic exocytosis of Cryptococcus neoformans from macrophages occurs in vivo and is influenced by phagosomal pH. *MBio* 2(4).
35. Takeuchi H, Furuta N, Morisaki I, Amano A (2011) Exit of intracellular Porphyromonas gingivalis from gingival epithelial cells is mediated by endocytic recycling pathway. *Cell Microbiol* 13(5):677–691.
36. Knodler LA, et al. (2010) Dissemination of invasive Salmonella via bacterial-induced extrusion of mucosal epithelia. *Proc Natl Acad Sci USA* 107(41):17733–17738.
37. Jeon MK, Klaus C, Kaemmerer E, Gassler N (2013) Intestinal barrier: Molecular pathways and modifiers. *World J Gastrointest Pathophysiol* 4(4):94–99.
38. Didier ES, Weiss LM (2006) Microsporidiosis: Current status. *Curr Opin Infect Dis* 19(5): 485–492.
39. Checroun C, Wehrly TD, Fischer ER, Hayes SF, Celli J (2006) Autophagy-mediated reentry of Francisella tularensis into the endocytic compartment after cytoplasmic replication. *Proc Natl Acad Sci USA* 103(39):14578–14583.
40. Collins CA, et al. (2009) Atg5-independent sequestration of ubiquitinated mycobacteria. *PLoS Pathog* 5(5):e1000430.

Supporting Information

Szumowski et al. 10.1073/pnas.1400696111

SI Materials and Methods

Strains. *Caenorhabditis elegans* were maintained on nematode growth media (NGM) plates seeded with *Escherichia coli* OP50-1, as described (1). We used N2 wild-type animals for all RNAi spore shedding experiments. The following transgenic strains were used in this study:

ERT106	*jyIs17[vha-6p::mCherry::ACT-5, ttx-3p::RFP] IV; dkIs166[opt-2p::PGP-1::GFP]*
HC722	*gk505[dyf-2(-) & sid-2(-)]; qtIs5(SID-2::GFP)]* (2)
MZE1	*unc-119(ed3); cbgIs91[pept-1p::PEPT-1::DsRed, unc-119(+)]; cbgIs98[pept-1p::GFP::RAB-11.1, unc-119(+)]* (3)
ERT213	*jyIs17[vha-6p::mCherry::ACT-5, ttx-3p::RFP] IV; cbgIs98[pept-1p::GFP::RAB-11.1, unc-119(+)]*
RT1102	*unc-119(ed3); pwIs428[vha-6p::RFP::RAB-11.1, unc-119(+)]* (4)
ERT260	*unc-119(ed3); cbgIs98[pept-1p::GFP::RAB-11.1, unc-119(+)]* 2x backcrossed
RT1239	*unc-119(ed3); pwIs480[vha-6p::RFP::RAB-5, unc-119(+)]* (4)
RT525	*unc-119(ed3); pwIs206[vha-6p::GFP::RAB-10, unc-119(+)]* (4)
GK288	*unc-119(ed3); dkIs166[opt-2p::PGP-1::GFP, unc-119(+)]* (5)
ERT197	*unc-119(ed3); pwIs428[vha-6p::RFP::RAB-11.1, unc-119(+); dkIs166[opt-2p::PGP-1::GFP]*
MZE4	*unc-119(ed3); cbgIs91[pept-1p::PEPT-1::DsRed, unc-119(+)];cbgIs103[pept-1p::SP12::GFP, unc-119(+)]* (3)
DA2123	*N2; adIs2122[lgg-1p::GFP::LGG-1; rol-6(su1006)]*) (6, 7)

Strains ERT106 and ERT213 contain an intestinally expressed actin *vha-6p::mCherry::ACT-5* (pET187) transgene that was made by PCR amplifying the *act-5* cDNA with its endogenous 3′ UTR and cloning it into the Gateway 3′ element vector pDONR P2R-P3. This vector was then recombined in a three-fragment Gateway LR recombination reaction with the *vha-6* promoter in the Gateway 5′ element vector pDONR P4-P1R, and mCherry in the Gateway middle element vector pDONR221, into the destination vector pDEST R4-R3. This *vha-6p::mCherry::ACT-5* transgene was injected into N2 worms at 10 ng/μL along with *ttx-3p::RFP* as a co-injection marker to generate an extrachromosomal array strain that was integrated with UV/psoralen treatment to create integrant *jyIs17[vha-6p::mCherry::ACT-5]IV*.

***Nematocida parisii* Spore Preps.** Spore preps were prepared as described (8). Briefly, *N. parisii* was cultured inside of *C. elegans*, and when animals were heavily infected, they were mechanically disrupted with silicon beads to isolate spores, which were then filtered through a 5-μm filter to remove intact *C. elegans* larvae and eggs. Spores were quantified by staining with Calcofluor white (Sigma-Aldrich) and counting with a hemocytometer (Cell-Vu). Aliquots of spores were stored at −80 °C before use.

Luminal Access Assays. To stain spores in contact with the lumen, Calcofluor white was fed to infected animals by applying 300 μL of Calcofluor white to 6-cm NGM/OP50 plates. Calcofluor white was spread evenly over the entire surface of the plate, the plate was dried in a sterile hood, and worms were allowed to feed on the dye for 2 h before imaging.

smGTPase RNAi Screen and Spore Shedding Assays. Feeding RNAi experiments were performed as described (8, 9). A library of 41 smGTPase RNAi clones was generated based on a list from ref. 10, and was divided roughly into quarters and prepped as 4 separate batches, each with their own L4440 empty vector controls, which were used to normalize the relative number of spores shed across the four batches. All RNAi clones were sequence verified. All clones were used undiluted, except for *rab-5* and *rab-11.1* RNAi clones, which were diluted 1:10 with L4440 (vector alone) control RNAi bacteria to allow for normal development. All experiments with these clones used these dilutions. Synchronized L2 animals were infected with 5.8×10^6 spores on 10-cm RNAi plates and incubated at 25 °C for 40 h to allow the infection to progress until the spore shedding stage of infection. Animals were washed three times in M9 at 24 h after infection (hpi) and 39 hpi and replated on fresh RNAi plates (at 24 hpi) or OP50 plates (at 39 hpi) to remove spores from cuticles. At 40 hpi, 50 animals were picked off of *E. coli* plates into microfuge tubes with 500 μL of 1:1 *E. coli* OP50 and M9. Spores excreted from 40 to 48 hpi were collected and quantified by staining with Calcofluor white and counting at 400×. All genes were tested in three biological replicates and screen hits were verified in triplicate in an independent biological replicate experiment.

To determine whether RNAi clones affected cell polarity, localization of the apically localized plasma membrane marker *PGP-1::GFP* in strain ERT106 was assessed at 630× in >30 RNAi-treated animals per RNAi clone.

RAB-11 Antibody Staining. Antibody staining with anti–RAB-11 antibodies was performed as described (11). Briefly, *C. elegans* intestines were dissected out, fixed in paraformaldehyde, washed, then incubated with 1:500 dilution of primary anti–RAB-11 peptide antibody (12) overnight at 4 °C, washed, then stained with 1:500 dilution of secondary antibody Cy3-labeled goat anti-rabbit IgG (Jackson Immunoresearch) for 2 h at room temperature, washed, then mounted in Vectashield with DAPI for viewing by fluorescence microscopy.

Spore Production Assays. The pathogen load in individual RNAi-treated animals was semiquantitatively measured by counting spores in ∼40 animals per treatment group fixed with acetone at 45 hpi, using a Zeiss AxioImager with Nomarski optics. The pathogen load in a population of animals was quantitatively determined by hydrolyzing infected animals and counting the spores released after host tissue was dissolved. RNAi-treated infected animals were fixed at 44 hpi with acetone and 50 animals were hydrolyzed for 30 min with 200 mM NaOH, 0.1% SDS, and 1:100 Calcofluor white. To ensure complete homogenization, infected *C. elegans* were repeatedly pipetted with

a 200-μL pipette tip. The suspension was neutralized by adding 100 μM of 1 M Tris·HCl at pH 7.4. *N. parisii* spores were then counted by using a Cell-Vu counting chamber. Three biological replicates were counted for each RNAi treatment.

Defecation Assays. The defecation contents of infected animals were analyzed for the ratio of *N. parisii* spores to control fluorescent beads. Briefly, spore-stage infected animals were fed a blend of 0.5-μm fluorescent beads (Polysciences; catalog no. 19507) and Calcofluor white (to label extracellular spores) for 2 h on OP50. Animals were then removed from the bead-feeding plate, briefly transferred to a clean OP50 plate to remove beads from the cuticle, and then transferred to a fresh OP50 plate and allowed to defecate undisturbed for 35 min, at which point they were removed from the plates and the presence of intracellular spores was verified with Nomarski optics at 630×. Each RNAi clone was tested on three independent plates, each containing eight animals during each of three independent biological experiments. The defecated materials were imaged with fixed exposure at 100×, and fluorescence intensity above background was quantified with ImageJ64 (version 1.46r) for the blue (Calcofluor white-stained spores) and red (beads) channels. For each defecation spot, the blue fluorescence value was divided by the total fluorescence (red plus blue). These values represent the fraction of each defecation spot that is comprised of spores and were normalized to the values obtained from analyzing defecated material from L4440 control RNAi animals.

Autophagy Assays. Autophagy pathway perturbation was assessed by quantifying the number of *GFP::LGG-1* puncta greater than 1.2 μm in size after feeding RNAi treatment. Animals were fixed in 4% (vol/vol) PFA at 24 hpi and imaged by using confocal microscopy then analyzed in ImageJ.

Statistical Analyses. For all datasets, *P* values reported were calculated in Prism 6 software and ns = not significant; $^{*}P < 0.05$; $^{**}P < < 0.001$. *P* values for spore shedding assays (Fig. 3*A* and Figs. S2*B* and S3), spore production in population assay (Fig. 3*C*), defecation contents assay (Fig. 3*D*), coat quantification assays (Fig. 5*A* and Fig. S6*D*), and LGG-1 puncta quantification assay (Fig. S2*D*) were calculated by using ANOVA with Dunnett's correction for multiple comparisons. *P* values reported in spore production in individual animals assay (Fig. 3*B*) were from Friedman's Test, ANOVA with Dunn's correction for multiple comparisons. Contagiousness assay (Fig. 5*B*) *P* values were calculated by a two-sided Fisher's exact test.

1. Brenner S (1974) The genetics of Caenorhabditis elegans. *Genetics* 77(1):71–94.
2. Winston WM, Sutherlin M, Wright AJ, Feinberg EH, Hunter CP (2007) Caenorhabditis elegans SID-2 is required for environmental RNA interference. *Proc Natl Acad Sci USA* 104(25):10565–10570.
3. Winter JF, et al. (2012) Caenorhabditis elegans screen reveals role of PAR-5 in RAB-11-recycling endosome positioning and apicobasal cell polarity. *Nat Cell Biol* 14(7): 666–676.
4. Chen CC, et al. (2006) RAB-10 is required for endocytic recycling in the Caenorhabditis elegans intestine. *Mol Biol Cell* 17(3):1286–1297.
5. Sato T, et al. (2007) The Rab8 GTPase regulates apical protein localization in intestinal cells. *Nature* 448(7151):366–369.
6. Meléndez A, et al. (2003) Autophagy genes are essential for dauer development and life-span extension in C. elegans. *Science* 301(5638):1387–1391.
7. Kang C, You YJ, Avery L (2007) Dual roles of autophagy in the survival of Caenorhabditis elegans during starvation. *Genes Dev* 21(17):2161–2171.
8. Estes KA, Szumowski SC, Troemel ER (2011) Non-lytic, actin-based exit of intracellular parasites from *C. elegans* intestinal cells. *PLoS Pathog* 7(9):e1002227.
9. Kamath RS, et al. (2003) Systematic functional analysis of the Caenorhabditis elegans genome using RNAi. *Nature* 421(6920):231–237.
10. Lundquist EA (2006) Small GTPases. *WormBook* 1–18.
11. Troemel ER, Félix MA, Whiteman NK, Barrière A, Ausubel FM (2008) Microsporidia are natural intracellular parasites of the nematode Caenorhabditis elegans. *PLoS Biol* 6(12):2736–2752.
12. Poteryaev D, Fares H, Bowerman B, Spang A (2007) Caenorhabditis elegans SAND-1 is essential for RAB-7 function in endosomal traffic. *EMBO J* 26(2):301–312.

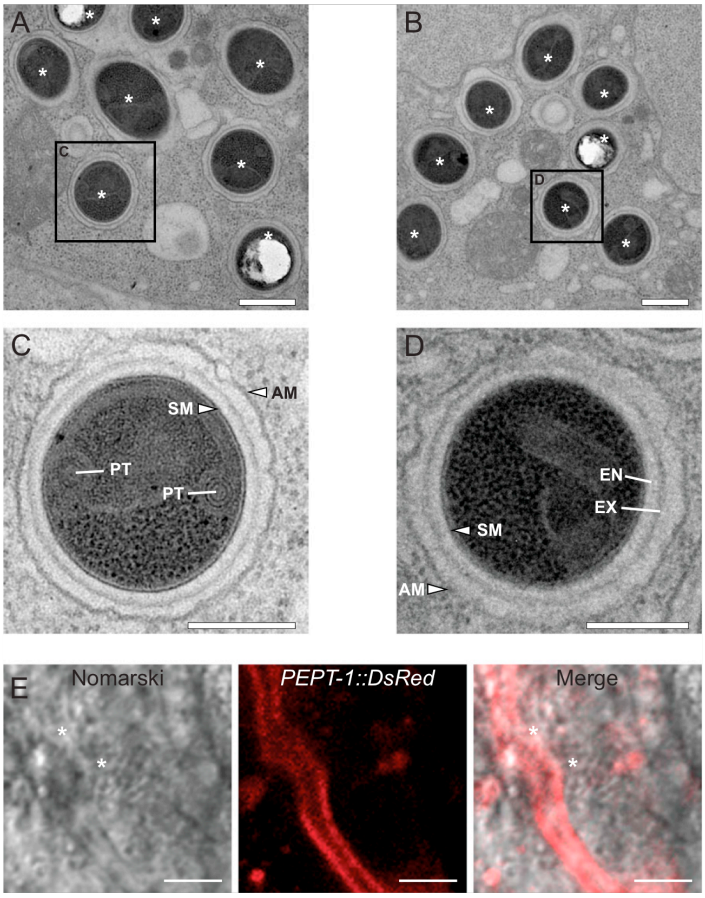

Fig. S1. *N. parisii* spores are surrounded by an additional membrane, and PEPT-1 does not localize to *N. parisii* spores. (*A* and *B*) Representative fields of view showing cross-sections of intracellular spores (asterisks) that are contained in an additional membrane. Boxed regions are expanded in *C* and *D*, respectively. (*C* and *D*) Magnified view of spores showing the spore membrane (SM) and an additional membrane (AM) surrounding spores. EN, endospore; EX, exospore; PT, polar tube. (*E*) *PEPT-1::DsRed* does not localize to *N. parisii* spores, which are marked with asterisks in Nomarski optics. (Scale bars: *A* and *B*, 500 nm; *C* and *D*, 250 nm; *E*, 5 μm.)

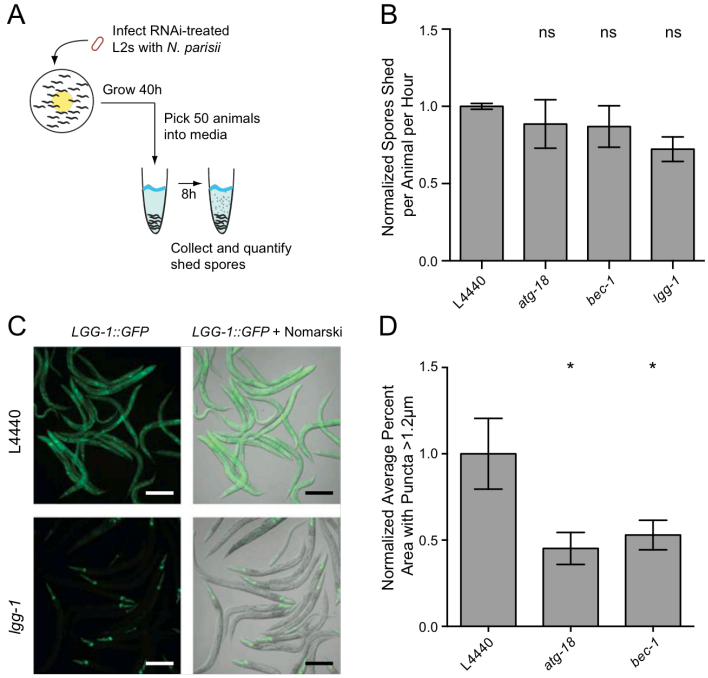

Fig. S2. RNAi against autophagy components *bec-1*, *atg-18*, and *lgg-1* does not significantly reduce spore shedding. (*A*) Spore shedding assay. (*B*) Spores shed by animals treated with control L4440 or RNAi against *bec-1*, *atg-18*, or *lgg-1*. The mean and SEM combined from three independent experiments are shown, normalized to the value for the L4440 RNAi control. $n = 150$ animals per treatment. (*C*) Intestinal expression of *GFP::LGG-1* is greatly reduced by *lgg-1* RNAi treatment. Remaining GFP expression is in the pharynx. (Scale bars: 200 μm.) (*D*) The number of *GFP::LGG-1* puncta greater than 1.2 μm in area is significantly reduced in *atg-18* and *bec-1* RNAi-treated animals. All results are normalized to the average L4440 control RNAi sample values. Mean and SEM from three combined independent experiments are shown. $n = 57$–64 animals per treatment group. ns, not significant; $^*P < 0.05$.

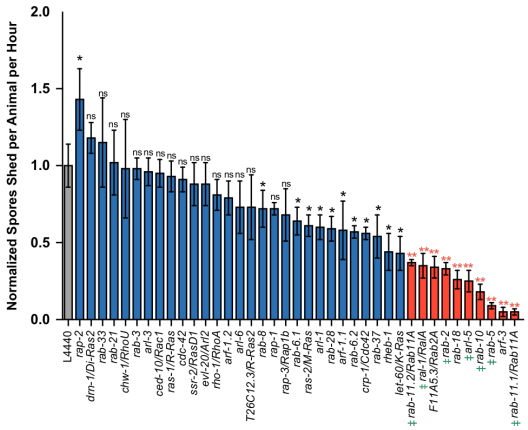

Fig. S3. Spore shedding screen using RNAi against 41 *C. elegans* predicted smGTPases. The mean and SD of biological triplicate samples is shown. $n = 50$ animals per treatment. L4440 is the empty vector control for RNAi to which all values are normalized. Red denotes samples scored as screen hits; blue denotes nonhits. Note that a lack of effect in this screen could be due to ineffective RNAi knockdown against the gene of interest. Green crosses denote characterized members of the recycling endosome pathway. When *C. elegans* gene names differ from those of human homologs, human gene names are listed after the *C. elegans* gene name. ns, not significant; $^*P < 0.05$; $^{**}P << 0.001$.

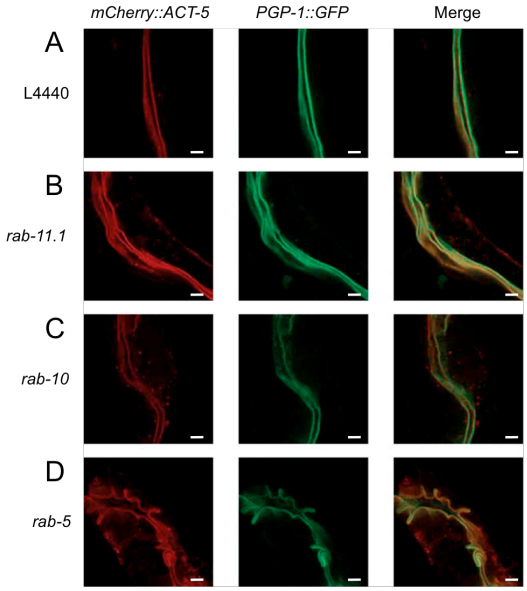

Fig. S4. Markers for intestinal cell polarity are unaffected by smGTPase RNAi treatment. The apical localizations of *mCherry::ACT-5* and *PGP-1::GFP* were unperturbed by treatment for each smGTPase spore shedding screen hit: (*A*) L4440 control, (*B*) *rab-11.1*, RNAi, (*C*) *rab-10* RNAi, (*D*) *rab-5* RNAi. Images are shown of *N. parisii*-infected animals, which is the reason for some actin localization to the basolateral side of intestinal cells (8). All genes included in screen were tested for polarity disruption, and representative images are shown. (Scale bars: 5 μm.)

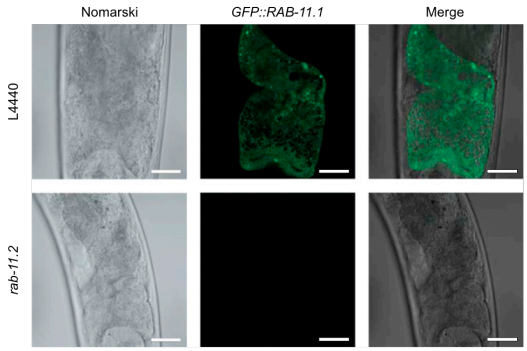

Fig. S5. *GFP::RAB-11.1* is knocked down by *rab-11.2* RNAi. *GFP::RAB-11.1* fluorescence is greatly reduced by *rab-11.2* RNAi. (Scale bars: 20 μm.)

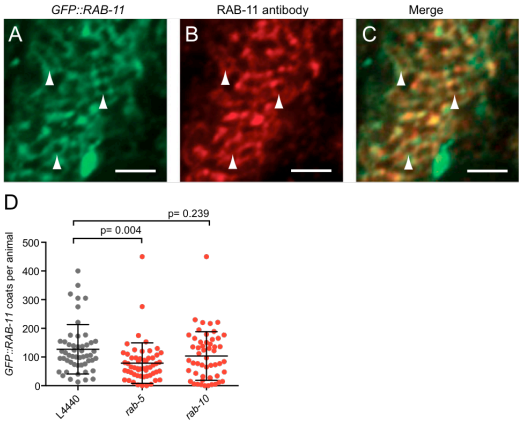

Fig. S6. Antibody against endogenous RAB-11 colocalizes with *GFP::RAB-11*–coated spores, and *rab-5* or *rab-10* RNAi knockdown does not substantially alter the number of *GFP::RAB-11*–coated spores. (*A*) The *GFP::RAB-11* transgene localizes to rod-shaped *N. parisii* spores (examples of spores shown in cross-section are highlighted by arrowheads), as shown in Fig. 4*E*. (*B*) RAB-11 antibody colocalizes with *GFP::RAB-11* transgene, as seen in the merged image in *C*. (Scale bars: 2.5 μm.) (*D*) Neither *rab*-5 nor *rab*-10 RNAi block the formation of *GFP::RAB-11* coats on SCCs. $n = 60$ animals per treatment group combined from two independent experiments. Each point represents the number of *GFP::RAB-11* coats in a single animal. Average is shown with error bars as SD.

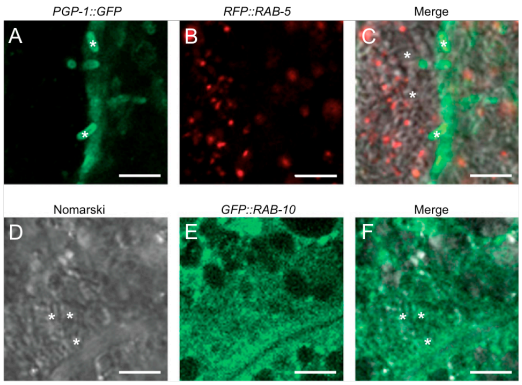

Fig. S7. RAB-5 and RAB-10 do not localize to spores. (*A*–*C*) *RFP::RAB-5* does not localize to *N. parisii* spores. Examples of spores are marked with asterisks in *A* and *C*. (*D*–*F*) *GFP::RAB-10* does not localize to *N. parisii* spores. Examples of spores are marked with asterisks in *D* and *F*. (Scale bars: 5 μm.)

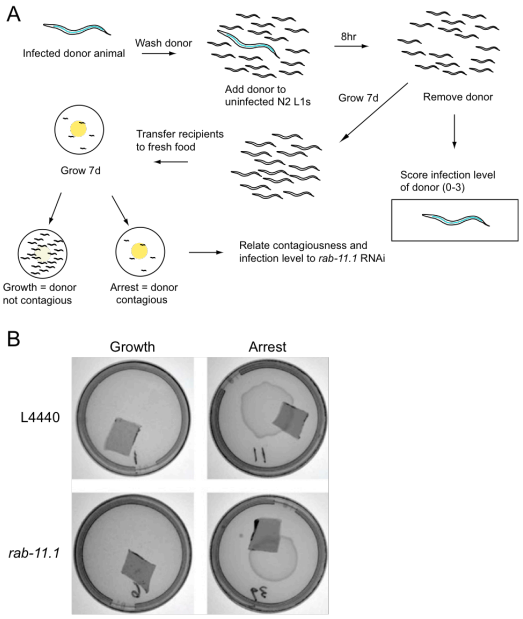

Fig. S8. Contagiousness assay design. (*A*) Experimental design for contagiousness assays. Donor animals were treated with either L4440 empty vector control RNAi bacteria, or *rab-11.1* RNAi bacteria. (*B*) Representative images of plates scored as growth-positive or arrested. The dark squares on the plates are chunks of agar used to transfer recipients to fresh food plates. The circle on arrested plates is an uneaten bacterial lawn, whereas on the growth-positive plates all bacteria have been consumed by the animals on the plate.

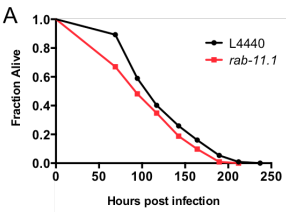

B

EXPERIMENTAL REPLICATE 1	Fraction Alive	
	L4440	*rab-11.1*
hpi	(n =112)	(n =112)
0.00	1.00	1.00
69.00	0.89	0.67
94.50	0.59	0.48
117.00	0.40	0.35
142.50	0.26	0.19
164.00	0.16	0.10
189.50	0.05	0.01
212.00	0.01	0.00
237.00	0.00	
median	117 hpi	94.5 hpi

C

EXPERIMENTAL REPLICATE 2	Fraction Alive	
	L4440	*rab-11.1*
hpi	(n =119)	(n=120)
0.00	1.00	1.00
65.50	0.90	0.74
87.25	0.66	0.55
109.75	0.45	0.45
134.25	0.37	0.29
158.00	0.24	0.16
182.25	0.10	0.08
206.25	0.06	0.03
230.25	0.01	0.01
255.00	0.00	0.00
median	109.75 hpi	109.75 hpi

D

EXPERIMENTAL REPLICATE 3	Fraction Alive	
	L4440	*rab-11.1*
hpi	(n = 94)	(n = 108)
0.00	1.00	1.00
60.50	0.89	0.83
85.25	0.67	0.59
92.75	0.63	0.56
130.50	0.46	0.28
158.50	0.33	0.13
179.10	0.16	0.06
182.00	0.05	0.03
205.50	0.01	0.00
230.50	0.00	
median	130.5 hpi	130.5 hpi

E

Uninfected	L4440	*rab-11.1*
Experiment 1	260.25	211.58
Experiment 2	263.75	190.92
Experiment 3	278.58	209.25

Fig. S9. *rab-11.1* RNAi effects on host survival in absence and presence of *N. parisii* infection. (*A*) Representative survival curve of independent biological replicates of infected *rab-11.1* RNAi and control animals. $n = 120$ animals per treatment group per experiment (three plates of 40 animals each). (*B–D*) Summary survival curve data for replicate experiments showing the fraction of animals alive at each time point animals were scored. The median survival time point for treatment groups is shown at the bottom of each table. *A* and *B* are data from the same experiment. (*E*) Summary of three experimental replicates comparing median survival time of uninfected *rab-11.1* RNAi and uninfected control animals. $n = 120$ animals per treatment group per experiment (three plates of 40 animals each).

4.1 Additional Acknowledgements

Chapter 4, in full, is reprinted from Proceedings of the National Academy of Sciences, 111, Szumowski, S.; Botts, M.; Popovich, J.; Smelkinson, M.; Troemel, E., RAB-11 directs polarized exocytosis of the intracellular pathogen *N. parisii* for fecal-oral transmission from *C. elegans*, 8215-20, (2014), with permission from Proceedings of the National Academy of Sciences. The dissertation author was the primary investigator and author of this material. Author contributions to manuscript are as follows: Szumowski, S.: Figure 1, Figure 2, Figure 3A, 3B, 3D, 3E, Figure 4, Figure 5, all Supplemental Figures, all experiments requested for peer review; Botts, M.: Figure 3C; Popovich, J.:, Figure 5A, Figure S6D; Smelkinson, M.: Figure S2D.

5 Small GTPases promote actin coat formation on pathogens exocytosing from *C. elegans* intestinal cells.

5.1 Summary

Exit of intracellular pathogens from host intestinal cells is a key stage in the transmission of foodborne and waterborne infections. However, little is known about this process *in vivo*. We have been studying the *in vivo* exit process of the microsporidian *Nematocida parisii,* which is an intracellular pathogen that infects intestinal cells of the nematode *Caenorhabditis elegans.* We recently demonstrated that *N. parisii* uses directional exocytosis to escape out of intestinal cells into the intestinal tract. We also found a requirement for an intestinal specific isoform of *C. elegans* actin called ACT-5 in *N. parisii* spore exit. Here, we show that ACT-5 forms coats around compartments that contain single exocytosing spores, and that these coats appear to form after fusion with the apical membrane. We performed a genetic screen for host factors required for actin coat formation and identified five small GTPases important for this process. Because animals with knock-down of these small GTPases have defects in spore shedding, we propose that actin coats are important for robust spore exit from the host. This finding illustrates how ACT-5 may promote pathogen exit, with striking similarity to the mechanistic role of actin to promote exocytosis by forming coats on vesicles of large, endogenous cargo.

5.2 Introduction

Actin is a dynamic, filament-forming protein that contributes to many important cellular functions. To regulate the activity of actin, an army of over 100 accessory proteins control actin polymerization and depolymerization, including the Rho small GTPases (smGTPases) Cdc42 and Rac1 (Heasman *et al.*, 2008, Pollard *et al.*, 2009). Cell motility, cell division, organelle movement, and vesicle trafficking are just a few

examples of complex cellular processes that are facilitated by actin. For example, studies of clathrin-mediated endocytosis have shown that actin can contribute to plasma membrane invagination, vesicle neck constriction, and the scission of vesicle budnecks (Kaksonen *et al.*, 2006). The role of actin in exocytosis is less well understood, and actin can be either a positive or negative regulator of exocytosis depending on the experimental system. An emerging theme is that actin promotes the last step of exocytosis by forming 'coats' around unusually large or insoluble cargo (Porat-Shliom *et al.*, 2013). For example, actin promotes exocytosis of large, endothelial-specific organelles called Weibel-Palade bodies (WPBs), which contain the von-Willebrand factor (VWF), an enormous multimeric protein that regulates blood clotting (Nightingale *et al.*, 2011). During exocytosis of large cargo such as VWF, vesicles first fuse with the target membrane, then actin forms a coat to stabilize the fused vesicle and promote expulsion of the cargo (Nightingale *et al.*, 2012). It is not well-understood which proteins regulate actin coat formation in exocytosis (Porat-Shliom *et al.*, 2013).

Intracellular pathogens exploit host actin machinery to facilitate multiple stages in their life cycles (Haglund *et al.*, 2011). For example, the bacterial pathogen *Listeria monocytogenes* stimulates actin-dependent restructuring and clathrin-mediated endocytosis to trigger its invasion into host cells (Pizarro-Cerda *et al.*, 2012). After invasion, several pathogens, including *Listeria,* exploit actin polymerization for intracellular motility, as well as cell-to-cell spread. The last stage within the life cycle of an intracellular pathogen is to egress from the host cell in order to propagate infection to new hosts. Here, too, there are examples of actin facilitating exit. Although exocytosis has been implicated in pathogen exit, the role of actin in this

process has not been clear, particularly *in vivo* (Chrisman *et al.*, 2010, Estes *et al.*, 2011, Friedrich *et al.*, 2012, Szumowski *et al.*, 2014).

We have been studying the *in vivo* life cycle and host cell exit strategy of an intracellular parasite called *Nematocida parisii*, which naturally infects the intestine of the nematode host *C. elegans* (Troemel *et al.*, 2008, Felix *et al.*, 2013). *N. parisii* belongs to the microsporidia phylum, which includes more than 1,400 species of intracellular parasites that are related to fungi (Williams, 2009, Texier *et al.*, 2010). Microsporidia can infect a wide range of hosts, including agriculturally relevant hosts such as fish and insects, as well as humans, where they can cause lethal diarrhea in immunocompromised patients (Didier *et al.*, 2011, Troemel, 2011). Microsporidia are obligate intracellular pathogens and thus undergo their entire replicative cycle inside of host cells (Keeling *et al.*, 2002, Vavra *et al.*, 2013). Microsporidia commonly infect intestinal cells, and here, the transparent *C. elegans* host system provides an excellent model to investigate the life cycle of an intestinal pathogen *in vivo*. The *C. elegans* intestine is composed of 20 epithelial cells that have striking structural and functional similarity to human intestinal epithelial cells (McGhee, 2007, Pukkila-Worley *et al.*, 2012). These cells are polarized, with microvilli on the apical side that are anchored into an actin-rich cytoskeletal structure called the terminal web. *N. parisii* spores invade the apical side of *C. elegans* intestinal cells, then replicate inside of these cells in a form called a meront, which then differentiates back into spores that exit exclusively out of the apical side of intestinal cells into the intestinal lumen (Troemel *et al.*, 2008, Estes *et al.*, 2011). Lumenal spores are then defecated out of the animal to infect new hosts as part of a fecal-oral life cycle.

Strikingly, a single live *C. elegans* animal can shed tens of thousands of spores in a few hours without lysis of intestinal cells, suggesting that the spore production and exit processes are carefully orchestrated inside of these cells (Estes *et al.*, 2011). Indeed, we previously described extensive cytoskeletal restructuring of *C. elegans* intestinal cells that likely facilitates the *N. parisii* life cycle. For example, during meront development, gaps form in the terminal web, which may remove a barrier to exit for spores. Interestingly, we also found that at early life stages, meronts replicate in direct contact with the cytosol, but once they differentiate into spores, they are found in separate membrane-bound, spore-containing compartments (SCCs) (Szumowski *et al.*, 2014). These SCCs then fuse with the apical plasma membrane for exit of spores into the intestinal lumen. The host smGTPase RAB-11 is a key player in this directional exocytosis: RAB-11 localizes to SCCs and is required for fusion of these compartments with the apical membrane. Accordingly, RAB-11 is also required for spore exit into the lumen, and for host contagiousness (Szumowski *et al.*, 2014). In summary, RAB-11-mediated directional exocytosis appears to be critical for *N. parisii* exit from *C. elegans* intestinal cells.

Our previous studies demonstrated that *N. parisii* spore exit is dependent on ACT-5, an intestinal-specific isoform of *C. elegans* actin, but the mechanism by which ACT-5 promoted spore exit was unclear (Estes *et al.*, 2011). Here, we present data showing that ACT-5 promotes exit through formation of actin coats around *N. parisii* SCCs that are exocytosing from intestinal cells into the lumen, similar to the formation of actin coats on large and insoluble kinds of endogenous cargo. We conducted an RNAi screen of *C. elegans* smGTPases to identify host factors that regulate ACT-5 coat formation on *N. parisii* SCCs. In particular, we found that formation of ACT-5

coats is dependent on the Rho GTPases *cdc-42* and *ced-10*/Rac1, as well as the Rab GTPases *rab-5*, *rab-10,* and *rab-11* that we previously identified in a screen for genes required for spore exit (Szumowski *et al.*, 2014). We found that actin coats form on exocytosing spores that are fused with the plasma membrane. Our results show that animals with normal numbers of ACT-5-coated spores excrete approximately twice as many spores as animals with reduced numbers of ACT-5-coated spores. These findings demonstrate an elegant application of host actin machinery that likely aids the pathogen in spreading to new hosts to propagate disease.

5.3 Results

5.3.1 Host actin forms coats around intracellular *N. parisii* spores at the apical membrane

Previously, we demonstrated a dose-dependent requirement for the actin isoform ACT-5 in *N. parisii* spore exit, although it was unclear how this host cytoskeletal structure promoted spore exit (Estes *et al.*, 2011). Here we show that *N. parisii* spores near the apical membrane acquire an ACT-5 'coat', while intracellular spores farther from the apical membrane or in the lumen do not exhibit ACT-5 coats (Figure 5-1A, B). We observed ACT-5 coats with several transgenic ACT-5 markers, including *YFP::ACT-5* (Figure 5-1A, B), as well as *mCherry::ACT*-5 and *GFP::ACT-5* (see Figures 5-2, 5-4). In order to confirm that the ACT-5-labeling was not due to an artifact from overexpressed transgenes, we also stained infected animals with antibodies specific for ACT-5 (MacQueen *et al.*, 2005), and saw similar localization around spores near the apical side of intestinal cells (Figure 5-1C).

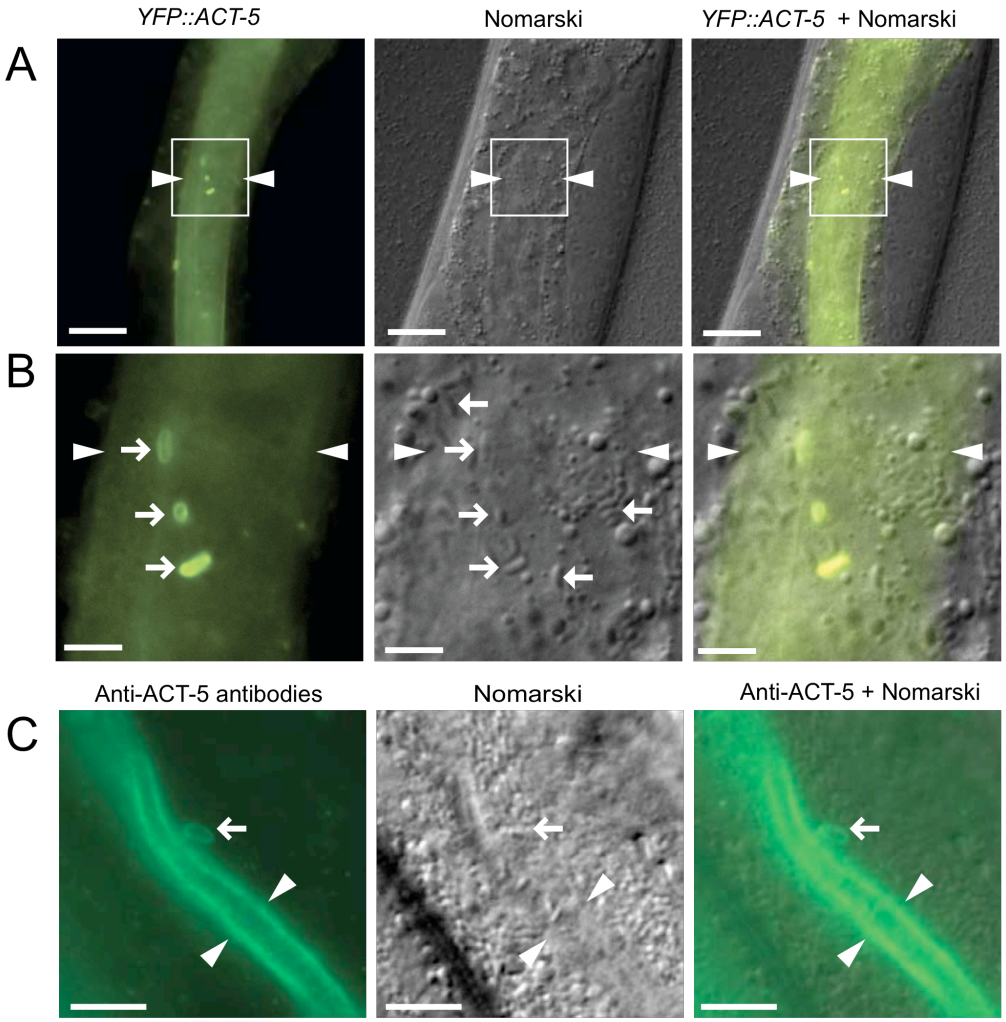

Figure 5-1. Intracellular *N. parisii* spores near the lumenal membrane of *C. elegans* intestinal cells acquire an actin "coat".
(A) *YFP::ACT-5* forms 'coats' around apically localized spores: region in white box is magnified in Panel B. Arrowheads indicate lumen. Scale bars are 20 μm. (B) Right-pointing arrows indicate apical spores with a *YFP::ACT-5* coat. Left-pointing arrows indicate spores further from the membrane that lack a *YFP::ACT-5* coat. Arrowheads indicate lumen. Scale bars are 5 μm. (C) Anti-ACT-5 antibody staining of infected animals. Arrow indicates spore near lumen with ACT-5 staining, similar to those observed with *YFP::ACT-5.* Arrowheads indicate lumen. Scale bars are 10 μm.

Additionally, we showed in earlier studies that *YFP::ACT-5* transgenic animals shed spores at the same frequency as wild type animals, suggesting that labeled ACT-5 does not impair function (Estes *et al.*, 2011). Using a strain that labels both

ACT-5 and IFB-2, an intermediate filament component in the terminal web at the apical side of intestinal cells, we did not see IFB-2 colocalizing with ACT-5 around spores (Figure 5-S1A), indicating that actin, but not intermediate filaments, is recruited to these apical spores.

To determine when these actin coats form, we examined the same animals at several different timepoints over the course of infection (Figure 5-S1B). We also analyzed populations of animals at single time points for the presence of spore coats (Figure 5-S1C). These experiments indicate that ACT-5 coats first appear around 42 hours post-inoculation (hpi), shortly after spores have differentiated and roughly when animals become contagious (Estes *et al.*, 2011). They also indicate that the fraction of a population of infected animals with ACT-5-coated spores increases over time. The correlation between the time at which ACT-5-coated spores appear and the time at which animals become contagious, as well as the apical localization of ACT-5-coated spores, suggested that these spores may be exiting from the host cell.

A

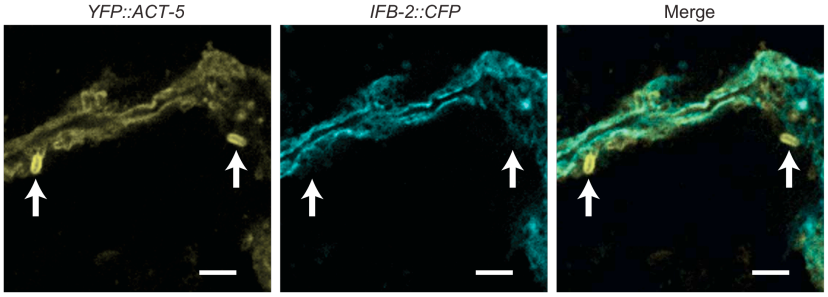

B

Study 1

Worm #	16.5 hpi	23 hpi	28 hpi	40 hpi	47 hpi
1	no	no	no	no	no
2	no	no	no	no	actin coated spores
3	no	no	no	no	actin coated spores
4	no	no	no	no	actin coated spores
5	no	no	no	no	no
6	no	no	no	no	no
7	no	no	no	no	no
8	no	no	no	no	actin coated spores
9	no	no	no	no	no
10	no	no	no	no	actin coated spores

Study 2

Worm #	24 hpi	29.5 hpi	34.5 hpi	48 hpi
1	no	no	no	actin coated spores
2	no	no	no	actin coated spores
3	no	no	no	actin coated spores
4	no	no	no	actin coated spores
5	no	no	no	actin coated spores
6	no	no	no	dead due to experimental error
7	no	no	no	actin coated spores
8	no	no	no	actin coated spores

C

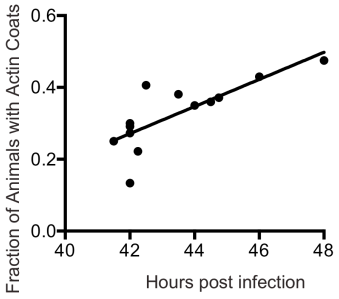

Figure 5-S1. Kinetics of actin coat formation around *N. parisii* spores. (A) *YFP::ACT-5*-coated spores (arrows) are not coated with *IFB-2::CFP*. Transgenic animals grown on L4440 empty vector RNAi bacteria were infected with microsporidia and observed at the actin spore coat stage, 43-46 hpi. Scale bars are 5 μm. (B) Individual infected animals carrying a *YFP::ACT-5* transgene were repeatedly imaged and recovered over the course of infection. Animals were examined at four timepoints in two independent experiments. Individual animals were imaged on a slide, recovered from the slide and then imaged again at a later timepoint for the presence of actin coats. (C) Synchronized populations of infected animals were examined to determine the frequency of actin spore coats at different timepoints after infection. Each data point represents an independent biological replicate, scoring a population of 20-60 animals.

5.3.2 ACT-5 forms coats on spores after they have fused with the apical membrane

Because we have been unsuccessful at visualizing pathogen trafficking using live imaging techniques, we assessed trafficking events using single timepoint analysis of spores with various markers. Our previous studies indicated that *N. parisii* SCCs fuse with the apical membrane of intestinal cells to ultimately exit out of these cells. Thus, we looked for colocalization of *mCherry::ACT-5*-coated spores with the host apical membrane marker *PGP-1::GFP* to determine whether these spores have fused with the host apical membrane. Indeed, we found that at 45 hpi, all spores with *mCherry::ACT-5* localization also showed localization of the apical membrane marker *PGP-1::GFP* (Figure 5-2A-B). In addition, some spores had *PGP-1::GFP* localization but did not have *mCherry::ACT-5* coats. These observations suggest that SCCs first fuse with the apical membrane, and then recruit ACT-5 to form coats. Next, we stained with the cell-impermeable dye Calcofluor white (CW) to determine which SCCs had access to the lumen (Szumowski *et al.*, 2014). In this assay, intracellular SCCs that have fused with the apical membrane and have access to the lumen via a fusion pore will be stained with CW as the dye diffuses into the SCC. Here, we found that some fused SCCs had access to the lumen without ACT-5 coats, while other fused SCCs had actin coats but no access to the lumen. However, most of the fused spores had both *mCherry::ACT-5* coats and CW staining (Figure 5-2A-B). Notably, exocytosed spores that were free in the lumen never exhibited *mCherry::ACT-5* or *PGP-1::GFP*, suggesting that these host factors remain inside the cell after exocytosis of the spore from the SCC. Altogether, these results suggest that SCCs likely fuse with the apical membrane before acquiring an ACT-5 coat or gaining

access to the lumen. After SCC fusion, it appears that either ACT-5 coat formation or lumenal access can occur first.

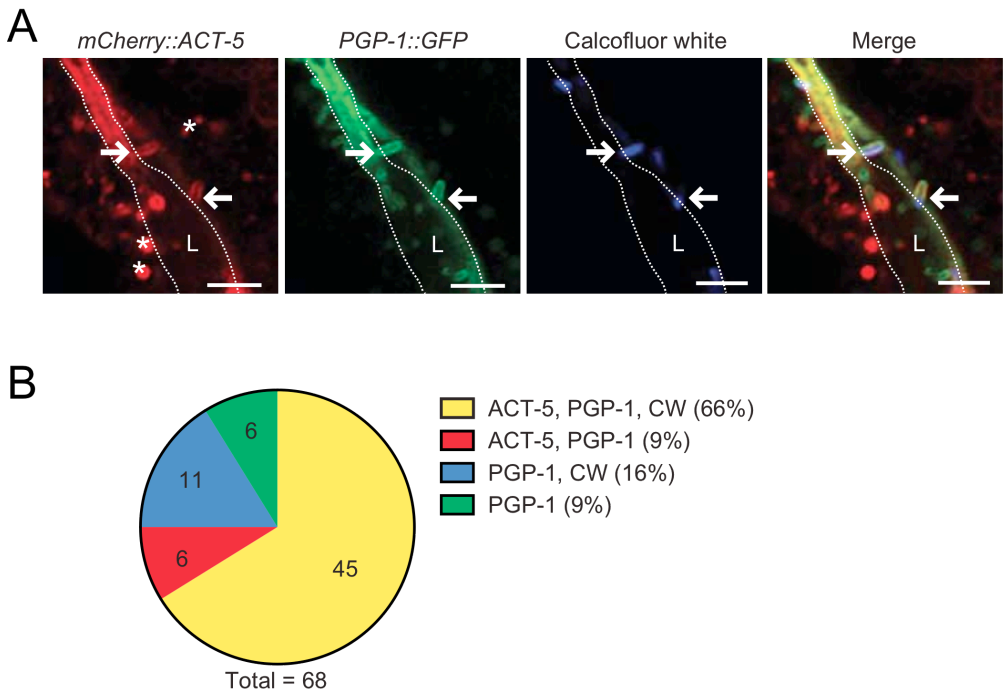

Figure 5-2. Actin-coated spores are labeled with host plasma membrane marker and have access to the lumen.
(A) Two *mCherry::ACT-5*-coated spores indicated with arrows are also labeled with the apical plasma membrane marker, *PGP-1::GFP*, indicating the SCC has fused with the host apical membrane. Right-pointing arrow shows a spore also stained with CW (blue), indicating it has access to the lumen. Left-pointing arrow only shows the edge of spore staining with CW, perhaps due to partial access to the lumen. Asterisks mark structures that are likely non-specific aggregations of mCherry. Lumenal walls indicated with dotted lines and lumenal space indicated with L. Scale bars are 5 μm. (B) Quantification at 45 hpi of ACT-5, PGP-1 and CW staining on 68 individual spores from 6 animals. Of note, all spores with actin coats also had *PGP-1::GFP* membrane surrounding them.

5.3.3 Small GTPases that regulate recycling endosomes and actin polymerization are required for actin coat formation

To investigate which host factors control ACT-5 coat formation, we conducted a feeding RNAi screen of 41 smGTPases, a class of genes involved in multiple intracellular trafficking events. After treatment with RNAi against these genes, the number of ACT-5-coated spores per animal was scored semi-quantitatively (Figure 5-3A, and see Experimental procedures). Our screen showed that RNAi knock-down of three members of the recycling endocytosis pathway, *rab-5, rab-10,* and *rab-11* caused defects in the number of ACT-5 coats per animal (Figure 5-3B). Previously we found that these three smGTPases were also important for spore exit, with *rab-11* required for fusion with the apical cell surface, and *rab-5* and *rab-10* not affecting fusion (Szumowski *et al.*, 2014). Here we also found that the Rho GTPases *cdc-42* and *ced-10* (Rac1) were required for actin coat formation (Figure 5-3B), although they were not previously identified in our screen for spore exit. The Rho GTPases *cdc-42* and *ced-10*/Rac1 are both known actin polymerization factors.

A

C. elegans gene	Homolog	# Actin Coats	*C. elegans* gene	Homolog	# Actin Coats
L4440	N/A	+++	rab-6.2	Rab6	++
arf-1.1	Arf1	++	rab-8	Rab8	+++
arf-1.2	Arf1	+++	rab-10	Rab10	0
arf-3	Arf5	+	rab-11	Rab11	0
arl-1	Arf1	+++	rab-18	Rab18	++
arl-3	Arf3	++++	rab-21	Rab21	+++
arl-5	Arf8	++	rab-28	Rab28	++
arl-6	Arf6	+++	rab-33	Rab33	+++
cdc-42	Cdc42	0	rab-37	Rab37	+++
ced-10	Rac1	0	ral-1	Ral-A	+
chw-1	Wrch1	+++	ran-1	Ran	sick
crp-1	Cdc42	+++	rap-1	Rap-1b	++++
drn-1	Di-Ras2	+++	rap-2	Rap-2a	+
evl-20	Arf2	+++	T26C12.3	Rap-2c	++++
let-60	K-Ras	++++	rap-3	Rap-1b	+++
rab-1	Rab1	++	ras-1	R-Ras	+
F11A5.3	Rab2	++	ras-2	M-Ras	+++
rab-2	Rab2	+	rheb-1	RheB	+
rab-3	Rab3	++++	rho-1	RhoA	+
rab-5	Rab5	0	sar-1	Sar1b	sick
rab-6.1	Rab6	+++	ssr-2	RasD1	++

B

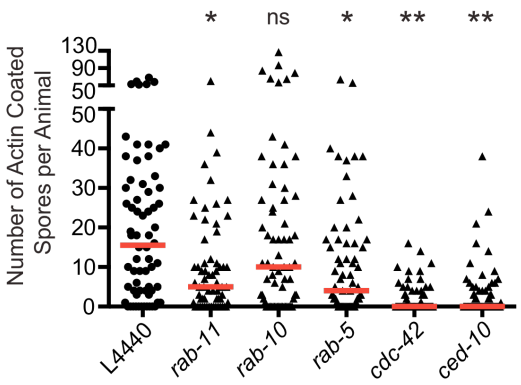

Figure 5-3. RNAi screen of smGTPases identifies factors required for ACT-5 coat formation on *N. parisii* spores.
(A) Feeding RNAi screen of smGTPases. Infected animals were analyzed at 43 hpi, when ACT-5 spore coats are first forming, and the number of ACT-5 spore coats per animal was determined using fluorescence microscopy. The number of + marks (0, +, ++, +++, ++++) indicates the fraction of animals examined (N > 60 per treatment) that had more than 20 actin coats per animal. The empty vector control L4440 received a score of +++, and screen hits with a score of 0 had a substantially reduced number of spore coat dense animals (see Experimental procedures for more information). (B) The number of actin-coated spores in screen hits was quantitatively analyzed in a blinded, independent biological replicate experiment. The y-axis changes scale at y = 50 to enable visualization of data points close to 0. Each data point represents the number of actin-coated spores in a single animal (n= >60 animals per sample). Red bar indicates the median value. P-value significance levels comparing each sample to L4440 using ANOVA are: ns = not significant; * = $p < 0.05$; ** = $p < 0.001$.

Because a defect in ACT-5 coat formation at the apical side of cells could be due to a disruption of cell polarity, we examined whether knocking down these smGTPases affected cell polarity, as assessed by apical localization of *PGP-1::GFP* and *mCherry::ACT-5*. Our previous analysis of spore exit indicated that *rab-5*, *rab-10*, and *rab-11* RNAi do not affect cell polarity with this assay (Szumowski *et al.*, 2014), and here we found that *cdc-42* and *ced-10* also do not affect cell polarity (Figure 5-S2). Altogether, these studies indicate that the smGTPases *rab-5*, *rab-10*, *rab-11*, *cdc-42* and *ced-10/*Rac1 are important for actin coat formation on SCCs.

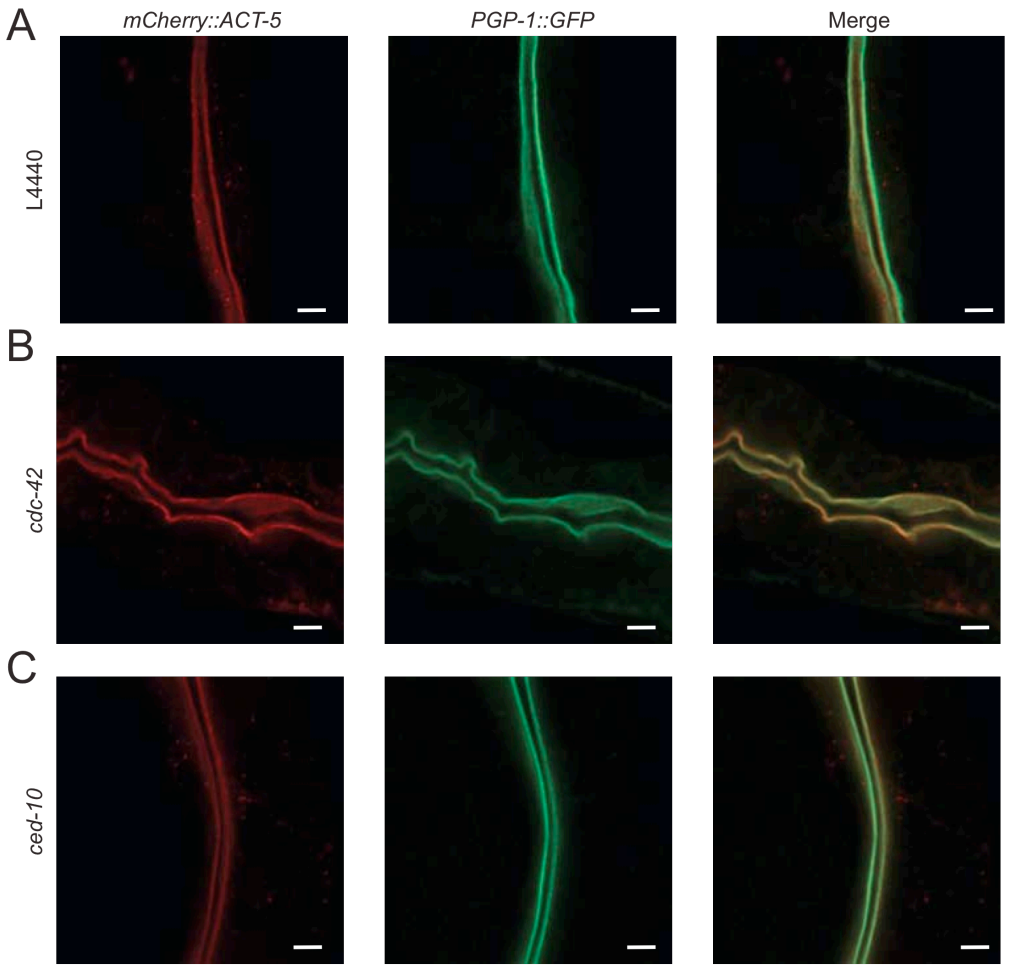

Figure 5-S2. Apical localization of PGP-1 and ACT-5 is not affected by smGTPase RNAi treatment.
(A) Empty vector RNAi treatment of infected animals shows that PGP-1 is normally localized along the lumen and colocalizes with ACT-5 at the apical cell surface. (B-C) Animals treated with smGTPase screen hit RNAi clones from late L2-adulthood (the treatment used for the screen) exhibit no change in *PGP-1::GFP* or *mCherry::ACT-5* apical localization. Scale bar in all images is 5 μm.

5.3.4 RAB-11 and CED-10/Rac1 localize to spores, but do not colocalize with ACT-5

To investigate whether the smGTPases identified in our screen had a direct role in the actin coat formation process, we next examined their localization to spores.

In our earlier work we found that RAB-5 and RAB-10 did not localize to spores, but that RAB-11 did (Szumowski *et al.*, 2014). Here, we compared RAB-11 localization to ACT-5 localization and did not observe any overlap between spores with *RFP::RAB-11* localization and spores with *GFP::ACT-5* or *PGP-1::GFP* localization (Figure 5-4A). This observation is consistent with the genetic findings that RAB-11 acts upstream of actin coat formation (Figure 5-3B) and fusion with the apical membrane (Szumowski *et al.*, 2014). Next, we used a *GFP::CED-10* transgene to examine CED-10/Rac1 localization around *N. parisii* spores (Lundquist *et al.*, 2001). Here we found that *GFP::CED-10* formed coats around spores, and like RAB-11-coated spores, these CED-10/Rac1-coated spores were distinct from the ACT-5-coated spores (Figure 5-4B). When comparing CED-10/Rac1 and RAB-11 localization in the same animals, we found that there were some spores with both CED-10/Rac1 and RAB-11 staining (Figure 5-4C), although these were less common than spores with only CED-10/Rac1 or only RAB-11 staining (Figure 5-4D). Specifically, of *GFP::CED-10*-coated spores, only 29% (n=15/52 spores, n=5 animals) also had *RFP::RAB-11* localization, while of *RFP::RAB-11*-coated spores, 5% (n=15/277 spores, n=5 animals) also had *GFP::CED-10* localization.

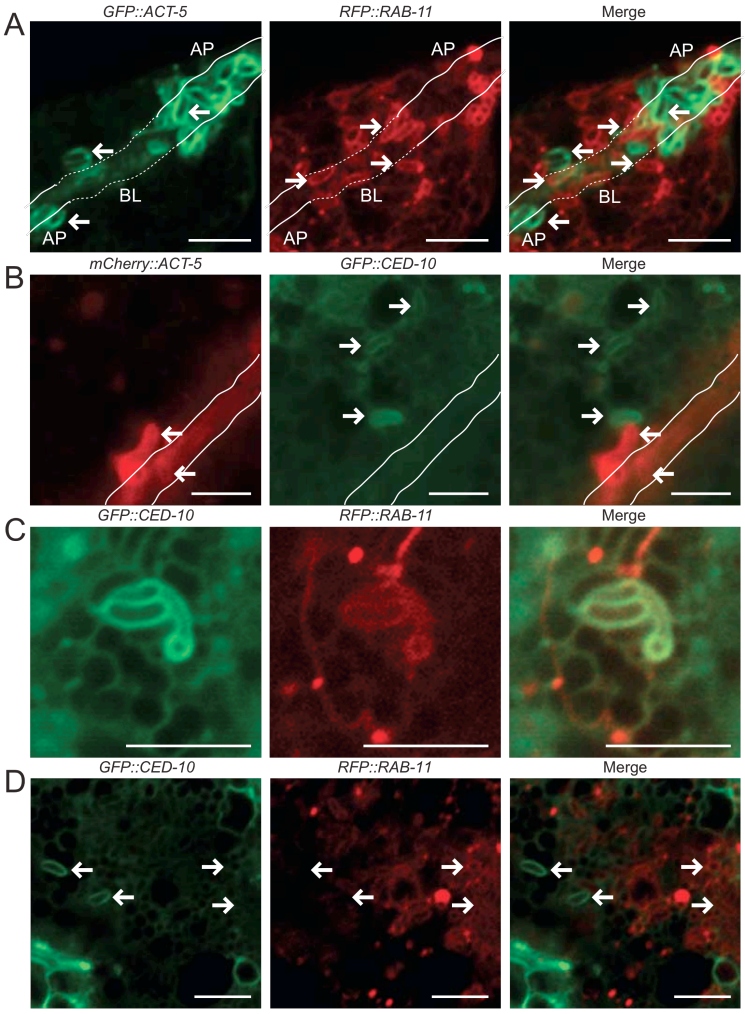

Figure 5-4. RAB-11 and CED-10 localize to *N. parisii* spores distinct from those where ACT-5 localizes.
(A) In *GFP*::*ACT-5*;*RFP::RAB-11* transgenic animals left-pointing arrows indicate examples of ACT-5-coated spores, which are distinct from the right-pointing arrows that mark RAB-11-positive spores. Because of the three-dimensional nature of the intestine, the lumen dips in and out of the Z-plane of focus. This tissue depth is indicated with the solid line marking apical regions (AP) and dotted line marking more basolateral (BL) regions of the intestine. (B) In *mCherry::ACT-5;GFP::CED-10* transgenic animals left-pointing arrows indicate examples of ACT-5-coated spores, which are distinct from the right-pointing arrows that mark CED-10 positive spores. Solid white lines indicate the lumen. (C) In *GFP::CED-10*; *RFP::RAB-11* transgenic animals spores often exhibit only a *GFP::CED-10* coat (left-facing arrows), or a *RFP::RAB-11* coat (right-facing arrows). (D) In *GFP::CED-10*;*RFP::RAB-11* transgenic animals CED-10 and RAB-11 occasionally colocalize on spores. (A-D) All animals were infected with microsporidia and observed at 43-46 hpi. Scale bars are 5 μm.

5.3.5 Formation of ACT-5 coats correlates with spore exit but is not required for spore exit

Several lines of evidence suggested that ACT-5-coated spores could be exiting from host cells. First, as mentioned earlier, ACT-5 is required for spore exit (Estes *et al.*, 2011). Second, ACT-5-coated spores are localized apically and have access to the lumen (Figure 5-2). Third, we found that ACT-5 coats appear at about 42 hpi (Figure 5-S1), shortly after spores have differentiated and roughly when animals begin excreting spores (Estes *et al.*, 2011). Fourth, many of the smGTPases that regulate ACT-5 coat formation also were previously shown to regulate spore exit (Szumowski *et al.*, 2014). Therefore, we next examined contagiousness and therefore spore exit from individual animals that either had ACT-5-coated spores or did not have ACT-5-coated spores. Although contagiousness is an indirect measure of spore exit, it addresses the role of ACT-5 coats in pathogen exit by enabling direct comparison of the presence of ACT-5 coats and the ability to transmit infection in the same animal.

To assess contagiousness, infected *YFP::ACT-5* transgenic donor animals were individually placed on a plate with 200 uninfected, recipient animals. After exposure to recipients, these infected donor animals were removed and examined for the presence of ACT-5 spore coats; after an incubation period, the recipients were observed to determine whether or not they became infected (See Experimental procedures for more information). If the recipients became infected, this result indicated that they had been exposed to a contagious donor that was excreting spores. We found that 74% of contagious donors had ACT-5-coated spores inside their intestinal cells, while 26% did not. Of non-contagious donors, none had ACT-5

coated spores (Figure 5-5A). Together, these results indicate that ACT-5 coats are correlated with contagiousness, but are not required for contagiousness. Further supporting this correlation, we found that donors with actin spore coats were more contagious than donors without actin spore coats: 81% of donors with actin spore coats caused larval arrest, a phenotype of severe infection, in recipient animals, whereas only 44% of contagious animals lacking ACT-5-coated spores caused larval arrest. Therefore, donors with *YFP::ACT-5*-coated spores are more contagious. The fact that 26% of contagious animals did not exhibit ACT-5-coated spores could be explained if ACT-5 coats are transient and the animal was examined after an ACT-5 coat had formed and disappeared. However, another interpretation of these results is that ACT-5 coats are not required for spore exit, and the presence of ACT-5 coats is simply correlated with a stage of infection when animals excrete more spores.

To more directly examine whether ACT-5 coats are required for spore exit, we measured spore production and spore exit in animals treated with RNAi against genes important for formation of ACT-5 coats. One possible explanation for a reduction of ACT-5-coated spores is that there are fewer spores made under these RNAi conditions. We previously had shown that knock-down of *rab-5, rab-10,* and *rab-11* did not block spore production (Szumowski *et al.*, 2014). Here we show that *cdc-42* and *ced-10/*Rac1 also do not block spore production. In fact, *ced-10/*Rac1 RNAi caused a doubling in spore production (Figure 5-5B). Thus, these RNAi clones do not cause a reduction in ACT-5-coated spores due to a reduction in spore production. Next, we examined spore exit. Previously, we had shown that *rab-5*, *rab-10*, and *rab-11* RNAi-treated animals had strong spore exit defects, which suggested that ACT-5 coats played a role in spore exit (Szumowski *et al.*, 2014). Surprisingly

however, we found that RNAi against *ced-10/*Rac1 caused no significant decrease in spore shedding, while RNAi against *cdc-42* caused about a 50% decrease in spore shedding (Figure 5-5C), despite the fact that *cdc-42* and *ced-10/*Rac1 RNAi cause a nearly complete block in the number of ACT-5 coats (Figure 5-3B). However, when spore exit is adjusted by the number of spores produced (which is greater in *ced-10/*Rac1-defective animals), the fraction of intracellular spores that are shed for both *cdc-42* and *ced-10/*Rac1 RNAi-treated animals was about half that of the control animals (Figure 5-5D). These results suggest that while ACT-5 coat formation may not be absolutely required for spore exit, this process leads to a doubling of spore exit.

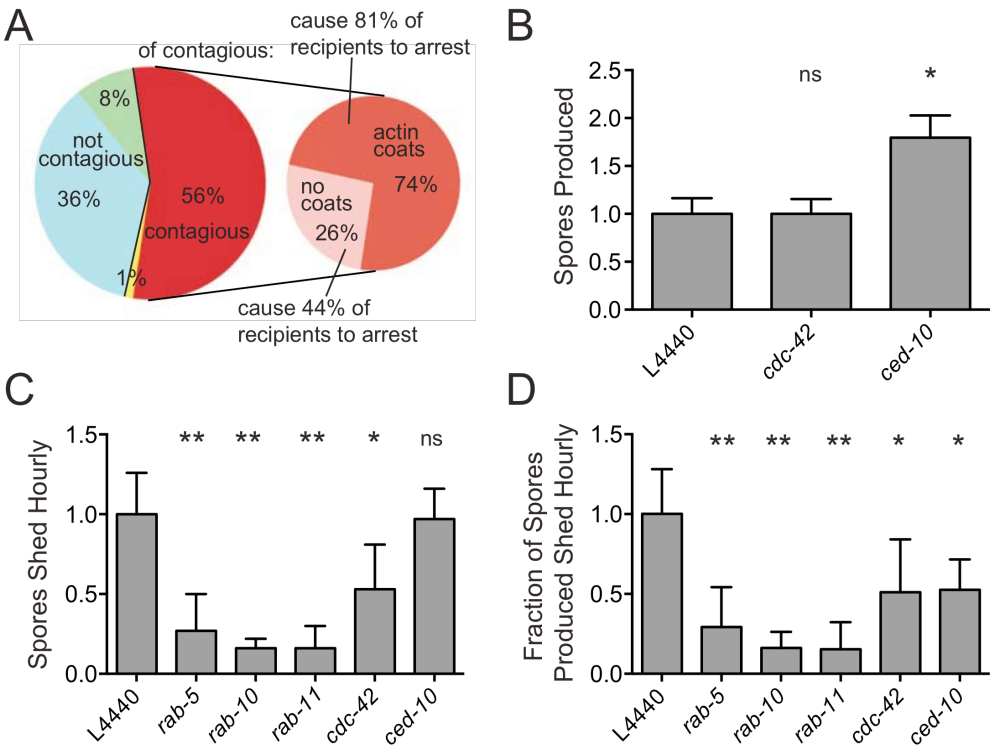

Figure 5-5. ACT-5 coats are correlated with spore exit and contagiousness, but are not required.
(A) Contagiousness of 84 infected donor animals was compared to the presence of spores and ACT-5 coats after exposure to recipients. Data combined from two biological replicate experiments. (B) Spore production in N2 RNAi-treated animals was quantified at 44 hpi. The total number of spores released from 50 lysed infected animals was quantified and normalized to the values from L4440-treated animals. Mean is from three independent experiments. (C) Quantification of spore shedding in N2 animals treated with RNAi against genes identified Figure 5-3 as regulators of ACT-5-coated spores. The normalized number of spores excreted per animal per hour is shown on the y-axis (mean is from three to four independent experiments for each sample), RNAi clone is shown on the x-axis. (D) Fraction of total spores produced that are excreted hourly. Normalized spore shedding data for each sample (Panel B) was divided by the normalized total number of spores produced for each sample (Panel C, and (Szumowski *et al.*, 2014) for Rab values) to give the fraction of the total spores produced that are excreted hourly. Propagation of error from combined experiments was calculated by taking the square root of the sum of standard deviations from all experiments squared, N = 6. Panels B-D show mean and standard deviation of independent experiments, normalized to L4440 values. ANOVA was used to calculate P-values indicated above graphs, comparing each sample to the L4440 control: ns = not significant; * = $p < 0.05$; ** = $p < 0.001$.

5.4 Discussion

Exit from the host cell is a key stage in the spread of intracellular pathogens. Here, we describe important mechanistic insights about the role of actin in the directional exoctyosis of *N. parisii*, a microsporidian pathogen that naturally infects the intestinal cells of *C. elegans.* In earlier studies we have shown that *N. parisii* spores are enclosed in membrane-bound compartments that are directed for exocytosis out of the apical side of intestinal cells into the lumen by the smGTPase RAB-11. We now show data supporting the model that after spores traffic to and fuse with the host apical membrane, most of these fused spores become coated with the intestinal-specific actin, ACT-5 (Figure 5-2), in a process that is dependent on the host smGTPases *rab-5, rab-10, rab-11, cdc-42,* and *ced-10/*Rac1 (Figure 5-3). Based on actin coat quantification and assays of spore exit, we propose actin coat-dependent and actin-coat-independent routes of exit for *N. parisii* spores (Figure 5-6). RNAi against actin polymerization factors *cdc-42* and *ced-10*/Rac1 almost completely eliminated ACT-5 coats on spores, but only reduced spore exit in half (Figure 5-5D). Because RNAi against the recycling endosome factors *rab-5*, *rab-10*, and *rab-11* caused a stronger block in spore exit, we propose they act upstream of both routes of exit, while *cdc-42* and *ced-10*/Rac1 are only important for promoting exit of actin-coated spores. Based on the spore shedding defect caused by RNAi against these actin polymerization factors, we propose that the ability to form ACT-5 coats roughly doubles the exocytic output of spores, a process that we described earlier as being dependent on ACT-5 (Estes *et al.*, 2011).

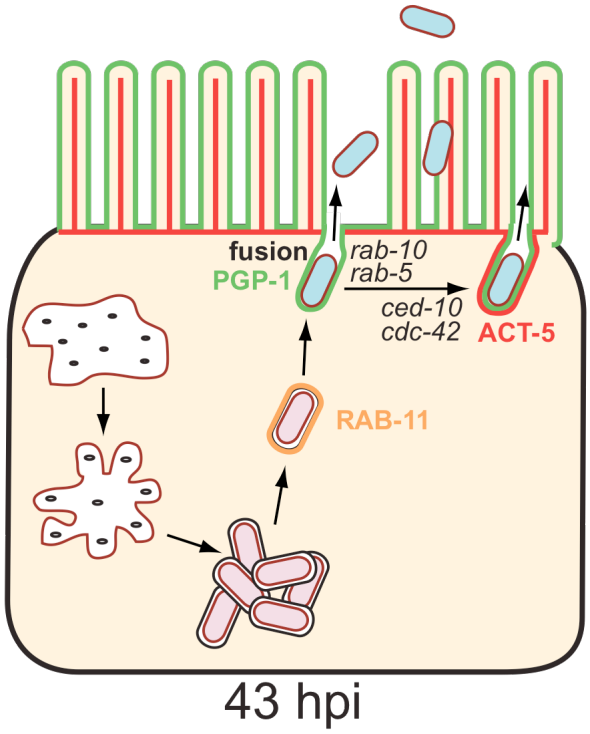

Figure 5-6. Model for actin regulation of *N. parisii* spore exocytosis and compensatory endocytosis in *C. elegans* intestinal cells.
At 43 hpi, meronts have differentiated into spores that are enclosed in membrane-bound spore-containing compartments (SCCs) labeled with RAB-11. These SCCs traffic up to the apical cell surface and fuse with host membrane, acquiring PGP-1 membrane marker. After fusion, spores have access to the lumen and are able to exit from the host cell, sometimes acquiring an ACT-5 coat. Formation of ACT-5 coats is dependent on the Rho GTPases *ced-10* and *cdc-42*, as well as *rab-5*, *rab-10* and *rab-11*.

Our findings about actin coats forming around *N. parisii* spores and likely promoting their exit are novel in terms of pathogen exit strategies, although these observations are intriguingly similar to descriptions of actin structures surrounding secretory vesicles containing large or insoluble endogenous cargo, where actin can form ‘coats’ or ‘rings’ around these vesicles after fusing with the plasma membrane (Nightingale *et al.*, 2012). For example, vascular endothelial cells secrete an extremely large glycoprotein called VWF, which is contained in enormous cigar-

shaped organelles called Weibel-Palade bodies (WPBs) that are up to 1-5 μm long (Metcalf *et al.*, 2008), similar in length to the 2 μm-long or 3 μm-long *N. parisii* spores (Troemel *et al.*, 2008). WPBs acquire actin rings upon fusion with the apical membrane and recent studies have shown that in this context actomyosin contractility squeezes VWF out into the extracellular environment (Nightingale *et al.*, 2012). As with exocytosis of *N. parisii* spores, Rabs are recruited to WPBs and are required for VWF secretion, although the exact Rabs involved in actin coat formation have not been well-defined (Zografou *et al.*, 2012). Our studies provide insight into smGTPases that regulate actin coat formation, identifying three Rabs involved in recycling endocytosis and two Rhos involved in actin polymerization. Actin has been shown to form coats around exocytosing vesicles in other systems as well, such as lung surfactant-containing vesicles (Miklavc *et al.*, 2012), cortical granules in frog oocytes (Sokac *et al.*, 2003, Sokac *et al.*, 2006), and amylase-containing vesicles in pancreatic cells (Turvey *et al.*, 2004, Jang *et al.*, 2012). In these systems, actin coats form after vesicles fuse with the membrane, are often stable for over 30 s, and likely serve to squeeze the cargo outside of the cell (Sokac *et al.*, 2006). Similarly, the actin coats appear to form around *N. parisii* spores after fusion with the membrane and may serve to expel these pathogens out of the cell. Although we are currently unable to visualize spore release in real-time, calculations based on approximately 2000 spores exiting per animal per hour (Figure 5-5C, L4440 prior to normalization) and approximately 19 actin coated spores per animal at any time (Figure 5-3B, L4440) suggest an approximate actin coat duration time of 35 s, which is consistent with the kinetics of exocytosis of large endogenous cargo.

Defining the precise role of actin in secretory events has been challenging for endogenous cargo, with some studies showing that actin promotes secretion and other studies showing that actin inhibits secretion (Cingolani *et al.*, 2008, Trifaro *et al.*, 2008). Recent imaging studies with WPBs have clarified the opposing roles that actin can play in secretion of VWF, with actin inhibiting the initial fusion event, but promoting release once fusion has occurred (Nightingale *et al.*, 2011). Similarly, we believe that ACT-5 plays opposing roles in the *N. parisii* exit process, with inhibition early during the exit process, and promotion later in the process (Estes *et al.*, 2011). Our previous studies showed that during the early stage of *N. parisii* development ACT-5 ectopically localizes to the basolateral side of cells and is then followed by formation of gaps in the terminal web. Because actin knock-down causes gap formation in the absence of infection, we hypothesized that actin relocalization triggers gap formation, perhaps to remove a barrier to exit. These findings suggested that early during infection actin can obstruct exit. However, we found that a reduction of ACT-5 expression impaired overall spore exit, which we now show is likely due in part to the role of ACT-5 forming coats around spores to promote expulsion. This dual role of actin first inhibiting and then promoting secretion appears to be common for exocytosis of vesicles containing large cargo such as the VWF protein or *N. parisii* spores. Interestingly, actin has also been shown to play opposing roles in the secretion of dense core vesicles, although here the mechanism of promoting secretion is likely distinct from the actin coats that form on *N. parisii* spores (Wollman *et al.*, 2012).

N. parisii is only one of more than 1,400 species of microsporidia, and very little is known about the exit process for any of these species. In particular, it would

be interesting to examine the exit process of microsporidian species that infect human intestinal cells, to determine whether this large cargo also acquires actin coats during the process of exiting from host cells. In this way it will be possible to determine whether the mechanistic insights we have gained from studying microsporidia transmission in *C. elegans* are conserved in medically relevant microsporidia infections of humans.

5.5 Experimental procedures

5.5.1 Strains

C. elegans were maintained on nematode growth media (NGM) plates seeded with *E. coli* OP50-1, as described (Brenner, 1974). We used N2 wild-type animals. See Table 5-1 for a complete list of strains used.

Table 5-1. Strains used in this study.

Strain	Transgene	Source	Figures used
N2	N/A	*Caenorhabditis* Genetics Center	5-5B, 5-5C, 5-5D
ERT38	*kcIs6[ifb-2p::IFB-2::CFP]; caIs[ges-1p::YFP::ACT-5]*	(Estes et al., 2011)	5-1A, 5-1B, 5-5A, 5-S1A-C
ERT60	*jyIs13[act-5p::GFP::ACT-5]*	UV psoralen integration of *act-5p::GFP::ACT-5* (Kang *et al.*, 2009)	used for crosses, 5-S1C
ERT99	*jyIs13[act-5p::GFP::ACT-5]; pwIs428[vha-6p::RFP::RAB-11.1]*	ERT60 x RT1102	5-4A
ERT106	*jyIs17[vha-6p::mCherry::ACT-5]; dkIs166 [opt-2p::PGP-1::GFP]*	(Szumowski *et al.*, 2014)	5-2, 5-3, 5-S1C, 5-S2A-C
ERT197	*jyIs17 [vha-6p::mCherry::ACT-5]IV; nEx1039[ced-10p::GFP::CED-10]; unc-76(e911)V pwIs428[vha-6p::RFP::RAB-11.1];*	ERT104 x MT10865	5-4B
ERT202	*nEx1039[ced-10p::GFP::CED-10]; unc-76(e911)V*	RT1102 x MT10865	5-4C, 5-4D
MT10865	*nEx1039 [ced-10p::GFP::CED-10]; unc-76(e911)V*	(Lundquist *et al.*, 2001)	used for crosses
RT1102	*pwIs428[vha-6p::RFP::RAB-11.1]*	(Chen *et al.*, 2006)	used for crosses

5.5.2 *N. parisii* Spore Preps and Infection Assays

Spore preps were prepared by culturing *N. parisii* inside of *C. elegans*, and when animals were heavily infected, they were mechanically disrupted with silicon beads to release spores, which were filtered to remove intact larvae and eggs. Aliquots of spores were quantified and stored at -80C prior to use. See (Estes *et al.*, 2011) for more information on spore preps. Infection assays were conducted with synchronized L1 larvae grown for 24 hours on 10 cm NGM plates seeded with OP50 at 20°C until approximately L3 stage, when they were infected with 2×10^6 *N. parisii* spores and then incubated at 25°C. To stain spores in contact with the lumen (Figure 5-2), CW was fed to infected animals 2 hours prior to imaging by applying 300 µl of CW to each 6 cm NGM/OP50 plate. The timing of actin coat formation (Figure 5-S1C) was assessed in a population of animals in independent experiments using different ACT-5 fusion proteins including: *GFP::ACT-5*, *YFP::ACT-5*, and *mCherry::ACT-5* (see Table 5-1 for strain names).

5.5.3 Microscope Image Acquisition

Symptoms of infection (Figure 5-S1B) were tracked by mounting approximately 50 animals on agarose pads and then viewing animals with Nomarski optics and/or fluorescence on a Zeiss AxioImager.M1 at 630X magnification (Zeiss EC Plan-NEOFLUAR Oil, DIC, 1.4 NA objective), using Axiovision 4.8 software and a Zeiss AxioCam MRm camera. These imaging conditions were also used to assess the presence of spores inside infected donor animals in contagiousness assays (Figure 5-5A), and the number of ACT-5 coated spores in RNAi screen (Figure 5-3). All other images were acquired on a confocal Zeiss LSM700 Observer.Z1 at 630X

magnification (Zeiss PLAN-APOCHOMAT Oil, 1.4 NA objective) using ZEN2010 software and a LSM T-PMT camera.

5.5.4 Anti-ACT-5 Antibody Staining

N. parisii-infected animals were fixed in a mixture of formaldehyde, n-heptane and methanol, freeze-thawed in liquid nitrogen, and then treated with collagenase. Samples were blocked with goat serum, incubated with normal goat serum and BSA, incubated with 1:10 anti-ACT-5 rabbit polyclonal antibodies, then incubated with goat anti-rabbit conjugated with Alexa488 secondary antibodies diluted 1:300 and mounted on agarose pads with Vectashield for viewing. See MacQueen et al., 2005 for more details on ACT-5 antibodies.

5.5.5 Spore-Shedding Assays

Synchronized L3 animals were infected with 2.0 x 10^5 spores on 6 cm plates and incubated at 25˚C for 39 hours to allow the infection to progress until the spore shedding stage of infection. Animals were then washed three times in M9 to remove spores from cuticles and placed in microfuge tubes with 500µl of 1:1 *E. coli* OP50 and M9. The spores excreted by 50 animals from 40-48 hpi were collected and quantified. See Estes et al., 2011 for more details on spore shedding assays.

5.5.6 RNA Interference Assays

Feeding RNAi experiments were performed as described (Estes *et al.*, 2011). Briefly, synchronized populations of L1 animals were seeded on plates of RNAi bacteria. All RNAi clones were used undiluted except for *rab-5* and *rab-11.1*, which

were diluted 1:10 with L4440 (vector alone) control RNAi bacteria to allow for normal development.

5.5.7 Contagiousness Assays

A synchronized population of ERT38 *kcIs6 [IFB-2::CFP], caIs[YFP::ACT-5]* animals was infected at the early L3 stage with 2 million spores/6 cm plate and allowed to reach 38 hpi. At this time point, animals were washed three times in M9 to remove any spores for their cuticles, and replated onto a clean OP50 plate. From this plate individual donor animals were cloned out onto plates containing 200 N2 L1s. The infected donor and the recipient N2s were allowed to cohabit the plate for 8 hours at 25˚C, at which point the infected donor animal was removed from the plate and mounted onto an agarose pad for microscopy. Each individual donor animal was assessed for the presence of any intracellular spores using Nomarski optics, and the presence of *YFP::ACT-5* coats using fluorescence. Results were recorded on a spreadsheet and later compared with the degree of infection of the recipients. After removal of the donor animal, the recipients were maintained at 25˚C for 7 days and then a 1 cm x 1 cm region of agarose plate containing animals was transferred to a fresh OP50 plate and allowed to grow for 7 days at 25˚C. At the end of this period, plates were assessed for larval arrest and lack of food clearing, traits associated with heavily infected animals. This information was paired with the actin phenotypes observed from the donor animal. As controls, animals that did not yet have fully developed spores were verified to be non-contagious.

5.5.8 RNAi Screen for Small GTPases that Block Formation of Actin Coats

A library of 41 *C. elegans* smGTPase RNAi clones was divided roughly into quarters and prepared as 4 separate batches, each with the empty vector control, L4440. All clones were sequence verified. A synchronized population of 200 L1 animals containing *mCherry::ACT-5* and *PGP-1::GFP* transgene markers were plated on a lawn of RNAi bacteria and allowed to develop to the L3 stage before infecting with 2 million *N. parisii* spores per 6 cm plate. Infection proceeded at 25˚C for 43 hours to the ACT-5 spore coat stage. Animals were fixed in 4% PFA and stored at 4˚C until analyzed. To determine whether an RNAi clone affected the formation of ACT-5 spore coats, approximately 60-80 animals were mounted on an agarose pad and examined under the microscope for the number of actin spore coats per animal. Hits were defined as reducing the proportion of the population with greater than 20 ACT-5 coats per animal by at least 70% relative to L4440. RNAi treatments were grouped into bins relative to the control (0-30% of control value = 0, 31-50% = +, 51-70% = ++, 71-130% = +++, 131-200% = ++++). After testing each clone once, hits were validated by performing a biological replicate experiment along with clones that were not initially hits used as negative controls. Of note, there are two *rab-11* isoforms, *rab-11.1* and *rab-11.2*, which have high sequence similarity. An RNAi clone against *rab-11.2* was used during the screen. However, for validation *rab-11.1* RNAi (diluted 1:10 with L4440) was used instead of *rab-11.2* RNAi because 1) we found direct localization of RAB-11.1 protein to *N. parisii* spores, 2) the *rab-11.2* RNAi clone knocks down *rab-11.1* and 3) using *rab-11.1* directly was found to have a stronger phenotype (Szumowski *et al.*, 2014). To determine whether the clone was affecting cell polarity, the localization of the apically-localized plasma membrane marker, *PGP-*

1::GFP was assessed. The spore production of RNAi-treated animals was measured at 44hpi by dissolving host tissue of infected animals and counting the spores released. Infected animals were fixed with acetone and 50 animals were hydrolyzed for 30 min with 200 mM NaOH, 0.1% SDS, and 1:100 CW. See (Szumowski *et al.*, 2014) for more details.

5.6 Additional Acknowledgements

We thank Keir Balla, Robert Luallen, Kirthi Reddy, Aaron Reinke, and Roy Wollman for helpful comments on the manuscript. Some strains were provided by the CGC, which is funded by NIH Office of Research Infrastructure Programs (P40 OD010440). This work was supported by NIH predoctoral training grant T32 GM008666 and a NSF Predoctoral Fellowship to S.C.S.; NIH Training in Immunology Grant 5T32AI060536 to K.A.E., and NIAID R01 AI087528, the Searle Scholars Program, Packard Foundation and Burroughs Wellcome Fund fellowships to E.R.T. We claim no conflicts of interest.

Chapter 5, in full, is currently being prepared for re-submission and publication, Szumowski, S.; Estes, K.; Popovich, J.; Botts, M.; Sek, G.; Troemel, E., Small GTPases promote actin coat formation on pathogens exocytosing from *C. elegans* intestinal cells. The dissertation author was the primary investigator and author of this material. Author contributions to manuscript are as follows: Szumowski, S.: Figure 2, Figure 3, Figure 4, Figure 5A, 5C, 5D, Figure 6, Figure S1A, Figure S1C, Figure S2; Estes, K.: Figure 1, Figure S1B; Popovich, J.: Figure 3A; Botts, M.: Figure 5B; Sek, G.: Figure 3A.

5.7 References

Brenner, S. (1974). The genetics of Caenorhabditis elegans. *Genetics* **77,** 71-94.

Chen, C.C., Schweinsberg, P.J., Vashist, S., Mareiniss, D.P., Lambie, E.J. and Grant, B.D. (2006). RAB-10 is required for endocytic recycling in the Caenorhabditis elegans intestine. *Molecular Biology of the Cell* **17,** 1286-1297.

Chrisman, C.J., Alvarez, M. and Casadevall, A. (2010). Phagocytosis of Cryptococcus neoformans by, and nonlytic exocytosis from, Acanthamoeba castellanii. *Applied and Environmental Microbiology* **76,** 6056-6062.

Cingolani, L.A. and Goda, Y. (2008). Actin in action: the interplay between the actin cytoskeleton and synaptic efficacy. *Nature Reviews Neuroscience* **9,** 344-356.

Didier, E.S. and Weiss, L.M. (2011). Microsporidiosis: not just in AIDS patients. *Current Opinion in Infectious Disease* **24,** 490-495.

Estes, K.A., Szumowski, S.C. and Troemel, E.R. (2011). Non-lytic, actin-based exit of intracellular parasites from C. elegans intestinal cells. *PLoS pathogens* **7,** e1002227.

Felix, M.A., Jovelin, R., Ferrari, C., Han, S., Cho, Y.R., Andersen, E.C., Cutter, A.D. and Braendle, C. (2013). Species richness, distribution and genetic diversity of Caenorhabditis nematodes in a remote tropical rainforest. *BMC Evolutionary Biology* **13,** 10.

Friedrich, N., Hagedorn, M., Soldati-Favre, D. and Soldati, T. (2012). Prison break: pathogens' strategies to egress from host cells. *Microbiology and Molecular Biology Reviews : MMBR* **76,** 707-720.

Haglund, C.M. and Welch, M.D. (2011). Pathogens and polymers: microbe-host interactions illuminate the cytoskeleton. *The Journal of Cell Biology* **195,** 7-17.

Heasman, S.J. and Ridley, A.J. (2008). Mammalian Rho GTPases: new insights into their functions from in vivo studies. *Nature Reviews Molecular Cell Biology* **9,** 690-701.

Jang, Y., Soekmadji, C., Mitchell, J.M., Thomas, W.G. and Thorn, P. (2012). Real-Time Measurement of F-Actin Remodelling during Exocytosis Using Lifeact-EGFP Transgenic Animals. *PloS One* **7,** e39815.

Kaksonen, M., Toret, C.P. and Drubin, D.G. (2006). Harnessing actin dynamics for clathrin-mediated endocytosis. *Nature Reviews Molecular Cell Biology* **7,** 404-414.

Kang, J., Shin, D., Yu, J.R. and Lee, J. (2009). Lats kinase is involved in the intestinal apical membrane integrity in the nematode Caenorhabditis elegans. *Development* **136,** 2705-2715.

Keeling, P.J. and Fast, N.M. (2002). Microsporidia: biology and evolution of highly reduced intracellular parasites. *Annual Review of Microbiology* **56,** 93-116.

Lundquist, E.A., Reddien, P.W., Hartwieg, E., Horvitz, H.R. and Bargmann, C.I. (2001). Three C. elegans Rac proteins and several alternative Rac regulators control axon guidance, cell migration and apoptotic cell phagocytosis. *Development* **128,** 4475-4488.

MacQueen, A.J., Baggett, J.J., Perumov, N., Bauer, R.A., Januszewski, T., Schriefer, L. and Waddle, J.A. (2005). ACT-5 is an essential Caenorhabditis elegans actin required for intestinal microvilli formation. *Molecular Biology of the Cell* **16,** 3247-3259.

McGhee, J.D. (2007). The C. elegans intestine. *WormBook***,** 1-36.

Metcalf, D.J., Nightingale, T.D., Zenner, H.L., Lui-Roberts, W.W. and Cutler, D.F. (2008). Formation and function of Weibel-Palade bodies. *Journal of Cell Science* **121,** 19-27.

Miklavc, P., Hecht, E., Hobi, N., Wittekindt, O.H., Dietl, P., Kranz, C. and Frick, M. (2012). Actin coating and compression of fused secretory vesicles are essential for surfactant secretion - a role for Rho, formins and myosin II. *Journal of Cell Science* **125,** 2765-2774.

Nightingale, T.D., Cutler, D.F. and Cramer, L.P. (2012). Actin coats and rings promote regulated exocytosis. *Trends in Cell Biology* **22,** 329-337.

Nightingale, T.D., White, I.J., Doyle, E.L., Turmaine, M., Harrison-Lavoie, K.J., Webb, K.F., Cramer, L.P. and Cutler, D.F. (2011). Actomyosin II contractility expels von Willebrand factor from Weibel-Palade bodies during exocytosis. *The Journal of Cell Biology* **194,** 613-629.

Pizarro-Cerda, J., Kuhbacher, A. and Cossart, P. (2012). Entry of Listeria monocytogenes in mammalian epithelial cells: an updated view. *Cold Spring Harbor Perspectives in Medicine* **2**.

Pollard, T.D. and Cooper, J.A. (2009). Actin, a central player in cell shape and movement. *Science* **326,** 1208-1212.

Porat-Shliom, N., Milberg, O., Masedunskas, A. and Weigert, R. (2013). Multiple roles for the actin cytoskeleton during regulated exocytosis. *Cellular and Molecular Life Sciences* **70,** 2099-2121.

Pukkila-Worley, R. and Ausubel, F.M. (2012). Immune defense mechanisms in the Caenorhabditis elegans intestinal epithelium. *Current Opinion in Immunology* **24,** 3-9.

Sokac, A.M. and Bement, W.M. (2006). Kiss-and-coat and compartment mixing: coupling exocytosis to signal generation and local actin assembly. *Molecular Biology of the Cell* **17,** 1495-1502.

Sokac, A.M., Co, C., Taunton, J. and Bement, W. (2003). Cdc42-dependent actin polymerization during compensatory endocytosis in Xenopus eggs. *Nature Cell Biology* **5,** 727-732.

Szumowski, S.C., Botts, M.R., Popovich, J.J., Smelkinson, M.G. and Troemel, E.R. (2014). The small GTPase RAB-11 directs polarized exocytosis of the intracellular pathogen N. parisii for fecal-oral transmission from C. elegans. *Proceedings of the National Academy of Sciences of the United States of America* **111,** 8215-8220.

Texier, C., Vidau, C., Vigues, B., El Alaoui, H. and Delbac, F. (2010). Microsporidia: a model for minimal parasite-host interactions. *Current Opinion in Microbiology* **13,** 443-449.

Trifaro, J.M., Gasman, S. and Gutierrez, L.M. (2008). Cytoskeletal control of vesicle transport and exocytosis in chromaffin cells. *Acta Physiologica (Oxf)* **192,** 165-172.

Troemel, E.R. (2011). New Models of Microsporidiosis: Infections in Zebrafish, C. elegans, and Honey Bee. *PLoS Pathogens* **7,** e1001243.

Troemel, E.R., Felix, M.A., Whiteman, N.K., Barriere, A. and Ausubel, F.M. (2008). Microsporidia are natural intracellular parasites of the nematode Caenorhabditis elegans. *PLoS Biology* **6,** 2736-2752.

Turvey, M.R. and Thorn, P. (2004). Lysine-fixable dye tracing of exocytosis shows F-actin coating is a step that follows granule fusion in pancreatic acinar cells. *Pflugers Archiv* **448,** 552-555.

Vavra, J. and Lukes, J. (2013). Microsporidia and 'the art of living together'. *Advances in Parasitology* **82,** 253-319.

Williams, B.A. (2009). Unique physiology of host-parasite interactions in microsporidia infections. *Cellular Microbiology* **11,** 1551-1560.

Wollman, R. and Meyer, T. (2012). Coordinated oscillations in cortical actin and Ca2+ correlate with cycles of vesicle secretion. *Nature Cell Biology* **14,** 1261-1269.

Zografou, S., Basagiannis, D., Papafotika, A., Shirakawa, R., Horiuchi, H., Auerbach, D., Fukuda, M. and Christoforidis, S. (2012). Rab-genome analysis reveals novel insights in Weibel-Palade body exocytosis. *Journal of Cell Science,* **125,** 4780 - 4790.

6 Discussion: Using *C. elegans* infected by *N. parisii* to understand disease transmission and host cell exit by microsporidia

The work presented in this dissertation comprises the bulk of what is known about host cell exit by any species of microsporidia. Prior to these experiments, it was largely assumed that parasite proliferation overloaded the host cell, which then burst open to expel spores. Contrary to this lytic model, I found that many host processes are elegantly re-purposed to facilitate exocytosis of microsporidia spores from living hosts. This work expands our understanding of how diseases are spread by examining how an intracellular pathogen can escape from its replicative host cell environment. In this chapter I will discuss the implications of my work on microsporidia-host interactions, intracellular pathogen exit, and disease transmission. I also present several hypotheses derived from my findings and suggest how these hypotheses could be tested in future studies.

6.1 Host cell exit is non-lytic and carefully orchestrated

My findings have shown that in the *N. parisii-C. elegans* model system of microsporidia infection, host cell exit is a tightly regulated and carefully orchestrated exocytic process. Rather than simple bursting of the host cell, we observed careful manipulation of the host environment and non-lytic, actin-dependent exit of *N. parisii* spores. Even prior to spore formation, substantial remodeling of cytoskeletal structures occurs in the intestines of infected animals, including ectopic localization of host ACT-5 and the formation of gaps in intermediate filaments of the terminal web (Chapter 3). We propose that this cytoskeletal remodeling is in preparation for spore exit. Removal of cytoskeletal material from the apical side of the host cell and accumulation of ectopic material at the basolateral side of the cell could physically bias spores toward exit from the apical side of the host cell. Such a bias would contribute to the apical-specific directionality of *N. parisii* exit that is important for

fecal-oral spreading of infection. For fecal-orally transmitted intracellular pathogens such as microsporidia, it is important that the replicated pathogens not only exit the host cell, but also navigate passage out of the host organism so they can spread to new hosts. *N. parisii* is able to exit apically and reach the intestinal tract for defecation from the host animal in part due to remodeling of the host cytoskeleton.

6.2 *N. parisii* spores use host endocytic recycling pathway for apical exocytosis

In addition to garnering appreciation for the complexity and elegance of microsporidia-induced cytoskeletal arrangements preceding and during spore exit, my work suggests another mechanism by which pathogens can exit in a targeted direction out of the host cell. I found that apically directed exit is likely promoted by co-opting the host endocytic recycling pathway. Normally this pathway traffics intracellular cargo up to the host plasma membrane so that receptors and membrane can be recycled (Grant and Donaldson, 2009). In Chapter 4, I present evidence supporting a model in which the master regulator of endocytic recycling, RAB-11, localizes to spores and enables *N. parisii* to fuse with and thus exocytose from the apical side of the host cell. Animals with depleted RAB-11 excrete fewer spores and are less contagious to their neighbors. These findings expand our understanding of how basic host cell processes such as endocytic recycling can be repurposed to promote disease transmission during infection by intracellular pathogens. We now know that prolific spore exit from living animals is possible in part because *N. parisii* spores use host intracellular trafficking pathways to exit apically while causing minimal damage to the host organism.

6.2.1 Studies proposed to investigate autophagy as the source of intracellular membrane that is around spores prior to exit

Related to the topic of fusion with the host apical membrane, in Chapter 4 I also present electron micrographs that show an additional layer of membrane around intracellular spores. We believe this membrane is important for topologically enabling fusion of spore-containing compartments with host the membrane during exocytosis. What is the source of this additional layer of membrane? Literature suggests that the mitochondrial outer membrane can contribute to autophagosome formation during starvation-induced autophagy (Hailey et al., 2010). We have conducted several experiments investigating the hypothesis that the membrane surrounding intracellular spores is delivered by an autophagic process that uses mitochondria-derived membrane. In support of this hypothesis, I found that mitochondrial membrane fusion, fission and biogenesis genes to affect spore exit. However, we were unable to observe transfer of fluorescently tagged mitochondrial proteins onto *N. parisii* or to visualize mitochondria in the act of transferring membrane to the pathogen in electron micrographs (see Appendix A.1).

A second source of membrane that is thought to contribute to autophagosome formation during starvation-induced autophagy is Rab11 recycling endosomes (Longatti et al, 2012). In this model, starvation induces TBC1D14 to move from recycling endosomes to the Golgi. TBC1D14 is a GTPase activating protein that inhibits Rab11 activity. After TBC1D14 relocalizes away from recycling endosomes, Rab11 is freed from its prior inhibition by TBC1D14 and can promote recycling endosome membrane donation to newly forming autophagosomes during starvation. The authors show that autophagy proteins ULK1 (an *unc-51* homolog) and Atg9 are

found on Rab11 positive recycling endosomes and that Rab11 is required for autophagosome formation (Longatti et al, 2012). Interestingly, preliminary data from our lab has shown that knock down of *unc-51* increases the number of *N. parisii* spores formed and causes an approximately 4-fold increase in spore shedding. This membrane donation model is particularly relevant given my finding that *N. parisii* spores traffic through the recycling endosome pathway and are RAB-11 positive (Chapter 4). It would be interesting to test whether the RAB-11 observed around spores also colocalizes with UNC-51 or ATG-9, which would support the idea that the intracellular membrane around spores is derived from a process similar to starvation-induced autophagy. Additionally, we could test whether RNAi of the *C. elegans* TBC1D14 homolog, *tbc-12*, affects RAB-11 coat formation around spores or spore shedding. According to the recycling endosome model of starvation-induced autophagy, we would expect that depleting *tbc-12* would remove its inhibition of RAB-11 membrane donation and increase the number of RAB-11 spore coats and the number of spores excreted, assuming that membrane acquisition is a rate-limiting step in spore exit.

If starvation-induced autophagy is activated by microsporidia infection, it would be informative to quantify the metabolic status of host cells during microsporidia infection and determine if *C. elegans* is in a starved state. I have collected preliminary data that could be used for this purpose in collaboration with Chris Rath in Pieter Dorrestein's lab (Chapter 7, A.1). Preliminary analysis of imaging mass spectroscopy (IMS) data indicates substantial differences in the lipid profiles between infected and uninfected animals, though we have not yet attempted to determine a global metabolic profile. We could try using this technique to measure

cellular ATP levels, as microsporidia are known to consume ATP from their hosts. Alternatively, there are kits designed to measure ATP that could be used. Data demonstrating a reduction in ATP levels could provide an explanation of how starvation-induced autophagy would be induced upon *N. parisii* infection. If microsporidia infection is found to activate starvation-induced autophagy, which in turn could provide recycling endosome membrane to spores, it will also be interesting to investigate how microsporidia avoid degradation after activating autophagy.

6.3 Diverse uses of host actin during *N. parisii* exit from *C. elegans* cells

As mentioned earlier, ACT-5 is ectopically localized to the basolateral side of host cells early during infection, and this protein is also required for spore exit (Chapter 3). In Chapter 5, I show that later in infection, after spore compartments fuse with the apical membrane, host ACT-5 can form a “coat” around *N. parisii* spores. These fused spores are often in contact with the intestinal lumen, as assessed by Calcofluor white staining (Chapter 5). Exocytosis of actin-coated cargo, termed “kiss-and-coat” exocytosis, has been previously described, and it is thought that actin coating may stabilize large or insoluble cargo (Sokac et al., 2006). Although I did not find ACT-5 spore coats to be required for spore exit, there is a close correlation between the presence of ACT-5 coated spores and the excretion of spores. We conclude that there are likely parallel pathways to spore exit, at least one of which is not dependent on ACT-5 spore coats, since animals seemingly without ACT-5 coated spores have only partial defects in spore exit (Chapter 5).

6.3.1 Studies proposed to investigate the role of calcium and animal mobility in exocytosis of actin-coated spores

Studies of kiss and coat exocytosis have reported that exocytic release of cargo is dependent on calcium (Ca^{2+}). In the absence of Ca^{2+}, actin-coated cargo remains docked to the target membrane (Miklavc et al, 2009), much as we observe actin-coated spores to be arrested at the apical membrane in animals immobilized for visualization. Interestingly, it has also been reported that waves of Ca^{2+} travel across the *C. elegans* intestine as part of the normal defecation cycle, and that these Ca^{2+} waves are disrupted in immobilized animals (Nehrke et al, 2008). Based on this information, I hypothesized that the Ca^{2+} waves that occur in freely moving animals are required to trigger exocytosis of spores. I conducted several experiments testing for reduced spore exit in mutant animals defective for mobility, but ran into complications with immobile animals not being able to feed themselves (which greatly impairs spore production and thus spore exit), or not being immobilized if I tried to feed them in liquid culture. One approach to circumvent complications of animal immobility is to try and image exocytic release in freely moving animals, though this would likely be technically challenging.

Another approach to directly test whether spore exit is Ca^{2+} dependent is to stimulate exocytic release of actin-coated spores by adding Ca^{2+} to immobilized worms, either by providing it in the mounting media, or by using drugs that stimulate release of intracellular Ca^{2+}. If exocytosis of *N. parisii* spores was found to be dependent on Ca^{2+}, it would then be interesting to visualize Ca^{2+} dynamics in the infected *C. elegans* intestine using genetically encoded Ca^{2+} sensors such as GCaMP or chameleon. Whether or not Ca^{2+} is related to exocytosis of actin-coated spores, the finding that actin-coated spores only partially account for the requirement

of *act-5* during spore exit leaves open avenues for further investigating the role of ACT-5 during *N. parisii* infection.

6.3.2 Studies proposed to investigate use of ACT-5 in myosin-based trafficking of intracellular spores prior to exit

A final line of inquiry relating to the ACT-5 dependency of spore exit is whether ACT-5 plays a role in trafficking spores prior to exit. One hypothesis is that ACT-5 may contribute to movement of spores up to the apical membrane for exocytosis by providing a scaffold for myosin V-based translocation of RAB-11 coated *N. parisii* spores. In neuronal cells, myosin Vb has been shown to move recycling endosomes via the Rab11 adaptor protein FIP2 (Wang et al, 2008). Since we believe that *N. parisii* spores traffic through recycling endosome related compartments using RAB-11, I tested if *C. elegans* FIP-2 or the myosin Vb homolog HUM-2 is required for spore exit, but I found no effect. Similarly, the other non-muscle myosin homologs *myo-3*, *hum-1*, and *hum-6* also caused no change in spore shedding. However, it is possible that there are redundant myosin Vb genes in *C. elegans*, as a similar lack-of-effect when depleting *hum-2* was reported in a recent study of recycling endosomes (Winter et al, 2012). Perhaps additional experiments knocking down unconventional myosins in the *hum-2* background would reveal a role of myosins and thus actin in trafficking RAB-11 marked *N. parisii* spores that I missed by knocking down these genes individually. The inability to visualize movement of spores was a major technical obstacle in these studies. Details of various methods I attempted to overcome this obstacle are discussed in Appendix A.2.

We have shown that ACT-5 is mislocalized early during infection and that at late time points ACT-5 localizes to a subset of likely exiting spores. But actin coats do

not seem to account for the entire requirement for *act-5* during spore exit. Rather, it seems as though ACT-5 is involved in many aspects of the *N. parisii* life cycle, and separating these roles from one another in order to study a potential role of actin in spore trafficking will likely be very challenging, particularly because ACT-5 is an essential gene and is difficult to knock-down consistently without causing developmental problems or lethality. The challenges in teasing apart the many roles of ACT-5 during the microsporidia life cycle illustrate the degree to which *N. parisii* interacts with its host cell. Not only does this microsporidia target core cellular processes that have diverse downstream effectors, such as the host cytoskeleton and endocytic recycling pathway, but *N. parisii* also has the ability to use the same protein for different purposes during in various stages of its life cycle. My work shows that microsporidia host cell exit is a complex, meticulously orchestrated process.

6.4 Conclusions

To conclude, my dissertation uncovers mechanisms by which intracellular pathogens can transmit disease. I found host cytoskeletal and intracellular trafficking pathways to be carefully regulated and crucial in the apical exocytosis of microsporidia from host cells. Exiting specifically out of the apical side of the host cell and into the intestinal lumen facilitates fecal-oral spreading of microsporidia infection in the *C. elegans* – *N. parisii* model system. This naturally evolved host-pathogen pair enables study of host cell exit strategies in intact, living animals. Key advancements to our understanding of microsporidia host cell exit resulting from my dissertation are summarized below in Figure 6-1. Although this work greatly improves our understanding microsporidia disease transmission and host cell exit processes used

by intracellular pathogens, hypotheses building on these findings abound, and future experiments will undoubtedly yield even more insight into this fascinating system.

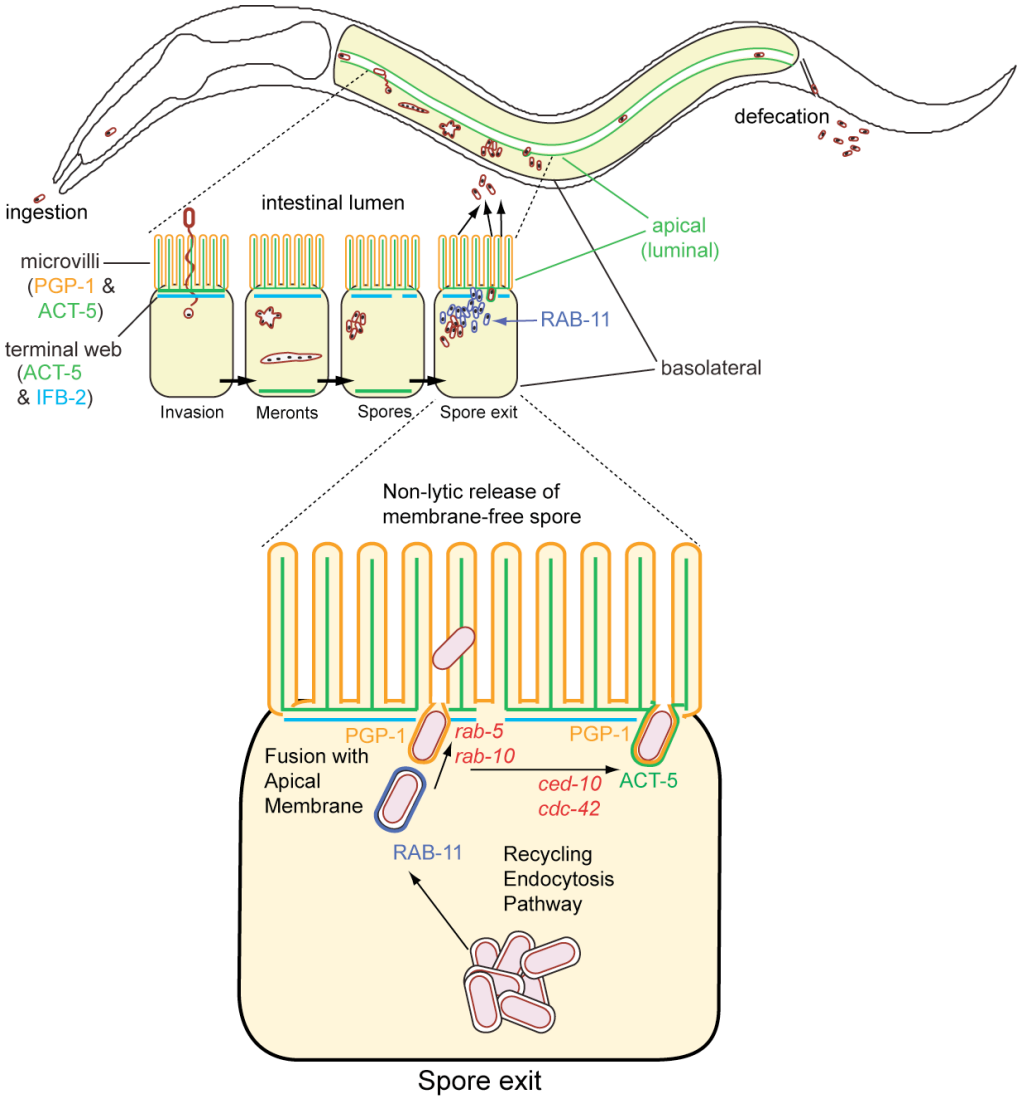

Figure 6-1. Advancements in understanding microsporidia exit.
After being ingested and gaining entry to the *C. elegans* intestinal cell, *N. parisii* replicates as meronts. During this stage ectopic, basolateral localization of host ACT-5 is observed. Just prior to spore formation, gaps form in the terminal web. Exocytosis of spores is dependent on the small GTPases *rab-5*, *rab-10*, and *rab-11*. RAB-11 and ACT-5 form coats on exiting spores, though at different stages during the exit process. The small GTPases *ced-10* and *cdc-42* are required for actin coat formation, as are *rab-5*, *rab-10*, and *rab-11.* After spores exocytose from the host cell into the intestinal lumen, they are defecated from the animal for fecal-oral spreading of infection.

6.5 References

Grant, B. and Donaldson, J. (2009). Pathways of endocytosis and endocytic recycling. *Nature Reviews Molecular Cell Biology* **10**, 597-608.

Hailey, D.W., Rambold, A.S., Satpute-Krishnan, P., Mitra, K., Sougrat, R., Kim, P.K. and Lippincott-Schwartz, J. (2010). Mitochondria supply membranes for autophagosome biogenesis during starvation. *Cell* **141**, 656-67.

Longatti. A., Lamb, C.A., Razi, M., Yoshimura, S., Barr, F.A. and Tooze, S.A. (2012). TBC1D14 regulates autophagosome formation via Rab11- and ULK1-positive recycling endosomes. *The Journal of Cell Biology* **197**, 659-75.

Nehrke, K., Denton, J. and Mowrey, W. (2008). Intestinal Ca2+ wave dynamics in freely moving C. elegans coordinate execution of a rhythmic motor program. *American Journal of Physiology- Cell Physiology* **294,** C333-44.

Miklavc, P., Wittekindt, O.H., Felder, E. and Dietl, P. (2009). Ca2+-dependent actin coating of lamellar bodies after exocytotic fusion: a prerequisite for content release or kiss-and-run. *Annals of the New York Academy of Sciences* **1152**, 43-52.

Shen, Q., He, B., Lu, N., Conradt, B., Grant, B. and Zhou, Z. (2013). Phagocytic receptor signaling regulates clathrin and epsin-mediated cytoskeletal remodeling during apoptotic cell engulfment in *C. elegans*. *Development* **140**, 3230-3243.

Sokac, A.M. and Bement, W.M. (2006). Kiss-and-coat and compartment mixing: coupling exocytosis to signal generation and local actin assembly. *Molecular Biology of the Cell* **17,** 1495-1502.

Wang, Z., Edwards, J.G., Riley, N., Provance, D.W., Karcher, R., Li, X.D., Davison, I.G., Ikebe, M., Mercer, J.A., Kauer, J.A. and Ehlers, M.D. (2008). Myosin Vb mobilizes recycling endosomes and AMPA receptors for postsynaptic plasticity. *Cell* **135**, 535-48.

Winter, J.F., Höpfner, S., Korn, K., Farnung, B.O., Bradshaw, C.R., Marsico, G., Volkmer, M., Habermann, B. and Zerial, M. (2012). Caenorhabditis elegans screen reveals role of PAR-5 in RAB-11-recycling endosome positioning and apicobasal cell polarity. *Nature Cell Biology* **14**, 666-76.

Appendix

A.1 Imaging mass spectrometry experiments

It is a well-established fact that microsporidia are dependent on host cells for nourishment. Perhaps because the intracellular environment is extremely nutrient dense, almost all microsporidia species lack the Tor (nutrient sensing) pathway that is otherwise present in all eukaryotes (Vavra and Lukes, 2013). Consistent with microsporidia obtaining nutrients from their host cell, when I image *C. elegans* intestinal cells infected with *N. parisii*, I have observed the disappearance of gut granules in the host cell during the course of infection. Gut granules are poorly characterized structures that are thought to act as fat storage organelles and lysosomal-related organelles in the *C. elegans* intestine. Based on the dependency of microsporidia on host cells for nutrients and the observation that fat storage organelles disappear during infection, I examined the metabolic status of host cells during microsporidia infection compared to uninfected host cells in order to investigate the hypothesis that *C. elegans* cells infected with *N. parisii* may be in a starved metabolic state.

The hypothesis that *N. parisii* causes a starvation response in its host was also related to a secondary hypothesis; that a state of starvation could activate ‘starvation-induced autophagy’. Starvation-induced autophagy could account for the acquisition of an additional layer of membrane around intracellular pathogen tissue prior to spore fusion with the apical host membrane (Chapter 6). In this way, an early observation that meronts develop in direct contact with the host cytoplasm (Troemel et al, 2008) could be reconciled in terms of membrane topology with my finding that mature spores are capable of fusing with the host apical membrane. One explanation for this ability to fuse with the host apical membrane is that the spores obtain a layer

of fusion-competent, host-derived membrane during their development, possibly as a result of autophagy. It is also possible that this host membrane fusion competent membrane is of pathogen origin rather than host-derived. As discussed in Chapter 6, published findings show that the outer membrane of mitochondria can supply membrane during starvation-induced autophagy (Hailey et al, 2010). This finding that was of particular interest to us due to the frequent juxtaposition of mitochondria and meronts in electron microscopy (EM) images of infected cells. A postdoc in our lab, Margie Smelkinson, tried to quantify whether mitochondria were more frequently next to meronts than one would expect by chance in such a crowded intracellular environment. To do so, she compared the number of mitochondria next to meronts with the number of gut granules next to meronts in EM images. She found there to be no significant difference between associations of meronts and mitochondria vs. meronts and gut granules. However it is difficult to draw conclusions from these data because mitochondria can be much larger than gut granules, and it is unclear if gut granules are an appropriate negative control. For example, meronts could actively associate with gut granules to access their nutrients and could thus be over-represented next to meronts.

In summary, we were investigating the hypothesis that mitochondria supply membrane to developing pathogen tissue via starvation-induced autophagy. I took a different approach to this investigation and sought to determine the metabolic status of the host cell to determine if infected *C. elegans* cells were in a state of starvation.

The technique I used to explore the metabolic status of infected *C. elegans* was proposed to us by Chris Rath, a post-doc in the lab of Pieter Dorrestein. The Dorrestein group specializes in imaging mass spectrometry (IMS) techniques

including MALDI-TOF and nanoDESI. MALDI stands for 'Matrix-assisted laser desorption/ionization' and TOF is 'Time of flight'. MALDI-TOF imaging relies on mass spectrometry to identify samples ionized by a laser at specific points on a two-dimensional grid. This results in a mass spectrometry profile that can be false-colored and interpreted to deduce the localization and diffusion patterns of the small molecules with respect to colony identity and location (Yang et al, 2009). NanoDESI is 'nanospray desorption ionization' and is very similar to MALDI-TOF but allows for greater resolution. These techniques have been successfully used in microbiology studies to identify metabolite exchange between colonies of different bacterial species in direct contact with one another (Phelan et al, 2011; Watrous et al, 2012). Chris Rath wanted to find new applications for this technology and investigate metabolite exchange in more complex organisms. In this collaboration, I prepared samples of *C. elegans* feeding on a number of different bacteria, as well as infected with microsporidia, and Chris operated the IMS equipment and analyzed the data.

We spent almost 6 months optimizing sample preparation conditions, and running controls. Some of the optimizations we made included: 1) use large plates (10 cm, poured thin with 10 mL media); 2) use developmentally synchronized *C. elegans* with harvest time of 4hpi for bacterial infections and 48hpi for microsporidia infections; 3) use whole-plate bacterial lawn coverage to prevent avoidance of the lawn by *C. elegans*; and 4) use a very high density of animals on the plate to increase signal from small molecules. The final procedures (2 biological replicates) were conducted on 12/2/11 and 12/20/11. See Table A-1 for a list of the samples prepared in each of these biological replicates and why each type of sample was collected (in

bold). Table A-2 shows how these plates and the animals on them were processed in different ways to obtain data.

Table A.1-1. List of 17 10 cm plate samples collected, plus 2 media-only control plate samples. The media used, microbe plated, and strain of worms used for each plate are listed. Plates were poured with 10 mL of media. All bacteria was GFP labeled and grown on SK plates except for *S. aureus* which was grown on TSA. For each bacteria, 3 combinations of worms were used: WT (*jyIs17* [N2/*mCherry::ACT-5*]), *zip-2 (-)* (ERT105 [*zip-2* (*tm4248*); *myo-2::mCherry*]), and no worms. ZIP-2 mutants are more susceptible to PA14 infection. Plates 13 and 14 were with younger worms than on plates 2 and 3.

Plate 1. SK *E. coli* DH5α = **Non-pathogenic, few secondary metabolites**
Plate 2. SK *E. coli* DH5α + *jyIs17* (WT) worms
Plate 3. SK *E. coli* DH5α + ERT105 (*zip-2*$^{(-)}$) worms
Plate 4. SK *B. subtilis* 3610 = **Non-pathogenic, well-characterized secondary metabolites**
Plate 5. SK *B. subtilis* 3610 + *jyIs17* (WT) worms
Plate 6. SK *B. subtilis* 3610 + ERT105 (*zip-2*$^{(-)}$) worms
Plate 7. SK *P. aeruginosa* PA14 = **Pathogen model 1**
Plate 8. SK *P. aeruginosa* PA14 + *jyIs17* (WT) worms
Plate 9. SK *P. aeruginosa* PA14 + ERT105 (*zip-2*$^{(-)}$) worms
Plate 10. SK *Microsporidia* ERTm1 +*E. coli* DH5α = **Intracellular pathogen model**
Plate 11. SK *Microsporidia* ERTm1 +*E. coli* DH5α + *jyIs17* (WT) worms
Plate 12. SK *Microsporidia* ERTm1 +*E. coli* DH5α + ERT105 (*zip-2*$^{(-)}$) worms
Plate 13. SK *E. coli* DH5α + *jyIs17* (WT) worms
Plate 14. SK *E. coli* DH5α + ERT105 (*zip-2*$^{(-)}$)worms
Plate 15. TSA *S. aureus NCTC8325* = **Pathogen model 2**
Plate 16. TSA *S. aureus NCTC8325* + *jyIs17* (WT) worms
Plate 17. TSA *S. aureus NCTC8325* + ERT105 (*zip-2*$^{(-)}$) worms
Plate 18. Blank media-only SK
Plate 19. Blank media-only TSA

Table A.1-2. Purpose of different sample types (plate, intact worms on slide, dissected worms on slide). For each of the plates listed in Table A-1, 4 infected worms were moved onto IMS slide intact; and 4 different infected worms were dissected on the slide. This was repeated for 3 slides total. The 4 worms are for biological replicates, the 3 slides are for positive mode, negative mode, and washed positive mode sample processing.

	Sample Type	Purpose
A	PLATE: agar lawn imaging mass spectrometry (IMS)	gross changes in bacterial/worm secreted metabolites
B	PLATE: Fluorescent imaging of entire plates (Typhoon)	Worm density determination for comparison with A
C	PLATE: Extract worms from 1/4 plate, agar from 1/4 plate, and agar + worms from 1/4 plate	Save for potential follow-up (e.g PCR/LCMS/NMR)
D	SLIDE: Intact worms (IMS)	Localization of metabolites to worm surface.
E	SLIDE: Intact worms (IMS, desalted)	Localization of peptides/proteins to worm surface.
F	SLIDE: Worm dissected (IMS)	Gut specific localization of metabolites.
G	SLIDE: Worm dissected (IMS, desalted)	Gut specific localization of peptides/proteins.
H	DIC/fluorescent imaging of individual worms (AxioImager microscope)	Compare with D-G for un/infected determination.

We collected data from two experimental batches. The first batch consisted of PA14, *S. aureus*, *B. subtilis*, and a DH5α *E. coli* control. We used this batch to perfect our harvesting procedure and found the best method for detecting signal from animals is to dissect the intestine on metal-coated slides. However, animals desiccate almost instantly on this surface and thus I found it crucial to transfer just the right amount of liquid onto the slide with the animal: enough liquid to allow dissection by cuticle nicking with a syringe before desiccation occurs, but not so much liquid as to create a puddle throughout which metabolites would diffuse and eliminate any spatial-specific signal in the metabolite data. I acquired fluorescent images of each worm to overlay with chemical images from IMS. We processed 4 intact and 4 dissected animals per group x 3 technical replicates (slides) and saw very consistent results. I also prepared thin-poured 10cm plates with or without animals for each species of bacteria. We hoped these controls would show different metabolites in the presence/absence of animals but preliminary analysis suggested that they look the same. Interestingly though, we found *Staph aureus* to have a very different metabolite signatures from other bacteria. Chris carried out all of the sample processing and chemical extractions in various solvents (polar/non-polar), etc. I do not have records of the precise methods that he used. We examined the raw data resulting from these preliminary experiments together and found numerous differences when comparing signals from different samples. However, I was eager to examine microsporidia-infected animals now that we had the conditions worked out, so we did that, and I am unsure of whether Chris ever completely analyzed the data from the first experiment. I do not have any analyzed results, but the raw data exists in the Dorrestein lab.

The second batch of samples I prepared was *C. elegans* +/- 48hpi microsporidia. Our hope was that we would be able to identify differentially secreted small molecules that would cluster into a biosynthetic or signaling pathway. I would then target these pathways with RNAi and assess the effects on *N. parisii* infection. In particular Chris was going to focus on examining ATP levels in the sample, but he was skeptical that the technique would be useful for measuring ATP. Preliminary analysis of the microsporidia infection data indicated substantial differences in the lipid profiles between infected and uninfected animals. These findings were promising, especially when coupled with the disappearance of gut granules over the course of infection. Apparently analyzing the raw data in order to obtain the exact identity of a spectrometry signal is a labor-intensive step, however it is much easier to place a compound in a category, such as ‘lipid’ or ‘sugar’. So, we never got to the point of fully analyzing the data to the compound-level and pulling out pathways for further analysis because Chris had to focus on a different project, and then he ended up getting a job before completing this work. My impression is that standard algorithms exist for this sort of analysis, and another collaborator could likely be found in the Dorrestein group. Below is the extent of the data I have, copied from a project summary sheet that Chris gave to me when we put the project on hold.

Summary of Project Workflow (steps in bold font were never completed):

Chemical imaging of *C. elegans* with mass spectrometry

1. Samples prepared (agar plates)

   Samples to be prepared to examine host-microbe metabolite exchange.

   1a. *E. coli* DH5a +/- *C. elegans* (jyls17 and ERT105)

   1b. *B. subtilis* 3610 +/- *C. elegans* (jyls17 and ERT105)

   1c. *P. aeruginosa* PA14 +/- *C. elegans* (jyls17 and ERT105)

   1d. *S. aureus* NCTC8325 +/- *C. elegans* (jyls17 and ERT105)

   1e. *N. parisii* + *E. coli* DH5a +/- *C. elegans* (jyls17 and ERT105)

2. Fluorescent/optical imaging of samples

   Imaging to verify infection and align samples for imaging mass spec.

   2a. Microscopy

   2b. Photoscanner

3. Quarter plates (10cm) -Q1 Imaging mass spectrometry

   Chemical imaging reveals metabolite localization.

   3a. IMS of entire plates.

   3b. IMS of intact worms.

   3c. Data processing and data mining.

4. Quarter plates (10cm) -Q2 Extract plates

   Plate extracts reveal secreted compounds from worm and bacteria.

   4a. Extraction of plates with butanol and EtOAc.

   4b. LC MS/MS analysis of plate extracts.

   4c. Data processing and compound identifications.

5. Quarter plates (10cm) -Q3 Extract worms

   Worm extracts for LC MS validation of localized compounds.

   5a. Extraction of worms with butanol and EtOAc.

   5b. LC MS/MS analysis of worm extracts.

   5c. Data processing and compound identifications.

6. Quarter plates (10cm) -Q4 nanoDESI

   In situ analysis of worm and bacterial metabolites.

   6a. NanoDESI analysis.

   6b. Data processing and compound identifications.

Current status:

Experimental (wetlab) datasets collected. Data has passed initial “quality-checks”. Deep data-mining and processing to be performed (C. Rath) after K01 application is completed (1/31/12) and paper submission for primary funded project (soon).

Expected outcome:

1. Identify general and specific chemical responses of C. elegans to microbes.
2. Identify general and specific chemical responses of microbes to C. elegans.
3. Identification of unexpected response factors!

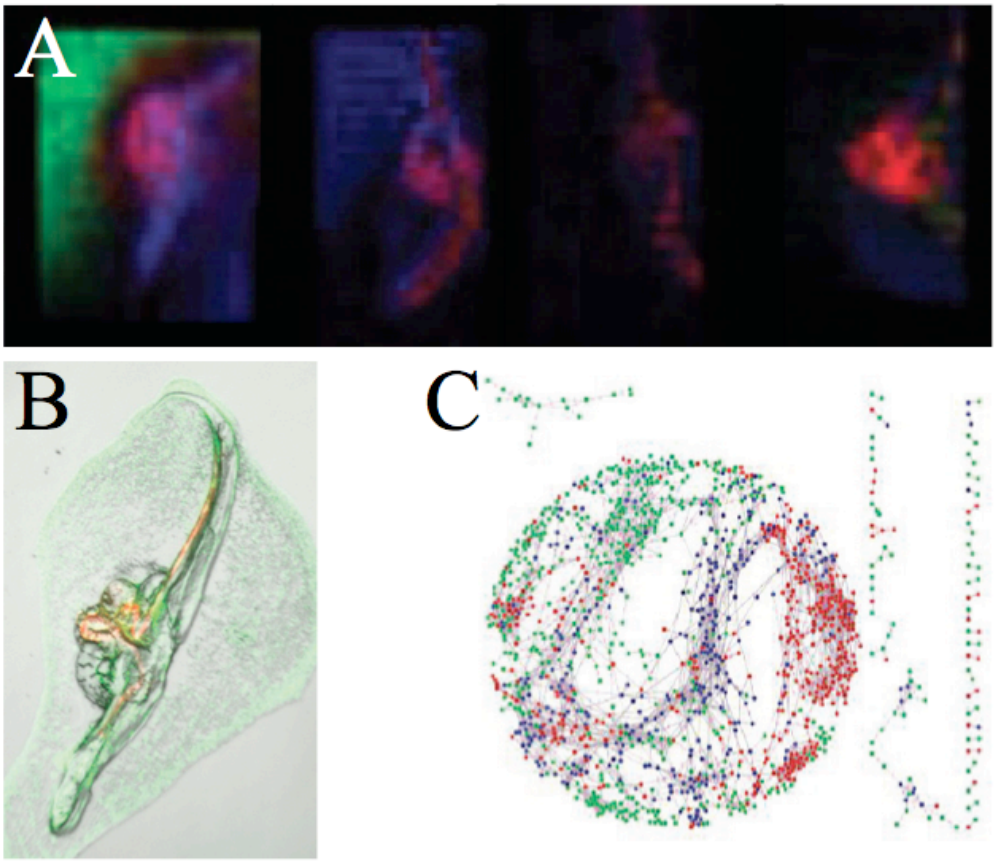

Figure A.1-1. Preliminary imaging mass spectrometry data. A. Chemical imaging data. B. Optical imaging using fluorescent microscopy. C. Data mining.

Exptl. Design

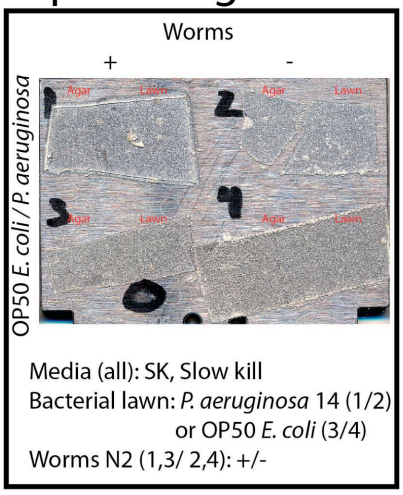

Media (all): SK, Slow kill
Bacterial lawn: *P. aeruginosa* 14 (1/2)
or OP50 *E. coli* (3/4)
Worms N2 (1,3/ 2,4): +/-

Petri Dish Visual

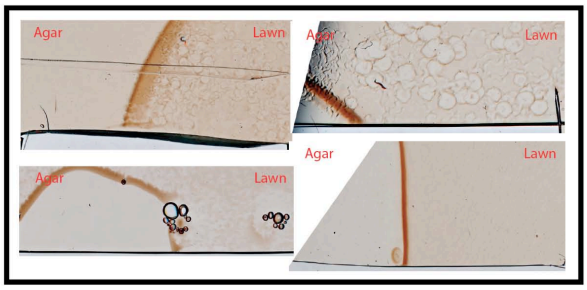

Hypothesis: Imaging mass spectrometry will allow specific ions to be localized on agar plates illustrating interspecies metabolic exchange between *C. elegans* and bacteria.

Ions Showing Specific Localization

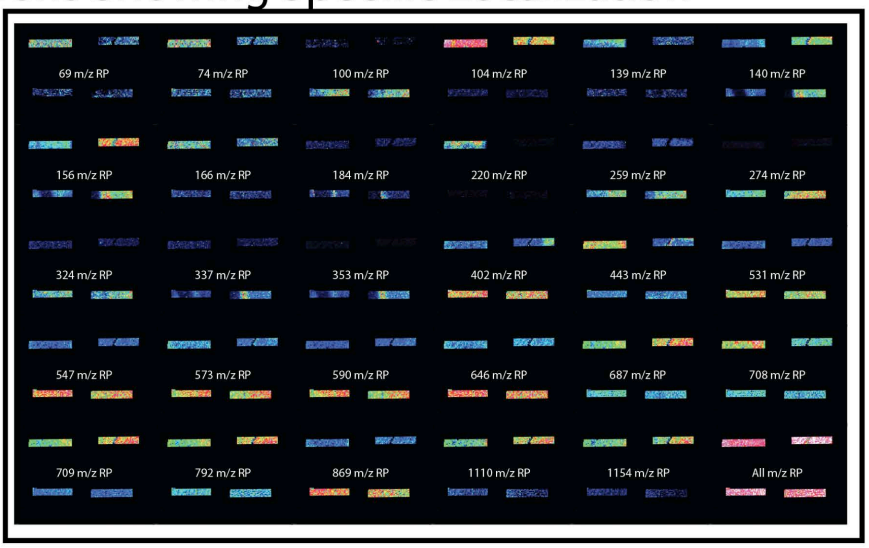

Figure A.1-2. Summary of results prepared by Chris Rath. Experimental design and results, including sample information, visualization of agar plates, and ions localized during sample processing are shown.

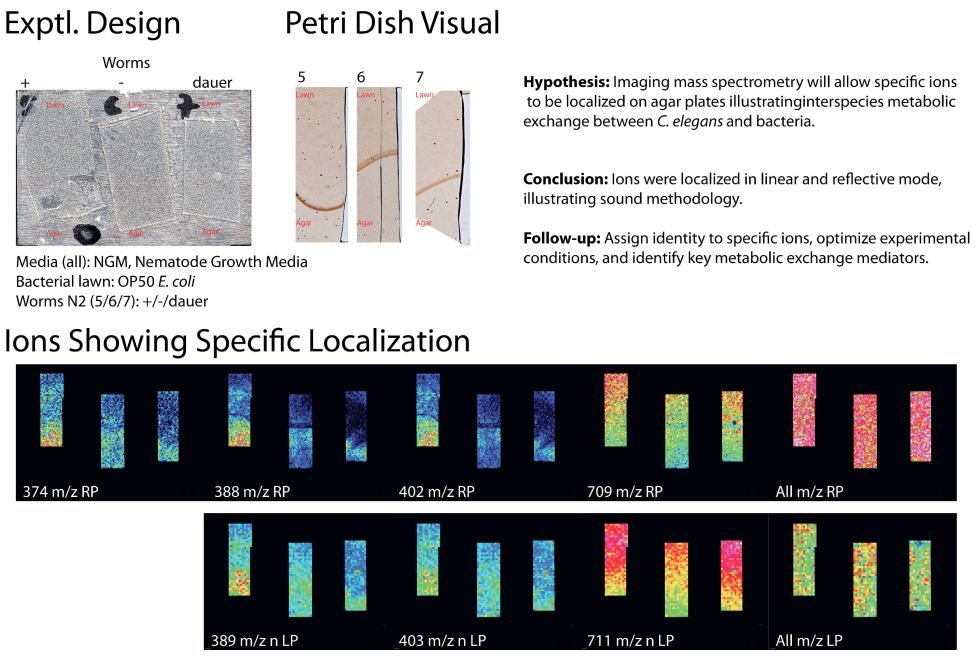

Figure A.1-3. Summary of results prepared by Chris Rath. Experimental design and results, including sample information, visualization of agar plates, and ions localized during sample processing are shown. Original (higher resolution and larger size) file can be found in the 'Chris Rath' folder of my electronic documents'.

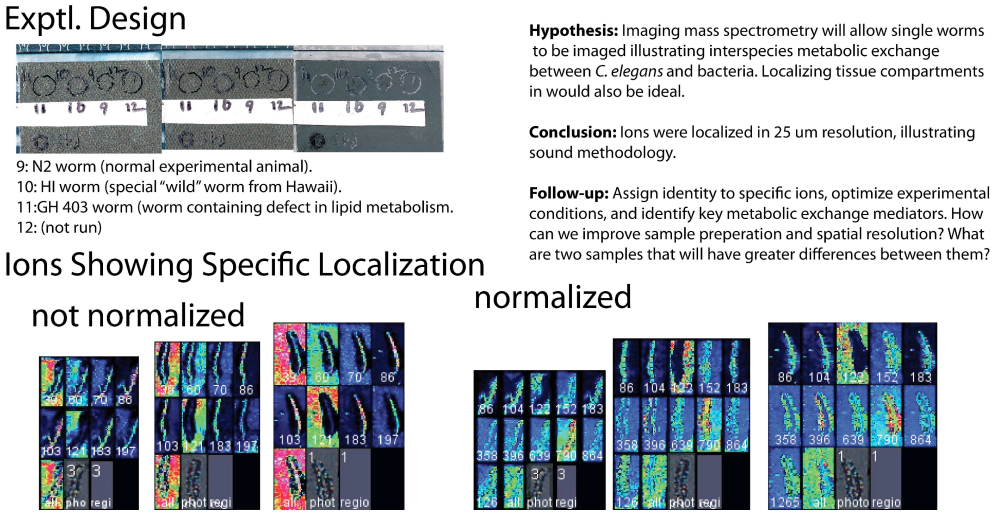

Figure A.1-4. Summary of results prepared by Chris Rath. Experimental design and results, including sample information, visualization of IMS metal-coated slides, and ions localized during sample processing are shown. The outline of the worm can be made out in the Ions Showing Specific Localization panel of IMS data.

In summary, there is a lot of carefully obtained, informative data that needs to be further analyzed by the Dorrestein lab. If this line of research is continued, I recommend finding a collaborator in the Dorrestein lab who is familiar with analysis of IMS/MALDI-TOF and nanoDESI data, and who ideally can get in contact with Chris Rath.

6.1 A.2 Live imaging

For many of my experiments investigating ACT-5 and spore exit, live imaging data would have been highly informative, both to establish the order of events and fluorescent markers associated with exit, as well as to visualize the direction of spore movement across the cell membrane and verify that spores are going out of rather than coming into the cell. I tried many different techniques but was not able to capture useful videos of ACT-5 in motion. While I believe I may have recorded movement of a few *GFP::RAB-11* coated spores, there are so many background spores that it is difficult to be sure the same spore is being visualized at different time points. Here I summarize the various methods I attempted, discuss a few technical challenges and the tools I used to attempt to overcome them, and present a protocol from the Worm Breeder's Gazette that uses agarose pads and microsphere beads to immobilize *C. elegans*. I found this protocol to be successful for other live imaging applications including *LGG-1::GFP* movement, but not ACT-5 live imaging.

A.2.1 Timelapse on Zeiss AxioImager and LSM 700 confocal

The first experiments I conducted to visualize changes in ACT-5 in living animals consisted of immobilizing animals in levamisole and mounting them on agarose pads for timelapse imaging with the Zeiss AxioImager microscope. During all

my attempts to monitor anesthetized animals on slides, ACT-5 structures appeared to be completely static. I also tried imaging in this way on several different microscopes, including a spinning disc confocal and a TIRF microscope, but experienced the same result.

One of the advantages to using levamisole to immobilize worms is that worms can make a full recovery after they are removed from the liquid and replaced on a plate. I conducted several “Image and Recover” experiments but these were foiled by either too many changes in ACT-5, such that the relation to the prior image was uninterpretable, or no changes, depending on the length of recovery time. A few times I was able to detect moderate changes between images, but it was very difficult to confidently identify the same spore at multiple time points. I tried to address this challenge by photoconverting spores using *DENDRA::ACT-5* animals. DENDRA is a fluorescent protein that changes its emission spectra from green light to red light when it is subjected to treatment with blue light. I was able to photoconvert and monitor large regions of spores over time, but I found difficult to control the targeting of photoconversion. However, this could be a fruitful avenue to pursue further.

Microscope drift

On the LSM700 confocal microscope, the stage cannot be adjusted in the middle of a time series, and the drift in focal plane that occurs during a long imaging session prohibits visualization of the same structure throughout an experiment. I tried to compensate for drift by setting up Z-stacks where the focal plane of interest starts at one point in the Z-stack and drifts through it over time, but this strategy is not ideal because movements across the Z-plane would be obscured by drift and it is difficult to analyze the resulting images. I also tried ‘manual’ timelapses, where I keep track of

time and acquisition manually so that I could correct for drift during the experiment, but this strategy also is not ideal since it is difficult to manually reset to the exact same focal plane for each image. Another problem with long timelapses is the evaporation of liquid off the slide, which in addition to drying out the sample and killing the animal, can also cause bubbles to form that move the animal during imaging and complicate analysis. One useful tool for timelapse analysis is called 'depth coding'. This feature is built into the LSM700 microscope software and flattens a Z-stack to a single image, where depth in the stack is coded by color. In this way movement in the Z-plane over time can be detected by changes in color at different time points. Again, drift is a problem, but everything should drift at the same rate in an image, so any outlying spores in terms of color shift can in theory be identified. In practice it is very difficult to find a single spore that changes color at a different rate when there are thousands of spores in each image.

A.2.2 Microfluidic trapping device designed by Edgar Guiterrez

A postdoc in Alex Groisman's lab, Edgar Guiterrez, designed microfluidic devices for use by Rebecca Green in the Oegma/Desei lab. I worked with Becky and Edgar extensively but obtained a time series with an immobilized animal. The microfluidic device that Edgar designed is a tiny chamber with ports, tubing, and a thin glass coverslip that is pulled down to gently squish animals and immobilize them when vacuum is applied to the device. However, if animals were near the edges of the chamber, they wouldn't trap well, and only a few animals could be put in the device at a time, or they wouldn't trap well. Actin phenotypes occur during specific time points in infection, and even with staggered infected plates it was very difficult image immobilized, actin-phenotype containing animals because the device had to be

reset (a lengthy process) if the two or three animals actually immobilized at any given time did not have actin coats. This is not a high-throughput imaging technique, at least in my experience. Furthermore, animals could only be trapped this way for 30-40 minutes before they would die. To work around this, the device was designed to release and re-trap animals. But often the animals moved to the edges of the chambers when released and then were not re-trapped. Or if they were immobilized again, they were at a different orientation, complicating imaging of very small and potentially moving spores. Lastly, although the animals often held still for brightfield imaging, they usually reacted to the laser used for imaging fluorophores by moving rapidly, making colocalization of different fluorescent markers impossible. I would not recommend pursuing this method of live imaging for analysis of small structures such as 2 μm long spores.

Animal movement

Whether the result of small gradual movements during a time course, or sporadic large movements, even “immobilized” animals often move at least a little bit during imaging. Additionally, when animals are imaged, recovered, and re-imaged, they often end up in a different orientation on the slide; either in terms of which side they are laying on, or how curled up they are. Coupled with the changes occurring during infection, this makes it very difficult to find the same structure that was imaged in the previous time point. I therefore created a ‘reference point’ line, using the transgene *DLG-1::GFP*, which marks epithelial cell junctions and creates a brick pattern that can be used to ensure the same region of the worm is being imaged across time points. These reference points could also be used in combination with imaging analysis software to measure movements of spores with respect to

hypothetically fixed structures. I crossed *DLG-1::GFP* with *mCherrry::ACT-5* to make a strain containing both markers, but research priorities shifted and I never worked with it very much. This approach would likely help correct for very small movements during imaging, although the use of GFP as a reference point limits studies of GFP/RFP colocalization with ACT-5, since GFP is being used as a place marker.

A.2.3 Worm Breeder's Gazette microsphere bead protocol

The method of immobilization for live imaging I found to be most successful is a protocol published by Fang-Yen et al. in the Worm Breeder's Gazette. In this method, animals are mounted on hard (10%) agarose pad and immobilized with microsphere beads that act like quicksand for the animal when the coverslip is added.

Agarose immobilization protocol (Fang-Yen et al., Worm Breeder's Gazette):

1. Prepare pads composed of 10% agarose in M9. The solution will be too viscous to pipette. To transfer agarose, scoop with a small spatula.
2. Add 0.25-0.5 µl of 0.1 µm diameter polystyrene microspheres (e.g. Polysciences 00876-15, 2.5% w/v suspension) onto the pad
3. Transfer worm(s) of any developmental stage to the pad using a platinum wire or eyelash pick.
4. Gently cover with a coverslip. The worms are ready for imaging.
5. To recover worms, lift the coverslip without sliding. Add a small amount of M9 to a worm and remove by pick or pipette.

Additional protocol notes:

- Use a double-boiler beaker set-up to avoid burning the agarose in the microwave
- Polystyrene beads are stored at 4C. Be sure to use the correct size beads, there are also larger, fluorescent beads stored at 4C.
- Unused agarose can be saved and reheated
- The volume of microspheres is the most important variable. Add too much and the 'quicksand' layer is too thick and worms are not pressed into the pad and are able to move; add too little and the slide dries out and worms desiccate during imaging. The volume you should use will depend on the area of the agarose pad, so it will be different each time. I recommend about 3 µl for a large pad. But this is a good place to try troubleshooting if you are having problems with the worms moving or dying.

In general, live imaging should not be this difficult. The 10% agarose and microsphere bead method works very well and will likely suffice for most purposes requiring live imaging. I have been able to visualize movement of LGG-1 in living animals using this method. Imaging ACT-5 and spore exit in immobilized animals was particularly challenging however. Possible reasons for these difficulties are explored in Chapter 6.

A.3 Endocytic vesicles contain multiple spores late in infection

Partially due to the inability to visualize movement of ACT-5 coated structures with live imaging, early in my investigations I conducted a line of experiments to determine whether actin-coated spores were going into or coming out of the host cell. Also, from very early on in monitoring actin dynamics over the course of infection, we knew that late in infection (>48hpi) large, ACT-5 coated vesicles were present that contained multiple spores. Here I show figures that I prepared for a short communication manuscript that is in preparation for publication in which these vesicles are described. Initially these figures were incorporated into the paper, “Small GTPases promote actin coat formation on pathogens exocytosing from *C. elegans* intestinal cells” that comprises Chapter 5, and many of the methods and markers shown below were also used in that paper. Refer to the experimental procedures provided in Chapter 5.5 for the information on strains used in this section. The only assay not used in Chapter 5 is described below:

Endocytosis Assays: Animals were picked into a 15 µl drop of 5 mg/mL TRITC-BSA and incubated for 4 hours. After TRITC-BSA feeding, animals were washed 3 times in M9 to dilute extracellular TRITC and then were immediately mounted on agarose pads for imaging.

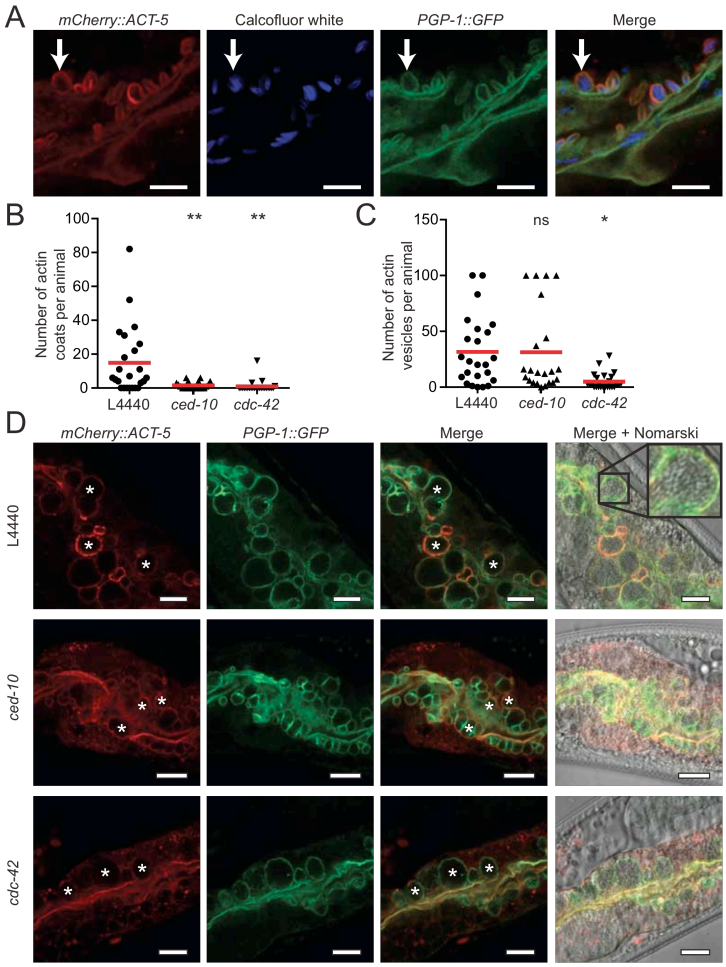

Figure A.3-1. Spore-filled vesicles are coated in ACT-5, which requires *cdc-42*, but not *ced-10*.
(A) Vesicles containing multiple spores (arrow) stain with *mCherry::ACT-5*, *PGP-1::GFP*, and CW. Scale bar is 5 μm. (B) RNAi knock down of Rho GTPases ced-10 or cdc-42 blocks actin coat formation. (C) RNAi knock-down of *ced-10* does not affect ACT-5 localization to vesicles, but RNAi knock-down of *cdc-42* blocks ACT-5 localization to vesicles. Quantification was capped at 100 vesicles per animal. For Panels B and C, red bar is the mean number of ACT-5 coats or vesicles per animal across the population examined. N = 22-25 animals per sample. ANOVA was conducted on the data, comparing each sample to the L4440 control. P-values are indicated above each sample: ns = not significant; * = $p < 0.05$; ** = $p < 0.001$. Data are representative of three independent assays. (D) Spore-filled vesicles (asterisks) marked with *mCherry::ACT-5* and *PGP-1::GFP* are visible in animals treated with L4440 empty vector control or with *ced-10* RNAi. L4440 panel shows magnification of an ACT-5 vesicle containing dozens of spores. Vesicles in animals treated with *cdc-42* RNAi are marked with *PGP-1::GFP* but lack ACT-5 staining. Scale bars are 10 μm.

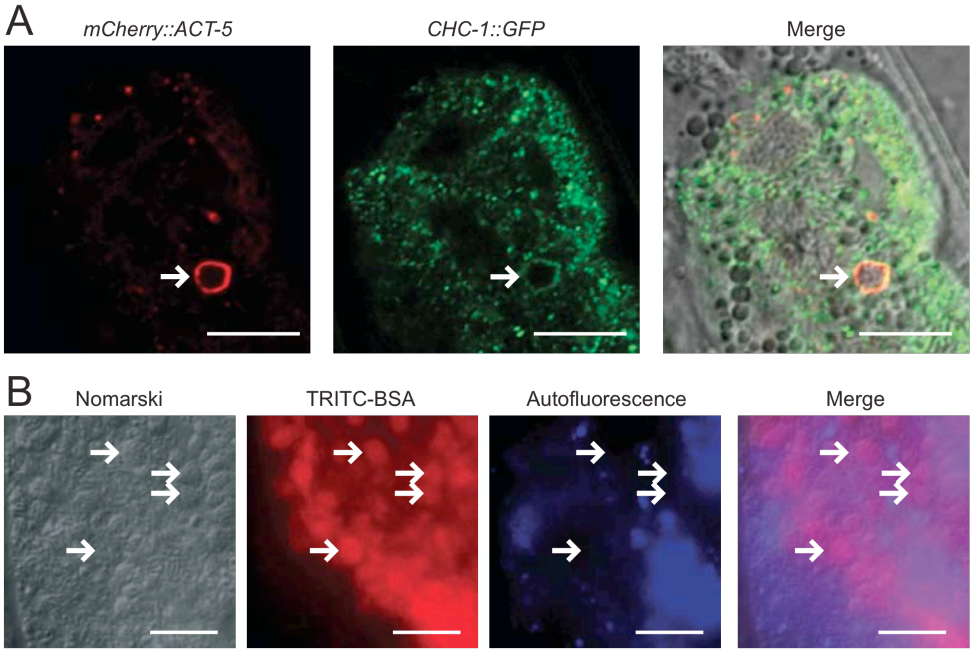

Figure A.3-2. Actin-coated spore-filled vesicles are labeled with clathrin and take up the endocytosis marker TRITC-BSA.
(A) Spore-filled vesicle (arrow) marked with *mCherry::ACT-5* colocalizes with clathrin, *CHC-1::GFP*. Scale bar is 10 µm. (B) TRITC-BSA fed to N2 animals accumulates in spore-filled vesicles. Arrows indicate examples of spore-filled vesicles that contain TRITC-BSA. Blue channel shows intestinal cell autofluorescence does not overlap with red channel signal indicating that staining of vesicles is TRITC-BSA, not autofluorescence. Scale bar is 10 µm.

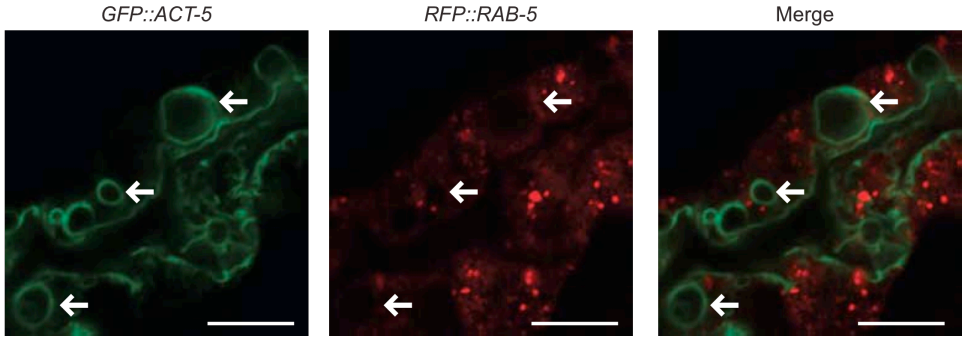

Figure A.3-3. Spore-filled vesicles do not label with the early endosome marker RAB-5.
GFP::ACT-5; *RFP::RAB-5* transgenic animals were infected with microsporidia and observed at the spore-filled vesicle stage, 47-48 hpi. Spore-filled vesicles marked with ACT-5 (arrows) do not stain with the early endosome marker RAB-5. Scale bars are 10 µm.

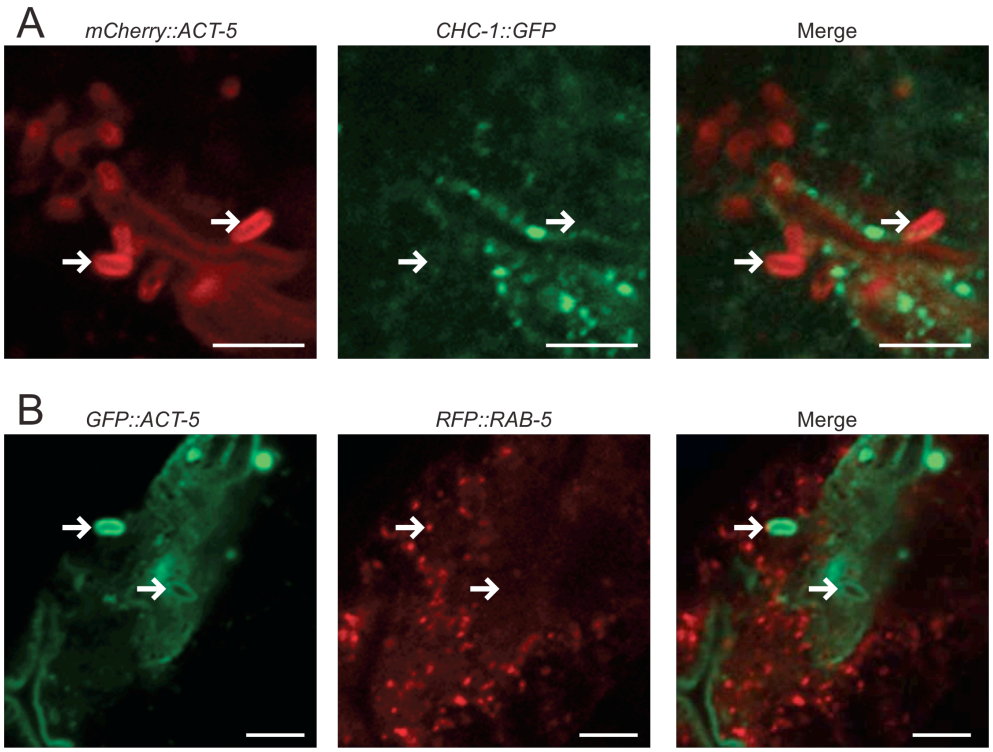

Figure A.3-4. Actin-coated individual spores do not label with clathrin CHC-1 or the early endosome marker RAB-5.
(A) *mCherry::ACT-5*; *CHC-1::GFP* transgenic animals were infected with microsporidia and observed at the actin spore coat stage, 43-46 hpi. The clathrin-mediated endocytosis marker *CHC-1::GFP* does not localize to *mCherry::ACT-5*-coated individual SCCs (arrows). Scale bars are 5 μm. (B) *GFP::ACT-5*; *RFP::RAB-5* transgenic animals were infected with microsporidia and observed at 47-48 hpi. SCCs marked with ACT-5 (arrows) do not stain with the early endosome marker RAB-5. Scale bars are 5 μm.

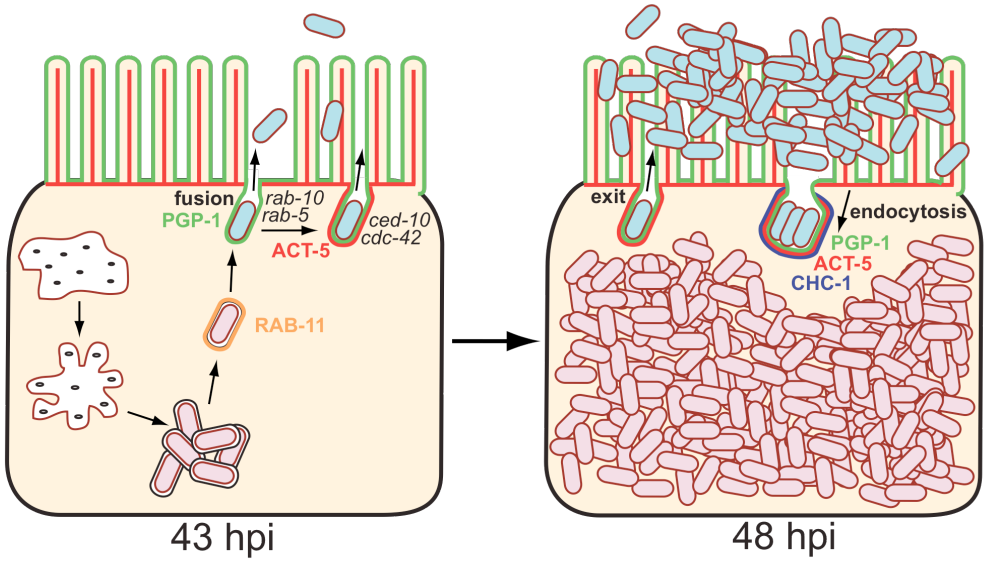

Figure A.3-5. Model for actin regulation of *N. parisii* spore exocytosis and compensatory endocytosis in *C. elegans* intestinal cells.
(A) Left panel: At 43 hpi, meronts have differentiated into spores that are enclosed in membrane-bound spore-containing compartments (SCCs) labeled with RAB-11. These SCCs traffic up to the apical cell surface and fuse with host membrane, acquiring PGP-1 membrane marker. After fusion, spores have access to the lumen and are able to exit from the host cell, sometimes acquiring an ACT-5 coat. Formation of ACT-5 coats is dependent on the Rho GTPases *ced-10* and *cdc-42*, as well as *rab-5*, *rab-10* and *rab-11*. Right panel: By 48 hpi, pathogen replication has overtaken the host intestinal cell and the lumen is packed with exited spores. Large membrane-bound, endocytic vesicles that contain multiple spores are coated in PGP-1 apical membrane, ACT-5 and clathrin (CHC-1). By taking in excess membrane from the apical surface that likely accumulates during bulk exocytosis of spores, host cells are able to maintain balance of their membrane pools.

These vesicles are interesting for several reasons. First, they are very large, to our knowledge they are the largest endocytic vesicles reported in *C. elegans*. Despite their large size, these vesicles are very stable. Although *mCherry::ACT-5* localizes to these vesicles, it does not seem to be required to stabilize them because PGP-1 staining clearly shows the presence of vesicle structures even when RNAi treatment against the actin polymerization factors *ced-10* and *cdc-42* reduces or eliminates ACT-5 localization to vesicles (Figure A.3-1D). It would be interesting to

determine whether clathrin still localizes to vesicles when ACT-5 localization is reduced by *ced-10* and *cdc-42* RNAi treatment. Perhaps clathrin stabilizes the vesicle in the absence of ACT-5. Barth Grant and colleagues have published a recent paper on the involvement of actin and clathrin in phagocytosis during cell corpse clearance in *C. elegans* that may provide useful insight (Shen et al, 2013).

Another interesting feature of these vesicles is that they do not appear to mature in the endocytic trafficking pathway. Due to an absence of RAB-5 staining (Figure A.3-3), we assume there is also no RAB-7 staining or targeting to the lysosome, though those hypotheses could be tested as well.

The current evidence strongly supports an endocytic origin for these structures. Late in infection, the lumen is so densely packed with spores that endocytosis of large numbers of spores from the lumen is entirely plausible. Many questions remain, however. For example, are these spores concentrated in the vesicles? Are they re-entering the cell as a distinct stage in their life cycle? What is the fate of these vesicles after internalization? Are the spores inside vesicles viable? Is it advantageous for the host or the pathogen for spores to be internalized *en masse*? Perhaps internalization of spores is a mechanism that maintains membrane homeostasis in the face of relentless exocytosis of spores (and thus internal host membrane material) from the apical cell membrane. Compensatory endocytosis could act as an emergency stop-gate measure, allowing the host to cope with the overwhelming *N. parisii* infection long enough to produce more progeny. Alternatively, perhaps internalization of spores in vesicles reduces the number of spores that are defecated into the environment, thereby reducing the probability of disease transmission to neighboring animals.

A.4 References

Fang-Yen, C., Wasserman, S., Sengupta, P. and Samuel, A. Agarose immobilization of C. elegans. *Worm Breeder's Gazette* **18**, 1.

Hailey ,D., Rambold, A., Satpute-Krishnan, P., Mitra, K., Sougrat, R., Kim, P. and Lippincott-Schwartz, J. (2010). Mitochondria supply membranes for autophagosome biogenesis during starvation. *Cell* **141**, 656-667.

Nehrke, K., Denton, J. and Mowrey, W. (2008). Intestinal Ca2+ wave dynamics in freely moving C. elegans coordinate execution of a rhythmic motor program. *American Journal of Physiology- Cell Physiology* **294**, C333-44.

Miklavc, P., Wittekindt, O.H., Felder, E. and Dietl, P. (2009). Ca2+-dependent actin coating of lamellar bodies after exocytotic fusion: a prerequisite for content release or kiss-and-run. *Annals of the New York Academy of Sciences* **1152**, 43-52.

Peters, M., Teramoto, T., White, J., Iwasaki, K. and Jorgensen, E. (2007). A calcium wave mediated by gap junctions coordinates a rhythmic behavior in C. elegans. *Current Biology* **17**, 1601-1608.

Phelan, V., Liu, W., Pogliano, K. and Dorrestein, P. (2011). Microbial metabolic exchange--the chemotype-to-phenotype link. *Nature Chemical Biology* **8**, 26-35.

Shen, Q., He, B., Lu, N., Conradt, B., Grant, B. and Zhou, Z. (2013). Phagocytic receptor signaling regulates clathrin and epsin-mediated cytoskeletal remodeling during apoptotic cell engulfment in C. elegans. *Development* **140**, 3230-3243.

Troemel, E., Felix, M., Whiteman, N., Barriére, A. and Ausubel, F. (2008). Microsporidia are natural intracellular parasites of the nematode Caenorhabditis elegans. *PLoS Biology* **6**, 2736-2752.

Vavra, J. and Lukes, J. (2013). Microsporidia and 'the art of living together'. *Advancements in Parasitology* **82**, 253-319.

Watrous, J., Roach, P., Alexandrov, T., Heath, B., Yang, J., Kersten, R., van der Voort, M., Pogliano, K., Gross, H., Raaijmakers, J., Moore, B., Laskin, J., Bandeira, N. and Dorrestein, P. (2012). Mass spectral molecular networking of living microbial colonies. *Proceedings of the National Academy of Sciences of the United States of America* **109,** E1743-52.

Yang, Y., Xu, Y., Straight, P. and Dorrestein, P. (2009). Translating metabolic exchange with imaging mass spectrometry. *Nature Chemical Biology* **5**, 885-887.